

The First Stars

Simon Glover

Abstract The first stars to form in the Universe – the so-called Population III stars – bring an end to the cosmological Dark Ages, and exert an important influence on the formation of subsequent generations of stars and on the assembly of the first galaxies. Developing an understanding of how and when the first Population III stars formed and what their properties were is an important goal of modern astrophysical research. In this review, I discuss our current understanding of the physical processes involved in the formation of Population III stars. I show how we can identify the mass scale of the first dark matter halos to host Population III star formation, and discuss how gas undergoes gravitational collapse within these halos, eventually reaching protostellar densities. I highlight some of the most important physical processes occurring during this collapse, and indicate the areas where our current understanding remains incomplete. Finally, I discuss in some detail the behaviour of the gas after the formation of the first Population III protostar. I discuss both the conventional picture, where the gas does not undergo further fragmentation and the final stellar mass is set by the interplay between protostellar accretion and protostellar feedback, and also the recently advanced picture in which the gas does fragment and where dynamical interactions between fragments have an important influence on the final distribution of stellar masses.

Simon Glover
Universität Heidelberg, Zentrum für Astronomie, Institut für Theoretische Astrophysik, Albert-
Ueberle-Str. 2, 69120 Heidelberg, e-mail: glover@uni-heidelberg.de

1 Formation of the first star-forming minihalo

1.1 The Jeans mass and the filter mass

In the currently dominant Λ CDM paradigm, gravitationally bound objects form in a hierarchical fashion, with the smallest, least massive objects forming first, and larger objects forming later through a mixture of mergers and accretion. The mass scale of the least massive objects to form from dark matter is set by free-streaming of the dark matter particles, and so depends on the nature of these particles. However, in most models, this minimum mass is many orders of magnitude smaller than the mass of even the smallest dwarf galaxies (Green, Hofmann & Schwarz, 2005). More relevant for the formation of the first stars and galaxies is the mass scale of the structures (frequently referred to as dark matter ‘minihalos’) within which the baryonic component of matter, the gas, can first cool and collapse.

A lower limit on this mass scale comes from the theory of the growth of small density perturbations in an expanding universe (see e.g. Barkana & Loeb, 2001). From the analysis of the linearized equations of motion, one can identify a critical length scale, termed the Jeans length, that marks the boundary between gravitationally stable and gravitationally unstable regimes. The Jeans length is given (in physical units) by

$$\lambda_J = c_s \sqrt{\frac{\pi}{G\rho_0}}, \quad (1)$$

where c_s is the sound speed in the unperturbed intergalactic medium and ρ_0 is the cosmological background density. Perturbations on scales $\lambda > \lambda_J$ are able to grow under the influence of their own self-gravity, while those with $\lambda < \lambda_J$ are prevented from growing by thermal pressure. We can associate a mass scale with λ_J by simply taking the mass within a sphere of radius $\lambda_J/2$ (Barkana & Loeb, 2001):

$$M_J = \frac{4\pi}{3} \rho_0 \left(\frac{\lambda_J}{2} \right)^3. \quad (2)$$

This mass, termed the Jeans mass, describes the minimum mass that a perturbation must have in order to be gravitationally unstable.

In the simplest version of this analysis, the value used for the sound speed in the equations for the Jeans length and Jeans mass is the instantaneous value; i.e. to determine λ_J and M_J at a redshift z , we use the value of c_s at that redshift. In this approximation, the Jeans mass is given in the high redshift limit (where the gas temperature is strongly coupled to the cosmic microwave background [CMB] temperature by Compton scattering) by the expression (Barkana & Loeb, 2001)

$$M_J = 1.35 \times 10^5 \left(\frac{\Omega_m h^2}{0.15} \right)^{-1/2} M_\odot, \quad (3)$$

where Ω_m is the dimensionless cosmological matter density parameter, and h is the value of the Hubble constant in units of $100 \text{ km s}^{-1} \text{ Mpc}^{-1}$. In the low redshift limit (where the coupling between radiation and matter is weak and the gas temperature evolves adiabatically), the Jeans mass is given instead by

$$M_J = 5.18 \times 10^3 \left(\frac{\Omega_m h^2}{0.15} \right)^{-1/2} \left(\frac{\Omega_b h^2}{0.026} \right)^{-3/5} \left(\frac{1+z}{10} \right)^{3/2} M_\odot, \quad (4)$$

where Ω_b is the dimensionless cosmological baryon density parameter. The evolution of M_J with redshift is also illustrated in Figure 1.

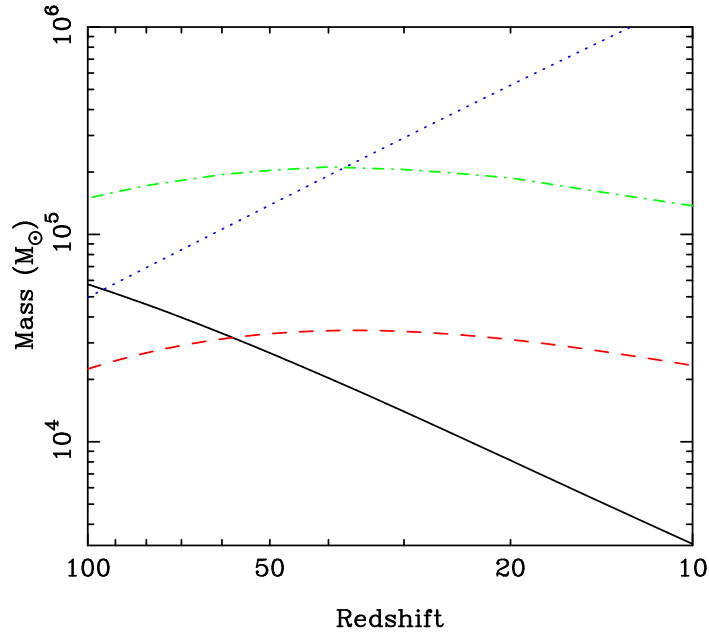


Fig. 1 Evolution with redshift of the Jeans mass (solid line), the filter mass computed in the limit where the relative streaming velocity between gas and dark matter is zero (dashed line) and the filter mass computed assuming a streaming velocity $v = \sigma_{\text{vbc}}$ (dash-dotted line). Also plotted is the critical minihalo mass, M_{crit} , required for efficient H_2 cooling (dotted line). The estimate of the filter mass in the no streaming limit comes from Naoz & Barkana (2007), who account for a number of effects not treated in the original Gnedin & Hui (1998) formulation, while the estimate of M_F in the streaming case comes from Tselikhovich, Barkana & Hirata (2011). The value of M_{crit} was computed using Equation 38.

A more careful treatment of the growth of linear density perturbations accounts for the fact that the sound speed, the Jeans length and potentially also the Jeans mass

may all change significantly during the time it takes for a perturbation to grow into the non-linear regime. Gnedin & Hui (1998) showed that in this case, the appropriate mass scale separating the gravitationally stable and gravitationally unstable regimes is a form of time-averaged Jeans mass that they denote as the “filter mass”, M_F . This is given in physical units by

$$M_F = \frac{4\pi}{3} \rho_0 \left(\frac{\lambda_F}{2} \right)^3, \quad (5)$$

where the filter wavelength λ_F is given in the high redshift limit by (Gnedin, 2000)

$$\lambda_F^2 = \frac{3}{1+z} \int_z^\infty \lambda_J^2 \left[1 - \left(\frac{1+z}{1+z'} \right)^{1/2} \right] dz'. \quad (6)$$

It is possible to improve further on this analysis by accounting for spatial variations in the sound speed (Barkana & Loeb, 2005; Naoz & Barkana, 2005) and by properly accounting for the separate rates of growth of the dark matter and baryonic perturbations in the high redshift limit in which the gas is mechanically coupled to the CMB by Compton scattering (Naoz & Barkana, 2007). The net result is to somewhat lower the filter mass in comparison with the predictions of Equations 5-6. Comparing the resulting filter mass with the Jeans mass (Figure 1), we see that the filter mass can be a factor of a few smaller than the Jeans mass at high redshift, but that for redshifts below $z \sim 50$, the filter mass is the larger of the two mass scales.

Another complication was recently pointed out by Tseliakhovich & Hirata (2010). They show that prior to the recombination epoch, the strong coupling between gas and radiation leads to the gas developing a non-zero velocity relative to the dark matter. While the gas and radiation are coupled, the sound-speed in the gas is approximately $c/\sqrt{3}$, where c is the speed of light, and the relative velocity between gas and dark matter is highly subsonic. Once the gas and radiation decouple, however, the sound-speed of the gas decreases enormously, becoming $\sim 6 \text{ km s}^{-1}$ at the end of the recombination epoch. Tseliakhovich & Hirata (2010) show that at the same time, the RMS velocity of the gas relative to the dark matter is about 30 km s^{-1} , implying that the gas is moving supersonically with respect to the dark matter. The coherence length of the supersonic flow is of the order of the Silk damping scale (Silk, 1968), i.e. several comoving Mpc, and so on the much smaller scales corresponding to the formation of the first star-forming minihalos, the gas can be treated as being in uniform motion with respect to the dark matter. Tseliakhovich & Hirata (2010) also show that the relative velocity between gas and dark matter acts to suppress the growth of small-scale structure in both components, and that because this effect is formally a second-order term in cosmological perturbation theory, it was not included in previous studies based on linear perturbation theory.

In a follow-up study, Tseliakhovich, Barkana & Hirata (2011) improve on the Tseliakhovich & Hirata (2010) analysis by accounting for spatial variations in the sound speed, and study the effect that the relative velocity between the gas and the dark matter has on the size of the filter mass. The magnitude of the relative velocity

v is randomly distributed with a Gaussian probability distribution function (PDF) with total variance σ_{vbc}^2 , i.e.

$$P_{\text{vbc}}(v) = \left(\frac{3}{2\pi\sigma_{\text{vbc}}^2}\right)^{3/2} 4\pi v^2 \exp\left(-\frac{3v^2}{2\sigma_{\text{vbc}}^2}\right). \quad (7)$$

Tseliakhovich, Barkana & Hirata (2011) show that for a relative velocity $v = \sigma_{\text{vbc}}$ (i.e. a one sigma perturbation), the effect of the relative velocity between gas and dark matter is to increase M_{F} by roughly an order of magnitude, as illustrated in Figure 1. Higher sigma perturbations lead to even greater increases in M_{F} , but Tseliakhovich, Barkana & Hirata (2011) show that the global average case (obtained by computing M_{F} for a range of different v and then integrating over the PDF given in Equation 7) is very similar to the one sigma case. Numerical studies of the effects of these streaming velocities (see e.g. Stacy, Bromm & Loeb, 2011; Greif et al., 2011b) have generally confirmed this result, although these studies still disagree somewhat regarding the influence of the streaming velocities on minihalos with masses greater than the revised M_{F} .

Nevertheless, even the most careful version of this analysis only tells us the mass scale of the first gravitationally bound structures to have a significant gas content, which is merely a lower limit on the mass scale of the first *star-forming* minihalos. The reason for this is that for stars to form within a minihalo, it is not enough that the gas be gravitationally bound; it must also be able to cool efficiently. In order for the gas within a minihalo to dissipate a large fraction of its gravitational binding energy – a necessary condition if pressure forces are not to halt the gravitational collapse of the gas (Hoyle, 1953; Rees, 1976; Rees & Ostriker, 1977) – it must be able to radiate this energy away. The timescale over which this occurs is known as the cooling time, and is defined as

$$t_{\text{cool}} = \frac{1}{\gamma - 1} \frac{n_{\text{tot}} k T}{\Lambda}, \quad (8)$$

where n_{tot} is the total number density of particles, γ is the adiabatic index, k is Boltzmann's constant, T is the gas temperature and Λ is the radiative cooling rate per unit volume. If the cooling time of the gas is longer than the Hubble time, then it is very unlikely that the minihalo will survive as an isolated object for long enough to form stars. Instead, it is far more likely that it will undergo a major merger with another dark matter halo of comparable or larger mass before any of its gas has cooled significantly, since major mergers occur, on average, approximately once per Hubble time (Lacey & Cole, 1993). Therefore, to determine the minimum mass of a star-forming minihalo, we must first understand how cooling occurs within primordial gas, a topic that we explore in the next section.

1.2 Cooling and chemistry in primordial gas

At high temperatures ($T \sim 10^4$ K and above), primordial gas can cool efficiently through the collisional excitation of excited electronic states of atomic hydrogen, atomic helium, and singly-ionized helium. However, it is relatively easy to show that most of the gas within a minihalo with $M \sim M_F$ will have a temperature significantly below 10^4 K. If we assume that the gas within the minihalo relaxes into a state of virial equilibrium, such that the total potential energy W and total kinetic energy K are related by $W = -2K$, then we can use this fact to define a virial temperature for the minihalo (Barkana & Loeb, 2001)

$$T_{\text{vir}} = \frac{\mu m_p v_c^2}{2k}, \quad (9)$$

where μ is the mean molecular weight, m_p is the proton mass, and v_c is the circular velocity of the minihalo. This can be rewritten in terms of the redshift z and the mass M of the minihalo as

$$T_{\text{vir}} = 1.98 \times 10^4 \left(\frac{\mu}{0.6} \right) \left(\frac{M}{10^8 h^{-1} M_\odot} \right)^{2/3} \left[\frac{\Omega_m}{\Omega_m(z)} \frac{\Delta_c}{18\pi^2} \right]^{1/3} \left(\frac{1+z}{10} \right) \text{K}, \quad (10)$$

where $\Omega_m(z)$ is the dimensionless cosmological density parameter evaluated at redshift z and $\Delta_c = 18\pi^2 + 82d - 39d^2$, with $d = \Omega_m(z) - 1$ (Bryan & Norman, 1998). In the standard Λ CDM cosmology, $\Omega_m(z) \simeq 1$ at $z > 6$, and hence the term in square brackets reduces to $\Omega_m^{1/3}$. If we rearrange Equation 10 and solve for the mass M_{atom} of a cloud that has a virial temperature $T_{\text{vir}} = 10^4$ K and that can therefore cool via atomic excitation, we find that

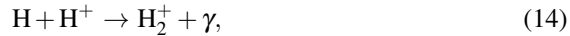
$$M_{\text{atom}} = 5 \times 10^7 h^{-1} \left(\frac{\mu}{0.6} \right)^{-3/2} \Omega_m^{-1/2} \left(\frac{1+z}{10} \right)^{-3/2} M_\odot, \quad (11)$$

significantly larger than our estimates for M_J and M_F above. Minihalos with masses close to M_J or M_F will therefore have virial temperatures much less than 10^4 K, placing them in the regime where molecular coolants dominate.

In primordial gas, by far the most abundant and hence most important molecule is molecular hydrogen, H_2 . The chemistry of H_2 in primordial gas has been reviewed in a number of different studies (see e.g. Abel et al., 1997; Galli & Palla, 1998; Stancil, Lepp & Dalgarno, 1998; Glover & Abel, 2008), and so we only briefly discuss it here. Direct formation of H_2 by the radiative association of two hydrogen atoms is highly forbidden (Gould & Salpeter, 1963), and so at low densities, most H_2 forms via the reaction chain (McDowell, 1961; Peebles & Dicke, 1968)



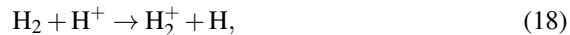
with a minor fraction forming via the reaction chain (Saslaw & Zipoy, 1967)



In warm gas, H_2 can be destroyed by collisional dissociation (see e.g. Martin, Keogh & Mandy, 1998)



or by charge transfer with H^+ (see e.g. Savin et al., 2004)



but at low temperatures there are no collisional processes that can efficiently remove it from the gas.

When the fractional ionization of the gas is low, the rate at which H_2 forms is limited primarily by the rate at which H^- ions form via reaction 12, as any ions that form are rapidly converted to H_2 by associative detachment with atomic hydrogen (reaction 13). If the fractional ionization is large, on the other hand, then many of the H^- ions formed by reaction 12 do not survive for long enough to form H_2 , but instead are destroyed by mutual neutralization with H^+ ions:



The ratio of the rates of reactions 13 and 19 is given by $k_{13}n_{\text{H}}/k_{19}n_{\text{H}^+}$, where n_{H} is the number density of atomic hydrogen, n_{H^+} is the number density of protons, and k_{13} and k_{19} are the rate coefficients for reactions 13 and 19, respectively. Mutual neutralization therefore becomes significant whenever $n_{\text{H}^+}/n_{\text{H}} \geq k_{13}/k_{19}$. Although the value of k_{13}/k_{19} is temperature dependent, the temperature dependence is weak if one uses the best available determinations of the rate coefficients (Kreckel et al. 2010 for reaction 13, Stenrup, Larson & Elander 2009 for reaction 19¹), and $k_{13}/k_{19} \sim 0.03$ to within 50% for all temperatures $100 < T < 10^4$ K. If we compare this value with the residual fractional ionization of the intergalactic medium (IGM) at this epoch, $x \sim 2 \times 10^{-4}$ (Schleicher et al., 2008), we see that mutual neutralization is unimportant within the very first star-forming minihalos. It becomes important once larger minihalos, with virial temperatures $T_{\text{vir}} \sim 10^4$ K or above, begin to form, as in these minihalos, substantial collisional ionization of the gas can occur, leading to an initial fractional ionization much higher than the residual value in the IGM. It also becomes an important process within the “fossil” HII regions left behind by the first generation of massive stars (Oh & Haiman, 2003; Nagakura & Omukai, 2005; Glover, Savin & Jappsen, 2006; Kreckel et al., 2010).

¹ A group lead by X. Urbain at the Université Catholique de Louvain has recently made new experimental measurements of the rate of this reaction at low temperatures, but at the time of writing, the results of this work remain unpublished

Although H_2 is by far the most abundant primordial molecule, it is actually not a particularly efficient coolant. The H_2 molecule has no dipole moment, and so dipole transitions between its excited rotational and vibrational levels are forbidden. Although radiative transitions between levels do occur, they are quadrupole transitions and the associated transition rates are small. In addition, application of the Pauli exclusion principle to the hydrogen molecule shows that it must have two distinct states, distinguished by the nuclear spin of the two hydrogen nuclei: para-hydrogen, in which the nuclear spins are parallel, and which must have an even value for the rotational quantum number J , and ortho-hydrogen, which has anti-parallel nuclear spins and an odd value for J . Radiative transitions between ortho-hydrogen and para-hydrogen involve a change in orientation of the spin of one of the nuclei and are therefore strongly forbidden. As a result, the least energetic rotational transition of H_2 that has any significant probability of occurring is the transition between the $J = 2$ and $J = 0$ rotational levels in the vibrational ground-state of para-hydrogen. This transition has an associated energy $E_{20}/k \simeq 512$ K. The H_2 molecule therefore has large energy separations between the ground state and any of the accessible excited rotational or vibrational states², and has only weak radiative transitions between these states.

These features of the H_2 molecule have two important consequences. First, it becomes a very inefficient coolant at temperatures $T \ll E_{20}/K$, as it becomes almost impossible to collisionally populate any of the excited states. The minimum temperature that can be reached solely with H_2 cooling depends somewhat on the H_2 abundance and the time available for cooling, but typically $T_{\min} \sim 150\text{--}200$ K. Second, its rotational and vibrational levels reach their local thermodynamic equilibrium (LTE) level populations at a relatively low density, $n_{\text{crit}} \sim 10^4 \text{ cm}^{-3}$. This means that at densities $n \gg n_{\text{crit}}$, the H_2 cooling rate scales only linearly with density and the cooling time due to H_2 becomes independent of density. Since other important timescales, such as the free-fall collapse time of the gas, continue to decrease with increasing density, the implication is that H_2 becomes an increasingly ineffective coolant as one moves to higher densities.

For these reasons, primordial molecules or molecular ions that do not share these drawbacks have attracted a certain amount of attention. In an early study, Lepp & Shull (1984) suggested that deuterated hydrogen, HD, and lithium hydride, LiH, may both be significant coolants in primordial gas. More recently, work by Yoshida et al. (2007) has suggested that H_2^+ may be an important coolant in some circumstances, while Glover & Savin (2006) show that H_3^+ is also worthy of attention. In practice, the only one of these molecules or ions that has proved to be important is HD. Detailed modelling of the chemistry of lithium in primordial gas (e.g. Stancil, Lepp & Dalgarno, 1996; Mizusawa, Omukai & Nishi, 2005) has shown that LiH is efficiently destroyed by the reaction



² For comparison, note that the energy separation between the $J = 0$ and $J = 1$ rotational levels of CO is roughly 5 K.

and that only a small fraction of the available lithium (which itself has an abundance of only 5×10^{-10} relative to hydrogen; see Cyburt, Fields & Olive 2008) is ever incorporated into LiH. Cooling from the molecular ion H_2^+ was re-examined by Glover & Savin (2009), who showed that the collisional excitation rates cited by Galli & Palla (1998) and used as a basis for the fits given in Yoshida et al. (2007) were a factor of ten too large, and that if the correct rates are used, H_2^+ cooling is no longer important. Finally, Glover & Savin (2009) also examined the possible role played by H_3^+ cooling in considerable detail, but found that even if one makes optimistic assumptions regarding its formation rate and collisional excitation rate, it still contributes to the total cooling rate at the level of only a few percent, and hence at best is a minor correction term.

These studies leave HD as the only viable alternative to H_2 as a coolant of primordial gas. HD has a small, but non-zero dipole moment, giving it radiative transition rates that are somewhat larger than those of H_2 , resulting in a critical density $n_{\text{crit}} \sim 10^6 \text{ cm}^{-3}$. Unlike H_2 , it is not separated into ortho and para states, and so the lowest energy transition accessible from the ground state is the $J = 1$ to $J = 0$ rotational transition, with an energy $E_{10}/k = 128 \text{ K}$. Although the cosmological ratio of deuterium to hydrogen is small [$\text{D}/\text{H} = (2.49 \pm 0.17) \times 10^{-5}$; Cyburt, Fields & Olive 2008], the ratio of HD to H_2 can be significantly boosted in low temperature gas by chemical fractionation. The reaction



that converts H_2 into HD is exothermic and so proceeds rapidly at all temperatures, while the inverse reaction



is endothermic and so proceeds very slowly at low temperatures. In equilibrium, these two reactions produce an HD-to- H_2 ratio given by

$$\frac{x_{\text{HD}}}{x_{\text{H}_2}} = 2 \exp\left(\frac{464}{T}\right) [\text{D}/\text{H}], \quad (23)$$

where $[\text{D}/\text{H}]$ is the cosmological D:H ratio. Together, these factors render HD a much more effective coolant than H_2 in low temperature gas.

In practice, for HD cooling to take over from H_2 cooling, the gas must already be fairly cold, with $T \sim 150 \text{ K}$ (Glover, 2008), and temperatures this low are typically not reached during the collapse of the first star-forming minihalos, meaning that HD remains a minor coolant (Bromm, Coppi & Larson, 2002). However, there are a number of situations, typically involving gas with an enhanced fractional ionization, in which HD cooling does become significant (see e.g. Nakamura & Umemura, 2002; Nagakura & Omukai, 2005; Johnson & Bromm, 2006; Yoshida et al., 2007; McGreer & Bryan, 2008; Greif et al., 2008; Kreckel et al., 2010).

1.3 The minimum mass scale for collapse

The relative simplicity of the chemistry discussed in the previous section allows one to construct a very simple model that captures the main features of the evolution of the H_2 fraction within low density gas falling into a dark matter minihalo. We start by assuming that radiative recombination is the only process affecting the electron abundance, and writing the rate of change of the electron number density as

$$\frac{dn_e}{dt} = -k_{\text{rec}}n_en_{\text{H}^+}, \quad (24)$$

where n_e is the number density of electrons, n_{H^+} is the number density of protons, and k_{rec} is the recombination coefficient. If we assume that ionized hydrogen is the only source of free electrons, implying that $n_e = n_{\text{H}^+}$, and that the temperature remains roughly constant during the evolution of the gas, then we can solve for the time evolution of the electron fraction:

$$x = \frac{x_0}{1 + k_{\text{rec}}ntx_0}, \quad (25)$$

where $x \equiv n_e/n$, n is the number density of hydrogen nuclei, and x_0 is the initial value of x . We next assume that all of the H_2 forms via the H^- pathway, and that mutual neutralization of H^- with H^+ (reaction 19) is the only process competing with associative detachment (reaction 13) for the H^- ions. In this case, we can write the time evolution of the H_2 fraction, $x_{\text{H}_2} \equiv n_{\text{H}_2}/n$, as

$$\frac{dx_{\text{H}_2}}{dt} = k_{12}xn_{\text{H}}p_{\text{AD}}, \quad (26)$$

where k_{12} is the rate coefficient of reaction 12, the formation of H^- by the radiative association of H and e^- , and p_{AD} is the probability that any given H^- ion will be destroyed by associative detachment rather than by mutual neutralization. Given our assumptions above, this can be written as

$$p_{\text{AD}} = \frac{k_{13}n_{\text{H}}}{k_{13}n_{\text{H}} + k_{19}n_{\text{H}^+}}, \quad (27)$$

where k_{13} is the rate coefficient for reaction 13 and k_{19} is the rate coefficient for reaction 19. If we again assume that $n_e = n_{\text{H}^+}$, and in addition assume that $n_{\text{H}} \simeq n$, then the expression for p_{AD} can be simplified to

$$p_{\text{AD}} = \left(1 + \frac{k_{19}}{k_{13}}x\right)^{-1}. \quad (28)$$

Substituting this into Equation 26, we obtain

$$\frac{dx_{\text{H}_2}}{dt} = k_{12}xn_{\text{H}} \left(1 + \frac{k_{19}}{k_{13}}x\right)^{-1}. \quad (29)$$

If the initial fractional ionization $x_0 \ll k_{13}/k_{19}$, then the term in parentheses is of order unity and this equation has the approximate solution

$$x_{\text{H}_2} = \frac{k_{12}}{k_{\text{rec}}} \ln(1 + k_{\text{rec}} n x_0 t), \quad (30)$$

$$= \frac{k_{12}}{k_{\text{rec}}} \ln(1 + t/t_{\text{rec}}), \quad (31)$$

where $t_{\text{rec}} = 1/(k_{\text{rec}} n x_0)$ is the recombination time. The growth of the H_2 fraction is therefore logarithmic in time, with most of the H_2 forming within the first few recombination times. In the more complicated case in which x_0 is comparable to or larger than k_{13}/k_{19} , but still significantly less than unity (so that $n_{\text{H}} \sim n$), the H_2 fraction is given instead by

$$x_{\text{H}_2} = \frac{k_{12}}{k_{\text{rec}}} \ln \left(\frac{1 + x_0 k_{19}/k_{13} + t/t_{\text{rec}}}{1 + x_0 k_{19}/k_{13}} \right). \quad (32)$$

From this analysis, we see that the main factor determining the final H_2 abundance is the ratio k_{12}/k_{rec} , since for times of the order of a few recombination times, the logarithmic term in Equation 32 is of order unity, implying that the final H_2 abundance is at most a factor of a few times k_{12}/k_{rec} . If we use the simple power-law fits to k_{12} and k_{rec} given by Hutchins (1976), namely $k_{12} = 1.83 \times 10^{-18} T^{0.8779} \text{ cm}^3 \text{ s}^{-1}$ and $k_{\text{rec}} = 1.88 \times 10^{-10} T^{-0.644} \text{ cm}^3 \text{ s}^{-1}$, then we can write the ratio of the two rate coefficients as

$$\frac{k_{12}}{k_{\text{rec}}} \simeq 10^{-8} T^{1.5219}. \quad (33)$$

The amount of H_2 produced is a strong function of temperature, but is of the order of a few times 10^{-3} for temperatures of a few thousand Kelvin. We see therefore that the formation of H_2 via H^- never results in a gas dominated by H_2 , as the H_2 abundance always remains much smaller than the abundance of atomic hydrogen.

Given this simple model for the amount of H_2 that will form in the gas, the obvious next step is to compare this to the amount of H_2 that is required to cool the gas efficiently. In order to determine the H_2 fraction necessary to significantly cool gas with a temperature T within some specified fraction of the Hubble time – say 20% of t_{H} – we can simply equate the two timescales, and solve for the H_2 fraction. Using our previous definition of the cooling time, we have

$$\frac{1}{\gamma - 1} \frac{n_{\text{tot}} k T}{\Lambda_0(T) n_{\text{H}_2}} = 0.2 t_{\text{H}}, \quad (34)$$

where we have assumed that H_2 is the dominant coolant and have written the cooling rate per unit volume in terms of Λ_0 , the cooling rate per H_2 molecule. Rearranging this equation, using the fact that when the H_2 fraction and the ionization level are low, $\gamma = 5/3$ and $n_{\text{tot}} = (1 + 4x_{\text{He}})n$, where x_{He} is the fractional abundance of helium (given by $x_{\text{He}} = 0.083$ for primordial gas), we obtain

$$x_{\text{H}_2, \text{req}} = 1.38 \times 10^{-15} \frac{T}{\Lambda_0(T)} t_{\text{H}}^{-1}. \quad (35)$$

In the high-redshift limit where $t_{\text{H}} \simeq H_0^{-1} \Omega_m^{-1/2} (1+z)^{-3/2}$, this becomes

$$x_{\text{H}_2, \text{req}} = 5.2 \times 10^{-32} \frac{T}{\Lambda_0(T)} \left(\frac{1+z}{10} \right)^{3/2}, \quad (36)$$

where we have used values for the cosmological parameters taken from Komatsu et al. (2011). Collisions of H_2 with a number of different species contribute to Λ_0 , as explored in Glover & Abel (2008), but in the earliest minihalos, the dominant contributions come from collisions with H and He. Λ_0 is therefore given to a good approximation by

$$\Lambda_0 = \Lambda_{\text{H}} n_{\text{H}} + \Lambda_{\text{He}} n_{\text{He}}. \quad (37)$$

Simple fits for the values of Λ_{H} and Λ_{He} as a function of temperature can be found in Glover & Abel (2008).

An illustration of the likely size of $x_{\text{H}_2, \text{req}}$ is given in Figure 2. In this Figure, we plot $x_{\text{H}_2, \text{req}}$ as a function of temperature, evaluated for three different redshifts: $z = 20, 30$ and 40 . In computing these values, we have assumed that the mean density of the gas in the minihalo is given by $\bar{\rho} = \Delta_c \rho_{b,0}$, where ρ_0 is the cosmological background density of baryons. In the Figure, we also show the actual H_2 fraction produced in the gas, $x_{\text{H}_2, \text{act}}$, as a function of temperature at times equal to 1, 5 and 10 recombination times, and where we have taken $x_0 \ll k_{13}/k_{19}$.

Figure 2 demonstrates that the amount of H_2 produced in the gas is a strongly increasing function of temperature, while the amount required to bring about efficient cooling of the gas is a strongly decreasing function of temperature. This means that for any given choice of comparison time t and redshift z , we can identify a critical temperature T_{crit} , such that gas with $T > T_{\text{crit}}$ will cool within a small fraction of a Hubble time, while gas with $T < T_{\text{crit}}$ will not. Moreover, because $x_{\text{H}_2, \text{act}}$ and $x_{\text{H}_2, \text{req}}$ are both steep functions of temperature, but are relatively insensitive to changes in t or z , the value of T_{crit} that we obtain is also relatively insensitive to our choices for t or z . We find that $T_{\text{crit}} \sim 1000$ K, and that at this temperature, the H_2 fraction required to provide efficient cooling lies somewhere between a few times 10^{-4} and 10^{-3} (c.f. Tegmark et al., 1997, who come to a similar conclusion using a very similar argument). If we convert this critical virial temperature into a corresponding critical minihalo mass using Equation 10, we find that

$$M_{\text{crit}} \simeq 6 \times 10^5 h^{-1} \left(\frac{\mu}{1.2} \right)^{-3/2} \Omega_m^{-1/2} \left(\frac{1+z}{10} \right)^{-3/2} M_{\odot}. \quad (38)$$

This mass scale is illustrated by the dotted line in Figure 1. At high redshift, it is smaller than the filter mass scale corresponding to $v_{\text{bc}} = \sigma_{\text{vbc}}$, demonstrating that at these redshifts, it is the streaming of the gas with respect to the dark matter that is the main process limiting the formation of Population III stars. Below a redshift of around 40, however, M_{crit} becomes the larger mass scale, implying that at these

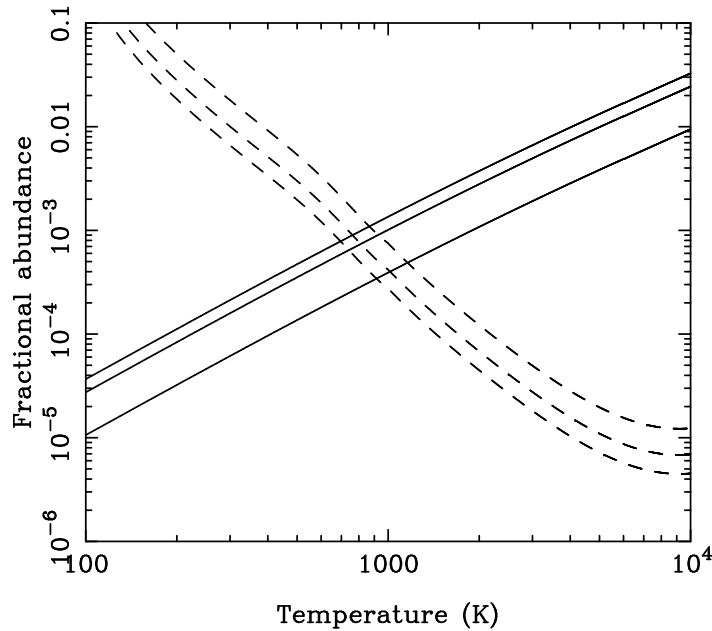


Fig. 2 Comparison of the fractional abundance of H_2 produced with our simple toy model for the chemistry (solid lines) versus the quantity of H_2 required in order to cool the gas within 20% of a Hubble time (dashed lines). From bottom to top, the solid lines correspond to the H_2 fraction produced at times $t = 1, 5$ and $10 t_{\text{rec}}$, respectively, where t_{rec} is the recombination time, and the dashed lines correspond to the H_2 fraction required at redshifts $z = 40, 30$ and 20 , respectively. We see that the minimum temperature that the gas must have in order to be able to cool within a fraction of a Hubble time – indicated by the point at which the lines cross – is relatively insensitive to our choices for t and z .

lower redshifts, there will be a population of small minihalos that contain a significant gas fraction, but that do not form stars, because their gas is unable to cool in less than a Hubble time. These small starless minihalos may be important sinks for ionizing photons during the epoch of reionization (Haiman, Abel & Madau, 2001).

To conclude our discussion of the first star-forming minihalos, we should mention one potentially important effect not taken into account in the analysis above. This is the influence of ongoing minor mergers and accretion on the thermal balance of the gas. Although major mergers occur only once per Hubble time, on average, minor mergers occur far more frequently, and act to stir up the gas, thereby heating it and lengthening the time required for it to cool. This phenomenon was noted by Yoshida et al. (2003) in their cosmological simulations of the formation of the first star-forming minihalos. Yoshida et al. (2003) show that in spite of the approximations made in its derivation, Equation 38 gives a reasonable guide to the minimum

mass of the minihalos that contain gas that can cool effectively. However, they also find that there are some minihalos with $M > M_{\text{crit}}$ in which the gas does not cool. They show that these minihalos have higher mass accretion rates than minihalos of the same mass in which cooling does occur, and hence ascribe the suppression of cooling to the effects of dynamical heating by the ongoing accretion and minor mergers. This effect was also treated more recently by Wang & Abel (2008), who show that it can be included into the simple thermal model described above by the addition of a heating term describing the effects of mergers and accretion. They show that if one writes this heating term as

$$\Gamma = \frac{k}{\gamma - 1} \frac{dT_{\text{vir}}}{dt}, \quad (39)$$

then one can relate the rate of change of the virial temperature to the mass growth rate of the minihalo in a relatively simple fashion.

2 Gravitational collapse and the formation of the first protostar

As the analysis in the previous section has shown, gas in minihalos with virial temperatures greater than about 1000 K (corresponding to masses $M \sim 10^6 M_{\odot}$) can form enough H_2 to cool within a small fraction of a Hubble time. This reduces the pressure and allows the gas to collapse further under the influence of its own self-gravity. As it does so, the value of the Jeans mass decreases. Many early studies of the formation of primordial stars assumed that as the Jeans mass decreases and the gas becomes more gravitationally unstable, it begins to undergo hierarchical gravitational fragmentation in a manner similar to that envisaged by Hoyle (1953), with the result that at any given moment, the mean fragment mass is approximately equal to the local Jeans mass (see Glover, 2005, for a historical summary of these models). In this picture, one could predict the final mass of the first stars simply by studying the evolution of the Jeans mass. Moreover, since the minimum Jeans mass reached during the collapse can be estimated with reasonable accuracy on purely thermodynamical grounds (Rees, 1976; Low & Lynden-Bell, 1976), in this view of Population III star formation, the dynamics of the gas is of secondary importance. Around ten years ago, however, it first became possible to model the coupled chemical, dynamical and thermal evolution of the gas within a primordial minihalo using high resolution 3D numerical simulations (Abel, Bryan & Norman, 2000, 2002; Bromm, Coppi & Larson, 1999, 2002). These studies showed that the picture outlined above is wrong: the gas does not undergo hierarchical fragmentation, and so one cannot predict the masses of the first stars simply by studying the evolution of the Jeans mass. These high resolution numerical simulations, and the many that have followed them (e.g. Yoshida et al., 2006; O’Shea & Norman, 2007; McGreer & Bryan, 2008, to name but a few), have for the first time given us a clear picture of exactly how gravitational collapse proceeds within one of these early minihalos. In

the next section, we will discuss the sequence of events that occur as we follow the collapse from the minihalo scale all the way down to the scale of a single Population III protostar. Following that, in Sections 2.2 and 2.3 we discuss two of the main uncertainties remaining in our model for the formation of the first Pop. III protostar: the role played by heating and ionization arising from dark matter self-annihilation (Section 2.2) and the role played by magnetic fields (Section 2.3).

2.1 Thermal and chemical evolution of the gas during collapse

2.1.1 Initial collapse

As gas falls into the minihalo from the intergalactic medium, it is shock-heated to a temperature close to T_{vir} . In the post-shock gas, the electron fraction decreases due to radiative recombination, but at the same time H_2 forms, primarily via reactions 12 and 13. As we have already seen, the H_2 fraction evolves logarithmically with time, with most of the H_2 forming within the first few recombination times. As the H_2 fraction increases, so does its ability to cool the gas, and so the gas temperature slowly decreases, reducing the pressure and allowing the gas to collapse to the centre of the minihalo.

At this point, the evolution of the gas depends upon how much H_2 it has formed. There are two main outcomes, and which one occurs within a given minihalo depends primarily on the initial ionization state of the gas.

The low ionization case

During the formation of the very first Population III stars (also known as Population III.1, to use the terminology introduced by Tan & McKee 2008), the initial fractional ionization of the gas is the same as the residual ionization in the intergalactic medium, i.e. $x_0 \sim 2 \times 10^{-4}$. In this case, the amount of H_2 that forms in the gas is typically enough to cool it to a temperature of $T \sim 200$ K but not below. At this temperature, chemical fractionation has already increased the HD/H_2 ratio by a factor of 20 compared to the cosmic deuterium-to-hydrogen ratio, and as a consequence, HD is starting to become an important coolant. However, the amount of HD that forms in the gas is not enough to cool it significantly below 200 K (Bromm, Coppi & Larson, 2002), and H_2 continues to dominate the cooling and control the further evolution of the gas. In this scenario, the collapse of the gas is greatly slowed once its temperature reaches 200 K and its density reaches a value of around 10^4 cm^{-3} , corresponding to the critical density n_{crit} , at which the rotational and vibrational level populations of H_2 approach their local thermodynamic equilibrium (LTE) values. At densities higher than this critical density, the H_2 cooling rate per unit volume scales only linearly with n (compared to a quadratic dependence, $\Lambda_{\text{H}_2} \propto n^2$ at lower densities), while processes such as compressional heating continue to increase more

rapidly with n . As a result, the gas temperature begins to increase once the density exceeds n_{crit} .

Gas reaching this point in the collapse enters what Bromm, Coppi & Larson (2002) term a “loitering” phase, during which cold gas accumulates in the centre of the halo but only slowly increases its density. This loitering phase ends once the mass of cold gas that has accumulated exceeds the local value of the Bonnor-Ebert mass (Bonnor, 1956; Ebert, 1955), given in this case by (Abel, Bryan & Norman, 2002)

$$M_{\text{BE}} \simeq 40T^{3/2}n^{-1/2}M_{\odot}, \quad (40)$$

which for $n \sim 10^4 \text{ cm}^{-3}$ and $T \sim 200 \text{ K}$ yields $M_{\text{BE}} \sim 1000M_{\odot}$.³ Once the mass of cold gas exceeds M_{BE} , its collapse speeds up again, and becomes largely decoupled from the larger-scale behaviour of the gas. The next notable event to occur in the gas is the onset of three-body H_2 formation, which is discussed in the next section.

The high ionization case

If the initial fractional ionization of the gas is significantly higher than the residual fraction in the IGM, then a slightly different chain of events can occur. A larger initial fractional ionization implies a shorter recombination time, and hence a logarithmic increase in the amount of H_2 formed after a given physical time. An increase in the H_2 fraction allows the gas to cool to a slightly lower temperature, and hence boosts the HD abundance in two ways: the lower temperature increases the HD/ H_2 ratio produced by fractionation, and the H_2 fraction itself is larger, so any given HD/ H_2 ratio corresponds to a higher HD abundance than in the low ionization case. If the additional ionization allows enough H_2 to be produced to cool the gas to $T \sim 150 \text{ K}$ (which requires roughly a factor of three more H_2 than is required to reach 200 K), then chemical fractionation increases the HD abundance to such an extent that it takes over as the dominant coolant (Glover, 2008). This allows the gas to cool further, in some cases reaching a temperature as low as the CMB temperature, T_{CMB} (e.g. Nakamura & Umemura, 2002; Nagakura & Omukai, 2005; Johnson & Bromm, 2006; Yoshida et al., 2007; McGreer & Bryan, 2008; Kreckel et al., 2010). The higher critical density of HD, $n_{\text{crit,HD}} \sim 10^6 \text{ cm}^{-3}$, means that the gas does not reach the loitering phase until much later in its collapse. Once the gas does reach this phase, however, its subsequent evolution is very similar to that in the low-ionization case discussed above. Cold gas accumulates at $n \sim n_{\text{crit}}$ until its mass exceeds the Bonnor-Ebert mass, which in this case is $M_{\text{BE}} \sim 40M_{\odot}$ if $T = 100 \text{ K}$ and $n = 10^6 \text{ cm}^{-3}$. Once the gas mass exceeds M_{BE} , the collapse speeds up again, and the gas begins to heat up. Aside from the substantial difference in the size of M_{BE} , the main difference between the evolution of the gas in this case and in the low

³ Discussions of Population III star formation often refer to the cold clump of gas at the centre of the minihalo as a “fragment”, and speak of M_{BE} as the “fragmentation mass scale”, but in the case of the very first generation of star-forming minihalos, this is actually something of a misnomer, as very seldom does more than one “fragment” form in a given minihalo

ionization case lies in the fact that in the high ionization case, the gas reheats from $T \sim 200$ K or below to $T \sim 1000$ K much more rapidly than in the low ionization case. As we shall see later, this period of rapid heating has a profound influence on the ability of the gas to fragment.

Several different scenarios have been identified that lead to an enhanced fractional ionization in the gas, and that potentially allow the gas to reach the HD-dominated regime. Gas within minihalos with $T_{\text{vir}} > 9000$ K will become hot enough for collisional ionization of hydrogen to supply the necessary electrons. However, as halos of this size will typically have at least one star-forming progenitor (Johnson, Greif & Bromm, 2008), it is questionable whether many Pop. III stars will form in such minihalos, as we would expect the gas in most of them to have been enriched with metals by one or more previous episodes of star formation.

Another possibility that has attracted significant attention involves the gas in the minihalo being drawn from a “fossil” HII region, i.e. a region that was formerly ionized by a previous Population III protostar but has now recombined (see e.g. Oh & Haiman, 2003; Nagakura & Omukai, 2005; Yoshida et al., 2007). Many studies have shown that the volume of the IGM ionized by a single massive Pop. III star is significantly larger than the volume that is enriched by the metals produced in the supernova occurring at the end of the massive star’s life (see e.g. the recent treatment by Greif et al. 2010, or Ciardi & Ferrara (2005) for a summary of earlier work). It is therefore possible that a significant number of Population III stars may form in such conditions.

A final possibility is that the required ionization can be produced by a flux of X-rays or high energy cosmic rays. Although X-ray ionization was initially favoured as a means of raising the ionization level of the gas, and hence promoting H_2 formation (Haiman, Abel & Rees, 2000), more recent work has shown that if one considers realistic models for the X-ray background that also account for the simultaneous growth of the soft UV background, then one finds that UV photodissociation of the H_2 is a more important effect, and hence that the growth of the radiation backgrounds almost always leads to an overall reduction in the amount of H_2 produced (Glover & Brand, 2003; Machacek, Bryan & Abel, 2003). Cosmic ray ionization may therefore prove to be the more important effect (Stacy & Bromm, 2007; Jasche, Ciardi & Ensslin, 2007), although we still know very little about the likely size of the cosmic ray ionization rate in high redshift minihalos.

2.1.2 Three-body H_2 formation

Once the collapsing gas reaches a density of around 10^8 – 10^9 cm^{-3} , its chemical makeup starts to change significantly. The reason for this is that at these densities, the formation of H_2 via the three-body reactions (Palla, Salpeter, & Stahler, 1983)



starts to become significant. These reactions quickly convert most of the hydrogen in the gas into H_2 . At the same time, however, they generate a substantial amount of thermal energy: every time an H_2 molecule forms via one of these three-body reactions, its binding energy of 4.48 eV is converted into heat. A simple estimate of the relative sizes of the compressional heating rate and the three-body H_2 formation heating rate helps to demonstrate the importance of the latter during this stage of the collapse. Let us consider gas at a density $n = 10^8 \text{ cm}^{-3}$ that has a temperature $T = 1000 \text{ K}$, collapsing at a rate such that $dn/dt = n/t_{\text{ff}}$, where t_{ff} is the gravitational free-fall time. In these conditions, the compressional heating rate is given by

$$\Lambda_{\text{pdv}} \simeq 1.25 \times 10^{-31} n^{1/2} T, \quad (44)$$

$$= 1.25 \times 10^{-24} \text{ erg s}^{-1} \text{ cm}^{-3}, \quad (45)$$

while the three-body H_2 formation heating rate has the value

$$\Lambda_{3\text{b}} \simeq 3.9 \times 10^{-40} T^{-1} n^3 x_{\text{H}}^3, \quad (46)$$

$$= 3.9 \times 10^{-19} x_{\text{H}}^3 \text{ erg s}^{-1} \text{ cm}^{-3}, \quad (47)$$

where we have adopted the rate coefficient for reaction 41 given in Palla, Salpeter, & Stahler (1983). Comparing the two heating rates, we see that three-body H_2 formation heating dominates unless x_{H} is very small (i.e. unless the gas is almost fully molecular). Therefore, even though the abundance of H_2 , the dominant coolant during this phase of the collapse, increases by more than two orders of magnitude, the gas typically does not cool significantly, owing to the influence of this three-body H_2 formation heating. Indeed, the temperature often actually increases.

One major uncertainty that remains in current treatments of this phase of the collapse of the gas is exactly how quickly the gas becomes molecular. Although reaction 41 is the dominant source of H_2 at these densities, the rate coefficient for this reaction is poorly known, with published values differing by almost two orders of magnitude at 1000 K, and by an even larger factor at lower temperatures (Glover, 2008; Turk et al., 2011). The effects of this uncertainty have recently been studied by Turk et al. (2011). They show that it has little effect on the density profile of the gas, and only a limited effect on the temperature profile. However, it has much more significant effects on the morphology of the gas and on its velocity structure. Simulations in which a high value was used for the three-body rate coefficient show find that gas occurs more rapidly, and that the molecular gas develops a much more flattened, filamentary structure. Significant differences are also apparent in the infall velocities and the degree of rotational support. Turk et al. (2011) halt their simulations at the point at which a protostar first forms, and so do not directly address the issue of whether these differences continue to have an influence during the accretion phase, and whether they affect the ability of the gas to fragment (see Section 3.2 below). A follow-up study that focussed on these issues would be informative.

2.1.3 Optically-thick line cooling

The next important event occurs at a density of around 10^{10} cm^{-3} , when the main rotational and vibrational lines of H_2 start to become optically thick (Ripamonti & Abel, 2004). The effect of this is to reduce the efficiency of H_2 cooling, leading to a continued rise in the gas temperature. In one-dimensional simulations (e.g. Omukai & Nishi, 1998; Omukai et al., 1998; Ripamonti et al., 2002), it is possible to treat optically thick H_2 cooling accurately by solving the full radiative transfer problem. These models show that although the optical depth of the gas becomes large at frequencies corresponding to the centers of the main H_2 emission lines, the low continuum opacity of the gas allows photons to continue to escape through the wings of the lines, with the result that the H_2 cooling rate is suppressed far less rapidly as the collapse proceeds than one might at first expect (see Omukai et al., 1998, for a detailed discussion of this point).

In three-dimensional simulations, solution of the full radiative transfer problem is not currently possible, due to the high computational expense, which has motivated a search for simpler approximations. There are two such approximations in current use in simulations of Population III star formation. The first of these was introduced by Ripamonti & Abel (2004). They proposed that the ratio of the optically thick and optically thin H_2 cooling rates,

$$f_\tau \equiv \frac{\Lambda_{\text{H}_2, \text{thick}}}{\Lambda_{\text{H}_2, \text{thin}}}, \quad (48)$$

could be represented as a simple function of density:

$$f_\tau = \min \left[1, \left(\frac{n}{n_0} \right)^{-0.45} \right], \quad (49)$$

where $n_0 = 8 \times 10^9 \text{ cm}^{-3}$. They showed that this simple expression was a good approximation to the results of the full radiative transfer model used by Ripamonti et al. (2002), and suggested that this approximation would be useful for extending the results of three-dimensional simulations into the optically thick regime. However, they also noted that it may only be accurate while the collapse remains approximately spherical, as the one-dimensional model on which it is based assumes spherical infall.

An alternative approach was introduced by Yoshida et al. (2006). They compute escape probabilities for each rotational and vibrational line of H_2 using the standard Sobolev approximation (Sobolev, 1960). In this approximation, the optical depth at line centre of a transition from an upper level u to a lower level l is written as

$$\tau_{ul} = \alpha_{ul} L_s, \quad (50)$$

where α_{ul} is the line absorption coefficient and L_s is the Sobolev length. The absorption coefficient α_{ul} can be written as

$$\alpha_{ul} = \frac{\Delta E_{ul}}{4\pi} n_l B_{lu} \left[1 - \exp\left(\frac{-\Delta E_{ul}}{kT}\right) \right] \phi(v_{ul}), \quad (51)$$

where E_{ul} is the energy difference between the two levels, n_l is the number density of H_2 molecules in the lower levels, B_{lu} is the usual Einstein B coefficient, and $\phi(v_{ul})$ is the line profile at the centre of the line. The Sobolev length is given by

$$L_s = \frac{v_{\text{th}}}{|dv_r/dr|}, \quad (52)$$

where v_{th} is the thermal velocity of the H_2 and $|dv_r/dr|$ is the size of the velocity gradient along a given line of sight from the fluid element of interest. Given τ_{ul} , the escape probability for photons emitted in that direction then follows as

$$\beta_{ul} = \frac{1 - \exp(-\tau_{ul})}{\tau_{ul}}. \quad (53)$$

To account for the fact that the velocity gradient may differ along different lines of sight from any particular fluid element, Yoshida et al. (2006) utilize a mean escape probability given by

$$\beta = \frac{\beta_x + \beta_y + \beta_z}{3}, \quad (54)$$

where β_x , β_y and β_z are the escape probabilities along lines of sight in the x , y and z directions, respectively. Finally, once the escape probabilities for each transition have been calculated, the optically thick H_2 cooling rate can be computed from

$$\Lambda_{\text{H}_2, \text{thick}} = \sum_{u,l} E_{ul} \beta_{ul} A_{ul} n_u, \quad (55)$$

where A_{ul} is the Einstein A coefficient for the transition from u to l and n_u is the population of the upper level u .

Strictly speaking, the Sobolev approximation is valid only for flows in which the Sobolev length L_s is much smaller than the characteristic length scales associated with changes in the density, temperature or chemical makeup of the gas, a requirement which is easy to satisfy when the velocity gradient is very large, but which is harder to justify in the case of Population III star formation, since the collapse speed is typically comparable to the sound-speed. Nevertheless, Yoshida et al. (2006) show that the optically thick H_2 cooling rates predicted by the Sobolev approximation are in very good agreement with those computed in the one-dimensional study of Omukai & Nishi (1998) by solution of the full radiative transfer problem.

Little work has been done on comparing these two approaches to treating optically-thick H_2 cooling. This issue was addressed briefly in Turk et al. (2011), who showed that the two approximations yielded similar values for f_τ for densities $n < 10^{15} \text{ cm}^{-3}$ during the initial collapse of the gas, with differences of at most a factor of two. However, as yet no study has examined whether this good agreement persists past the point at which the first protostar forms.

2.1.4 Collision-induced emission

A further significant point in the collapse of the gas is reached once the number density increases to $n \sim 10^{14} \text{ cm}^{-3}$. At this density, a process known as collision-induced emission becomes important. Although an isolated H_2 molecule has no dipole moment, and can only emit or absorb radiation through quadrupole transitions, when two H_2 molecules collide⁴ they briefly act as a kind of “supermolecule” with a non-zero dipole moment for the duration of the collision. This supermolecule can therefore absorb or emit radiation through dipole transitions, which have much higher transition probabilities than the quadrupole transitions available to isolated H_2 . If radiation is absorbed, this process is termed collision-induced absorption; if it is emitted, then we refer to the process as collision-induced emission (CIE). A detailed discussion of the phenomenon can be found in Frommhold (1993).

Collision-induced emission can in principle occur in gas of any density, but the probability of a photon being emitted in any given collision is very small, owing to the short lifetime of the collision state ($\Delta t < 10^{-12} \text{ s}$ at the temperatures relevant for Pop. III star formation; see Ripamonti & Abel 2004). For this reason, CIE becomes an important process only at very high gas densities. Another consequence of the short lifetime of the collision state is that the individual lines associated with the dipole transitions become so broadened that they actually merge into a continuum. This is important, as it means that the high opacity of the gas in the rovibrational lines of H_2 does not significantly reduce the amount of energy that can be radiated away by CIE. Therefore, once the gas reaches a sufficiently high density, CIE becomes the dominant form of cooling, as pointed out by several authors (Omukai & Nishi, 1998; Ripamonti et al., 2002; Ripamonti & Abel, 2004).

The most detailed study of the effects of CIE cooling on the collapse of primordial gas was carried out by Ripamonti & Abel (2004). They showed that CIE cooling could actually become strong enough to trigger a thermal instability. However, the growth rate of this instability is longer than the gravitational free-fall time, meaning that it is unlikely that this process can drive fragmentation during the initial collapse of the gas.

2.1.5 Cooling due to H_2 dissociation

The phase of the collapse dominated by CIE cooling lasts for only a relatively short period of time. The gas becomes optically thick in the continuum once it reaches a density $n \sim 10^{16} \text{ cm}^{-3}$ (Omukai & Nishi, 1998; Ripamonti & Abel, 2004), which strongly suppresses any further radiative cooling. Once this occurs, the gas temperature rises until it reaches a point at which the H_2 begins to dissociate. At these densities, this occurs at a temperature $T \sim 3000 \text{ K}$. Once this point is reached, the temperature rise slows, as most of the energy released during the collapse goes into dissociating the H_2 rather than raising the temperature. As it takes 4.48 eV of energy

⁴ A similar process can also occur during collisions of atomic hydrogen or atomic helium with H_2 , but it is the H_2 - H_2 case that is the most relevant here

to destroy each H_2 molecule, this H_2 dissociation phase continues for a while. However, it comes to an end once almost all of the H_2 has been destroyed, at which point the temperature of the gas begins to climb steeply. The thermal pressure in the interior of the collapsing core rises rapidly and eventually becomes strong enough to halt the collapse. At the point at which this occurs, the size of the dense core is around 0.1 AU, its mass is around $0.01 M_\odot$ and its mean density is of order 10^{20} cm^{-3} (Yoshida, Omukai & Hernquist, 2008). It is bounded by a strong accretion shock. This pressure-supported, shock-bounded core is a Population III protostar, and its later evolution is discussed in Section 3 below.

2.2 Dark matter annihilation

One complication not accounted for in the models of Pop. III star formation described above is the role that may be played by dark matter annihilation. The nature of dark matter is not yet understood, but one plausible candidate is a weakly interacting massive particle (WIMP) – specifically, the lightest supersymmetric particle predicted in models based on supersymmetry. The simplest supersymmetry models predict that this WIMP has an annihilation cross-section $\langle\sigma v\rangle \sim 3 \times 10^{-26} \text{ cm}^2$, a mass within the range of 50 GeV to 2 TeV, and a cosmological density consistent with the inferred density of dark matter (Spolyar et al., 2008). The rate per unit volume at which energy is produced by dark matter annihilation can be written as $Q_{\text{ann}} = \langle\sigma v\rangle \rho_X^2 / m_X$, where ρ_X is the mass density of dark matter and m_X is the mass of a single dark matter particle. For a plausible particle mass of 100 GeV, and a dark matter density equal to the cosmological background density of dark matter, this expression yields a tiny heating rate, $Q_{\text{ann}} \sim 6 \times 10^{-62} (1+z)^6 \Omega_m^2 h^4 \text{ erg cm}^{-3} \text{ s}^{-1}$, even before one accounts for the fact that much of the annihilation energy is released in the form of energetic neutrinos or gamma-rays that couple only very weakly with the intergalactic gas. WIMP annihilation therefore plays no significant role in the evolution of the intergalactic medium while the WIMPs remain uniformly distributed (Myers & Nusser, 2008). However, the ρ_X^2 density dependence of the heating rate means that it can potentially become significant in regions where the dark matter density is very high.

Spolyar et al. (2008) proposed that one situation in which the heating from dark matter annihilation could become important would occur during the formation of the very first Population III protostars. They assumed that any given star-forming minihalo would form only a single Pop. III protostar, and that this protostar would form at the center of the minihalo. As the gas collapsed at the center of the minihalo, its increasing gravitational influence would bring about a local enhancement of the dark matter density, via a process known as adiabatic contraction. The basic idea underlying this is very simple. For a collisionless particle on a periodic orbit, the quantity $\oint p dq$, where p is the conjugate momentum of coordinate q , is an adiabatic invariant, i.e. a quantity that does not vary when the gravitational potential varies, provided that the rate of change of the potential is sufficiently slow. If p represents

the angular momentum of a particle on a circular orbit of radius r within some spherically symmetric mass distribution, then one can show that the quantity $rM(r)$ is constant for that particle, where $M(r)$ is the mass enclosed within r , so long as this enclosed mass changes on a timescale that is long compared to the orbital period. Spolyar et al. (2008) show that if one starts with a simple NFW profile for the dark matter (Navarro, Frenk & White, 1997) and account for the effects of adiabatic contraction using a simple approach pioneered by Blumenthal et al. (1986), then one finds that for any WIMP mass less than 10 TeV, the effects of dark matter annihilation heating become significant during the collapse of the gas. Spolyar et al. (2008) identify the point at which this occurs by comparing the heating rate due to dark matter annihilation with the H_2 cooling rate. To determine a value for the latter, they make use of the simulation results of Yoshida et al. (2006) and Gao et al. (2007) and measure how the H_2 cooling rate of the gas in the central collapsing core evolves as the collapse proceeds. They show that for a 100 GeV WIMP, heating dominates at gas densities $n > 10^{13} \text{ cm}^{-3}$. Finally, they argue that once dark matter annihilation heating dominates over H_2 cooling, the gravitational collapse of the gas will come to a halt, and hence the gas will never reach protostellar densities. Instead, it will remain quasi-statically supported at a density of roughly 10^{13} cm^{-3} (for a 100 GeV WIMP), with a corresponding size scale of 17 AU, for as long as the dark matter annihilation rate remains large compared to the H_2 cooling rate. As the time required to consume all of the dark matter within a radius of 17 AU may be hundreds of millions of years, the resulting quasi-static gas distribution – dubbed a “dark star” by Spolyar et al. (2008) – could potentially survive for a very long time.

One criticism of the original Spolyar et al. (2008) model is its reliance on the Blumenthal et al. (1986) prescription for describing the effects of the adiabatic contraction of the dark matter. This prescription assumes that all of the dark matter particles move on circular orbits, which is unlikely to be the case in a realistic dark matter minihalo, and concerns have been expressed that it may yield values for the dark matter density after adiabatic contraction that are significantly higher than the true values (see e.g. Gnedin et al., 2004). For this reason, Freese et al. (2009) re-examined this issue using an alternative method for estimating the effects of adiabatic contraction, based on Young (1980). This alternative prescription does account for particles moving on radial orbits, and Freese et al. (2009) show that it predicts dark matter densities that are indeed systematically smaller than those predicted by the Blumenthal et al. (1986) prescription, but only by a factor of two. Freese et al. (2009) therefore conclude that although using the Young (1980) prescription for adiabatic contraction in place of the simpler Blumenthal et al. (1986) prescription will lead to some minor quantitative changes in the predicted outcome, the main qualitative results of the Spolyar et al. (2008) study are insensitive to this change, and one would still expect a “dark star” to form.

Another potential problem with the dark star hypothesis is the fact that it is not at all clear that the collapse of the gas will stop once the dark matter heating rate exceeds the H_2 cooling rate. For one thing, the values for the H_2 cooling rate used by Spolyar et al. (2008) do not account for the effects of the dark matter annihilation heating. If this leads to an increase in temperature, then this will also increase the

H_2 cooling rate, allowing more of the energy produced by dark matter annihilation to be radiated away. It is therefore unlikely that the point in the collapse at which the dark matter annihilation heating rate exceeds the Spolyar et al. estimate for the H_2 cooling rate is marked by any sharp jump in the temperature. Instead, we would expect to find a more gradual temperature increase, at least up until the point at which collisional dissociation of the H_2 starts to occur.

Once H_2 begins to dissociate, this provides another outlet for the energy generated by dark matter annihilation. Spolyar et al. estimate that for a 100 GeV WIMP, the power generated by dark matter annihilation within the central core is $L_{\text{dm}} \sim 140 L_{\odot}$, and the core mass is roughly $0.6 M_{\odot}$. The total energy stored within the core in the form of the binding energy of the H_2 molecules is roughly

$$E_{\text{H}_2, \text{bind}} = 4.48 \text{eV} \times 0.76 \times \frac{0.6 M_{\odot}}{m_{\text{H}_2}} \simeq 2.6 \times 10^{45} \text{ erg}, \quad (56)$$

and the time required for dark matter annihilation to produce this much energy is

$$t_{\text{dis}} = \frac{E_{\text{H}_2, \text{bind}}}{L_{\text{dm}}} \simeq 200 \text{ yr}. \quad (57)$$

For comparison, the free-fall time at this point in the collapse is roughly 15 years. H_2 dissociation will therefore allow the collapse of the gas to continue until either the dark matter heating rate becomes large enough to destroy the H_2 in the core in much less than a dynamical time, or the compressional heating produced during the collapse becomes capable of doing the same job. In either case, it is likely that much higher core densities can be reached than was assumed in the Spolyar et al. study.

A first attempt to hydrodynamically model the formation of a “dark star” while correctly accounting for these thermodynamical effects was made by Ripamonti et al. (2010). They used the 1D, spherically symmetric hydrodynamical code described in Ripamonti et al. (2002) to model the collapse of the gas up to densities of order 10^{15} cm^{-3} for a range of different WIMP masses between 1 GeV and 1 TeV. Adiabatic contraction of the dark matter was modelled using the algorithm described in Gnedin et al. (2004), and the effects of the dark matter annihilation heating and ionization were self-consistently accounted for in the chemical and thermal model. Ripamonti et al. (2010) show that even in the most extreme case that they study, the heating produced by the dark matter appears unable to halt the collapse for an extended period. After the dark matter heating rate exceeds the H_2 cooling rate, dissociation of H_2 in the core accounts for most of the “excess” energy not radiated away by the gas, allowing the collapse to continue. Once the H_2 in the core is exhausted, the temperature rises steeply, very briefly halting the collapse. However, the temperature quickly becomes large enough to allow other cooling mechanisms (e.g. H^- bound-free transitions or Lyman- α emission from atomic hydrogen) to operate, allowing the collapse to restart. Ripamonti et al. (2010) do not find any evidence for the formation of a hydrostatically supported “dark star” up to the highest densities that they study. Confirmation of this result in a 3D treatment of the collapse would be very useful.

2.3 The role of magnetic fields

2.3.1 Initial strength

The majority of the work that has been done on modelling the formation of the first stars assumes that magnetic fields play no role in the process, either because no magnetic field exists at that epoch, or because the strength of any field that does exist is too small to be significant. A number of mechanisms have been suggested that may generate magnetic seed fields during the inflationary epoch, the electroweak phase transition or the QCD phase transition (see Kandus, Kunze & Tsagas, 2011, for a recent comprehensive review). Observational constraints (e.g. Barrow, Ferreira & Silk, 1997; Schleicher, Banerjee & Klessen, 2008) limit the strength of the magnetic field at the epoch of first star formation to no more than about 1 nG (in comoving units), but it is quite possible that any primordial seed field resulting from one of these processes will actually have a much smaller strength.

An alternative source for magnetic fields within the first generation of star-forming minihalos is the so-called Biermann battery effect (Biermann, 1950). In a partially ionized gas in which the gradient of electron density does not perfectly align with the gradient of electron pressure, as can happen if there is a temperature gradient that does not align with the pressure gradient, the magnetic induction equation takes the form

$$\frac{\partial \mathbf{B}}{\partial t} = \nabla \times (\mathbf{v} \times \mathbf{B}) + \frac{c \nabla p_e \times \nabla n_e}{n_e^2 e}, \quad (58)$$

where \mathbf{B} is the magnetic field, \mathbf{v} is the velocity, n_e is the electron density, p_e is the electron pressure, and e is the charge on an electron. In the limit that $B \rightarrow 0$, the first term on the right-hand side of this equation also becomes zero, but the battery term does not. It can therefore act as the source of a magnetic field in a gas that is initially unmagnetized. An early investigation into the effectiveness of the Biermann battery during galaxy formation was made by Kulsrud et al. (1997), who considered the formation of massive galaxies and showed that the Biermann battery could generate a field of strength $B \sim 10^{-21}$ G during their assembly. More recently, Xu et al. (2008) have simulated the action of the Biermann battery during the formation of one of the first star-forming minihalos, finding that it is able to generate initial field strengths of the order of 10^{-18} G during this process.

2.3.2 Amplification

The seed fields generated by the Biermann battery, or by other processes acting in the very early Universe can be significantly amplified by flux-freezing during the gravitational collapse of the gas. If the diffusive timescale associated with ambipolar diffusion or Ohmic diffusion is long compared to the gravitational collapse

timescale, then the magnetic field will be “frozen” to the gas, and will be carried along with it when the gas collapses.

In the optimal case of spherical collapse, perfect flux freezing implies that the field strength evolves with density as $B \propto \rho^{2/3}$, and hence the magnetic pressure $p_{\text{mag}} = B^2/8\pi$ evolves as $p_{\text{mag}} \propto \rho^{4/3}$. In comparison, the thermal pressure p_{therm} evolves as $p_{\text{therm}} \propto \rho T$, and so if the temperature does not vary much during the collapse, the plasma β parameter, $\beta \equiv p_{\text{therm}}/p_{\text{mag}}$, evolves as $\beta \propto \rho^{-1/3}$. Therefore, if the gas is initially dominated by thermal pressure rather than magnetic pressure, it will remain so during much of the collapse, as a large change in the density is necessary to significantly alter β . In the case examined by Xu et al. (2008), the very small initial magnetic field strength means that β is initially very large, and remains so throughout the collapse, implying that the magnetic field never becomes dynamically significant. Moreover, even if we take an initial comoving field strength of 1 nG, comparable to the observational upper limit, at the mean halo density, $\beta \sim 10^4$ (assuming a halo formation redshift $z = 20$ and a virial temperature of 1000 K), and does not become of order unity until very late in the collapse. Furthermore, if the collapse of the gas is not spherical, whether because of the effects of gravitational forces, angular momentum, or the influence of the magnetic field itself, the amplification due to flux freezing and collapse will be less than in the spherical case (see e.g. Machida et al., 2006, who find a somewhat shallower relationship in some of their models).

Therefore, for magnetic fields to play an important role in Pop. III star formation, they must either start with a field strength very close to the observational upper limit, or we must invoke an amplification process that is much more effective than the amplification that occurs due to flux freezing and gravitational collapse. One obvious possibility is amplification via some kind of dynamo process, which could bring about exponential amplification of an initially small seed field. Of particular interest is the small-scale turbulent dynamo (Kraichnan & Nagarajan, 1967; Kazantsev, 1968; Kulsrud & Anderson, 1992). This produces a magnetic field that has no mean flux on the largest scales but that can have substantial mean flux within smaller-scale subregions. The growth rate of the magnetic field due to the turbulent dynamo is closely related to the rate of turnover of the smallest eddies. If the magnetic field is sufficiently small that it does not significantly affect the velocity field of the gas (the kinematic approximation), and if we assume that we are dealing with Kolmogorov turbulence, then Kulsrud & Zweibel (2008) show that the magnetic energy density grows exponentially, and that after a single gravitational free-fall time it is amplified by a factor $\exp(\text{Re}^{1/2})$, where Re is the Reynolds number of the flow. If we assume that the driving scale of the turbulence is comparable to the size of the minihalo, and that the turbulent velocity is of the same order as the sound speed (see e.g. Abel, Bryan & Norman, 2002), then $\text{Re} \sim 10^4\text{--}10^5$, implying that the magnetic field is amplified by an enormous factor during the collapse. In practice, the field will not be amplified by as much as this analysis suggests, as the kinematic approximation will break down once the magnetic energy density becomes comparable to the kinetic energy density on the scale of the smallest eddies. Nevertheless, this sim-

ple treatment implies that the turbulent dynamo can amplify the magnetic field to a strength at which it becomes dynamically important.

Although the importance of dynamo processes during the formation of the first galaxies has been understood for a number of years (see e.g. Pudritz & Silk, 1989; Beck et al., 1994; Kulsrud et al., 1997), they have attracted surprisingly little attention in studies of primordial star formation. Over the past couple of years, however, this has begun to change, with several recent studies focussing on the growth of magnetic fields during the formation of the first stars. The first of these was Schleicher et al. (2010), who studied the effectiveness of the turbulent dynamo during gravitational collapse using a simple one-zone Lagrangian model for the collapsing gas. Their model assumes that turbulence is generated by gravitational collapse on a scale of the order of the Jeans length, and that on smaller scales, the turbulent velocity scales with the length-scale l as $v_{\text{turb}} \propto l^\beta$. Schleicher et al. (2010) study both Kolmogorov turbulence, with $\beta = 1/3$ and Burgers turbulence, with $\beta = 1/2$, and show that in both cases, amplification of a weak initial seed field occurs rapidly, and that the field reaches saturation on all but the largest scales at an early point during the collapse. Because Schleicher et al. (2010) did not solve directly for the fluid velocities, they were unable to model the approach to saturation directly. Instead, they simply followed Subramanian (1998) and assumed that the strength of the saturated field satisfies

$$B_{\text{sat}} = \sqrt{\frac{4\pi\rho v_{\text{turb}}^2}{\text{Rm}_{\text{cr}}}}, \quad (59)$$

where $\text{Rm}_{\text{cr}} \sim 60$ is a critical value of the magnetic Reynolds number, $\text{Rm} = v_{\text{turb}}l/\eta$ (where η is the resistivity), that must be exceeded in order for exponential growth of the field to occur (Subramanian, 1998).

The main weakness of the Schleicher et al. (2010) study lies in the assumptions that it was forced to make about the nature of the turbulent velocity field. Therefore, in a follow-up study, Sur et al. (2010) used high-resolution adaptive mesh refinement simulations to directly follow the coupled evolution of the velocity field and the magnetic field within a 3D collapse model. For their initial conditions, Sur et al. (2010) took a super-critical Bonnor-Ebert sphere (Bonnor, 1956; Ebert, 1955) with a core density $n_c = 10^4 \text{ cm}^{-3}$ and a temperature $T = 300 \text{ K}$. They included initial solid-body rotation, with a rotational energy that was 4% of the total gravitational energy, and a turbulent velocity component with an RMS velocity equal to the sound speed and with an energy spectrum $E(k) \propto k^{-2}$. A weak magnetic field was also included, with an RMS field strength $B_{\text{rms}} = 1 \text{ nG}$, and with the same energy spectrum as the turbulence. For reasons of computational efficiency, Sur et al. (2010) did not follow the thermal and chemical evolution of the gas directly. Instead, they adopted a simple barotropic equation of state, $P \propto \rho^{1.1}$, inspired by the results of previous hydrodynamical models (e.g. Abel, Bryan & Norman, 2002). In view of the sensitivity of the turbulent dynamo to the Reynolds number, and the fact that numerical dissipation on the grid scale limits the size of Re in any 3D numerical simulation to be substantially less than the true physical value, there is good reason to expect that the dynamo amplification rate will be sensitive to the numerical resolution of

the simulation. Sur et al. (2010) therefore focussed on the effects of resolution, performing five different simulations with the same initial conditions, but with different grid refinement criteria. Starting with a model in which the refinement criterion ensures that the Jeans length is always resolved by 8 grid zones, they looked at the effects of increasing this number to 16, 32, 64 and 128 grid zones.

Sur et al. (2010) showed that in the 8 and 16 cell runs, the magnetic field strength increases with density at a slower rate than the $B \propto \rho^{2/3}$ that we would expect simply from flux freezing and roughly spherical collapse, indicating that in these runs, the turbulent dynamo does not operate. Starting with the 32 cell run, however, they found evidence for an increase in B with density that is larger than can be explained simply by compression, which they ascribe to the effects of the turbulent dynamo. They showed that as the number of grid zones used to resolve the Jeans length is increased, the rate at which the field grows also increases, and there is no sign of convergence at even their highest resolution. This resolution dependence explains why the earlier study of Xu et al. (2008) found no evidence for dynamo amplification, as their study used only 16 grid zones per Jeans length.

More recently, Federrath et al. (2011) have re-examined this issue of resolution dependence, and have shown that when the number of grid zones per Jeans length is small, the amount of turbulent energy on small scales is also significantly underestimated. The reason for this is the same as the reason for the non-operation of the turbulent dynamo: the effective Reynolds number is too small. Federrath et al. (2011) show that in gravitationally collapsing regions that undergo adaptive mesh refinement, the effective Reynolds number scales with the number of grid zones per Jeans length as $\text{Re}_{\text{eff}} = (N/2)^{4/3}$. Furthermore, an effective Reynolds number $\text{Re}_{\text{eff}} \sim 40$ is required in order for the turbulent dynamo to operate, implying that one needs $N \sim 30$ or more zones per Jeans length in order to begin resolving it, in agreement with the findings of Sur et al. (2010). It should also be noted that the operation of the turbulent dynamo in simulations of turbulence without self-gravity requires a similar minimum value for the Reynolds number (Haugen, Brandenburg & Dobler, 2004).

Together, these studies support the view that amplification of a weak initial magnetic field by the turbulent dynamo may indeed have occurred within the first star-forming minihalos. However, a number of important issues remain to be addressed. First, the three-dimensional studies carried out so far all adopt a simple barotropic equation of state, rather than solving self-consistently for the thermal evolution of the gas. This is a useful simplifying assumption, but may lead to incorrect dynamical behaviour, as one misses any effects due to thermal instabilities, or the thermal inertia of the gas (i.e. the fact that the cooling time is typically comparable in size to the dynamical time). Work is currently in progress to re-run some of these models with a more realistic treatment of the thermodynamics and chemistry in order to explore the effect that this has on the degree of amplification (T. Peters, private communication). Second, it will clearly be important to perform similar studies using more realistic initial conditions for the gas. Of particular concern is whether the turbulence that is generated during the gravitational collapse of gas within a primordial minihalo is similar in nature to that studied in these more idealized calculations,

and if not, what influence this has on the amplification of the field. Finally, and most importantly, there is the issue of the level at which the field saturates. Exponential amplification of the field by the small-scale dynamo will occur only while the kinematic approximation holds, i.e. while the energy stored in the magnetic field is much smaller than the energy stored in the small-scale turbulent motions. Once the field becomes large, the Lorentz force that it exerts on the gas will act to resist further folding and amplification of the field. In addition, the dissipation of magnetic energy by Ohmic diffusion and ambipolar diffusion will grow increasingly important. However, it remains unclear which of these effects will be the most important for limiting the growth of the magnetic field in dense primordial gas.

2.3.3 Consequences

If a strong magnetic field can be generated by dynamo amplification, then it will affect both the thermal and the dynamical evolution of the gas. The possible dynamical effects of a strong magnetic field have been investigated by Machida et al. (2006, 2008). In a preliminary study, Machida et al. (2006) used nested-grid simulations to investigate the influence of a magnetic field on the collapse of a small, slowly-rotating primordial gas cloud. For their initial conditions, they used a supercritical Bonnor-Ebert sphere with mass $5.1 \times 10^4 M_\odot$, radius 6.6 pc, central density $n_c = 10^3 \text{ cm}^{-3}$ and an initial temperature of 250 K. They assumed that this cloud was in solid body rotation with angular velocity Ω_0 and that it was threaded by a uniform magnetic field oriented parallel to the rotation axis, with an initial field strength B_0 . They performed simulations with several different values of Ω_0 and B_0 , with the former ranging from 10^{-17} s^{-1} to $3.3 \times 10^{-16} \text{ s}^{-1}$, and the latter from 10^{-9} G to 10^{-6} G . To treat the thermal evolution of the gas, they used a barotropic equation of state, based on the one-zone results of Omukai et al. (2005).

Machida et al. (2006) used this numerical setup to follow the collapse of the gas down to scales of the order of the protostellar radius. They showed that the magnetic field was significantly amplified by compression and flux freezing during the collapse, reaching strengths of order 6×10^5 – $6 \times 10^6 \text{ G}$ on the scale of the protostar. A very compact disk with a radius of few R_\odot formed around the protostar, and in models with initial field strength $B_0 > 10^{-9} \text{ G}$, the magnetic field became strong enough to drive a hydromagnetic disk wind that ejected roughly 10% of the infalling gas. Numerical limitations (discussed in Section 3 below) prevented Machida et al. (2006) from following the evolution of the system for longer than a few days after the formation of the protostar, and so it remains unclear whether an outflow would eventually be generated in the 10^{-9} G case, and whether the outflows continue to be driven as the protostar and disk both grow to much larger masses.

In a follow-up study, Machida et al. (2008) used a similar numerical setup, but examined a much broader range of values for $\beta_0 (\equiv E_{\text{rot}}/|E_{\text{grav}}|)$, the ratio of the initial rotational energy to the initial gravitational energy, and $\gamma_0 (\equiv E_{\text{mag}}/|E_{\text{grav}}|)$, the ratio of the initial magnetic energy to the initial gravitational energy. They found that the outcomes of the simulations could be classified into two main groupings.

Clouds with $\beta_0 > \gamma_0$, i.e. ones which were rotationally dominated, formed a prominent disk during the collapse that then fragmented into a binary or higher order multiple system. In these simulations, no jets were seen (with the exception of a couple of model in which $\beta_0 \sim \gamma_0$). On the other hand, when $\beta_0 < \gamma_0$, i.e. when the cloud was magnetically dominated, the disk that formed was much less prominent and did not fragment, but instead an outflow was driven that removed of order 10% of the gas that reached the disk, as in the Machida et al. (2006) study.

These results support the idea that outflows will be a natural consequence of the generation of strong magnetic fields during Population III star formation. However, it is important to note that the Machida et al. (2006, 2008) simulations only model the very earliest stages of outflow driving, on a timescale $t \ll 1$ yr. The evolution of outflows on much longer timescales, and their influence on the infalling gas have not yet been studied in detail, and it is unclear to what extent one can safely extrapolate from the very limited period that has been studied.

A strong magnetic field could also have a direct impact on the thermal evolution of the gas, through the heating arising from ambipolar diffusion. The effects of this process in gravitationally collapsing gas within the first star-forming minihalos have been investigated by Schleicher et al. (2009) using a simple one-zone treatment of the gas. They assume that in the absence of ambipolar diffusion, the magnetic field strength would evolve as $B \propto \rho^\alpha$, where $\alpha = 0.57(M_J/M_{J,\text{mag}})^{0.0116}$ and $M_{J,\text{mag}}$ is the magnetic Jeans mass (i.e. the minimum mass that a perturbation must have in order to be unstable to its own self-gravity when support against collapse is provided by a magnetic field, rather than by thermal pressure). This expression for α is an empirical fitting formula derived by Schleicher et al. (2009) from the results of Machida et al. (2006). In their treatment of the evolution of B within their one-zone models, Schleicher et al. (2009) also account for the loss of magnetic energy through ambipolar diffusion.

Another important simplification made in the Schleicher et al. (2009) model is the replacement of the full expression for the ambipolar diffusion heating rate (Pinto et al., 2008)

$$L_{\text{AD}} = \frac{\eta_{\text{AD}}}{4\pi} \frac{|(\nabla \times \mathbf{B}) \times \mathbf{B}|^2}{B^2}, \quad (60)$$

where $B = |\mathbf{B}|$ and η_{AD} is the ambipolar diffusion resistivity, with the simpler approximation

$$L_{\text{AD}} = \frac{\eta_{\text{AD}}}{4\pi} \frac{B^2}{L_B}, \quad (61)$$

where L_B is the coherence length of the magnetic field.

Schleicher et al. (2009) show that if the initial field strength is less than 0.01 nG (comoving), then ambipolar diffusion heating has almost no effect on the thermal evolution of the gas. For stronger fields, ambipolar diffusion heating leads to an increase in the gas temperature at densities between $n \sim 10^4 \text{ cm}^{-3}$ and $n \sim 10^{10} \text{ cm}^{-3}$, amounting to as much as a factor of three at $n \sim 10^8 \text{ cm}^{-3}$. However, at higher densities, three-body H_2 formation heating becomes a more important heat source than ambipolar diffusion, meaning that the temperature evolution becomes largely

independent of the magnetic field strength once again. Schleicher et al. (2009) did not examine initial field strengths larger than 1 comoving nG, as these are ruled out by observational constraints, but if one considers the effects of the turbulent dynamo acting during the collapse, then it is possible that much larger fields could be generated on smaller scales, and it would be useful to revisit this issue and examine whether ambipolar diffusion heating from these smaller-scale fields can significantly affect the collapse of the gas.

Finally, one important caveat to bear in mind regarding the Machida et al. (2006, 2008) and Schleicher et al. (2009) simulations is the fact that they adopt a correlated initial magnetic field, while the field generated by the turbulent dynamo will have little or no correlation on large scales (Maron, Cowley & McWilliams, 2004). The extent to which the dynamical and thermal effects of this uncorrelated field will be the same as those of a correlated field is unclear. Further investigation of this issue would be very valuable.

3 Evolution after the formation of the first protostar

As we saw in the last section, when it comes to the formation of the very first Population III protostar, there is broad agreement on the details of the process, with different groups, who use different numerical approaches, finding results that are in good qualitative agreement with each other. Some quantitative disagreements still exist (see e.g. Turk et al., 2011), but it is unclear to what extent these reflect real differences between numerical approaches as opposed to natural variation in the details of the collapse. The main uncertainties in this phase stem from uncertainties in the input physics, such as whether magnetic fields can become amplified to dynamically significant levels during the collapse, or whether dark matter annihilation significantly affects the outcome.

Once we move on to considering the evolution of the gas within star-forming minihalos *after* the formation of the first protostar, the situation becomes much less clear. The fundamental problem stems from the fact that although we can follow the gravitational collapse of the primordial gas down to scales as small as the protostellar radius (see e.g. Yoshida, Omukai & Hernquist, 2008), the numerical timestep in an explicit hydrodynamical code becomes extremely short during this process. This is a consequence of the Courant condition, which states that for such a code to be numerically stable, the timestep must satisfy

$$\Delta t \leq \frac{\Delta x}{c_s}, \quad (62)$$

where Δx is the size of the smallest resolution element, and c_s is the sound speed of the gas.

The Courant condition implies that if we take a value of Δx small enough to adequately resolve the structure of the protostar and the gas immediately surrounding it (e.g. $\Delta x = 1R_\odot$), then the required timestep will be extremely small: $\Delta t \leq 7 \times 10^4$ s

for $\Delta x = 1R_{\odot}$ and a sound speed of 10 km s^{-1} . This means that if we want to follow the later evolution of the protostar and the surrounding gas over a timescale of thousands of years in order to see how it grows in mass prior to reaching the main sequence, then we must use a very large number of timesteps: our simple estimate above yields a number of the order of a million. In practice, the computational expense of doing this within a three-dimensional hydrodynamical code is prohibitively large, meaning that it has so far proved impossible to study the evolution of the gas in this fashion.

Efforts to surmount this difficulty typically follow one of two approaches. One approach is simply to halt the numerical simulation at the point at which the Courant timestep becomes prohibitively small, and to model the later evolution of the protostar using a semi-analytical, or one-dimensional, fully numerical treatment. To do this, it is necessary to make some assumption about the behaviour of the gas surrounding the protostar. In general, models of this type assume that the gas does not fragment and form additional protostars, but instead is simply accreted by the existing protostar, either directly or via a protostellar accretion disk. The results obtained using this approach – what we afterwards refer to as the “smooth accretion model” – are discussed in Section 3.1 below.

The other approach that can be used to study the further evolution of the gas surrounding the protostar makes use of a technique developed for studies of contemporary star formation, which face a similar problem on protostellar scales. Gravitationally bound regions of gas that become smaller than some pre-selected size scale are replaced by what are usually termed sink particles (see e.g. Bate, Bonnell & Price, 1995). These particles can accrete gas from their surroundings and continue to interact gravitationally with the surrounding gas, but allow one to neglect the very small-scale hydrodynamical flows that would otherwise force one to take very small numerical timesteps owing to the Courant condition. The great advantage of the sink particle technique is that one need make no assumption about the dynamical evolution of the gas surrounding the protostar on scales much larger than the effective size of the sink particle (the so-called accretion radius, discussed in more detail below), as one can simply continue to model this using the same numerical techniques as were used to model the initial gravitational collapse. The main disadvantage of the technique is that, strictly speaking, it represents an *ad hoc* modification of the fluid equations, with consequences that may not be entirely straightforward to predict. The modification to the solution caused by replacing dense gas with sink particles is unlikely to significantly affect the evolution of the gas on scales that are much larger than the accretion radius, but will clearly have an effect on the flow on scales close to the accretion radius. In addition, the common strategy of treating sink particles as point masses may not be appropriate when dealing with close encounters between sinks, as one misses the tidal forces acting between the gas clumps represented by the sinks.

Although sink particles have been used in studies of Population III star formation for over a decade, simulations using the correct initial conditions, and with sufficient spatial resolution and mass resolution to capture the details of the gas flow on scales close to those of individual protostars have only recently become possible. These

simulations show that, contrary to the assumption made in the smooth accretion model, the gas generally fragments, rather than simply accreting onto a single, central protostar. The results obtained from studies using sink particles – afterwards referred to as the “fragmentation model” for Population III star formation – are discussed in Section 3.2 below.

3.1 The smooth accretion model

3.1.1 Determining the accretion rate

As we have already discussed above, at the point at which the protostar forms, its mass is very small ($M \sim 0.01 M_{\odot}$; see Yoshida, Omukai & Hernquist 2008), but it is surrounded by an infalling envelope of gas containing tens or hundreds of solar masses. If we assume that the gas in this infalling envelope does not undergo gravitational fragmentation, then it has only two possible fates – it must either be accreted by the central protostar (or protostellar binary; see e.g. Turk, Abel & O’Shea 2009), or it must be prevented from accreting, and possibly expelled from the immediate vicinity of the protostar, by some form of protostellar feedback. This means that the mass of the protostar at the point at which it forms has very little to do with its final mass. To determine the size of the latter, we must understand the rate at which gas is accreted by the protostar, and how this process is affected by protostellar feedback.

Since protostellar feedback involves a number of different processes, many of which are complicated to model, it is easiest to start by considering models in which feedback effects are not included. As feedback acts to reduce the accretion rate, models of this type allow us to place an upper limit on the final mass of the Pop. III star.

A useful starting point is a simple dimensional analysis. Suppose that the protostar is embedded in a gravitationally unstable cloud of mass M and mean density $\langle \rho \rangle$, and that the protostellar mass $M_* \ll M$, so that its gravity is negligible in comparison to the self-gravity of the cloud. The timescale on which the gas cloud will undergo gravitational collapse and be accreted by the protostar is simply the free-fall collapse time, $t_{\text{ff}} = \sqrt{3\pi/32G\langle \rho \rangle}$. Therefore, the time-averaged accretion rate will be given approximately by

$$\dot{M}_{\text{est}} \sim \frac{M}{t_{\text{ff}}} \sim M \sqrt{G\langle \rho \rangle}. \quad (63)$$

If the gas cloud were highly gravitationally unstable, then it would fragment rather than accreting onto a single object, so let us assume that it is only marginally unstable, i.e. that $M \sim M_{\text{J}}$. In that case, since $M_{\text{J}} \sim c_s^3 G^{-3/2} \rho^{-1/2}$, we can write our estimate of the time-averaged accretion rate as

$$\dot{M}_{\text{est}} \sim M_{\text{J}} \sqrt{G\langle \rho \rangle}, \quad (64)$$

$$\sim \frac{c_s^3}{G}. \quad (65)$$

We therefore find that the characteristic accretion rate scales as the cube of the sound speed. Moreover, since $c_s \propto T^{1/2}$, this implies that the accretion rate scales with temperature as $\dot{M} \propto T^{3/2}$.

This is an important result, because as we have already seen, the characteristic temperature of the dense, star-forming gas in a primordial minihalo is of the order of 1000 K, far larger than the 10 K temperatures found within prestellar cores in local regions of star formation (see e.g. Bergin & Tafalla, 2007). Our simple scaling argument therefore tells us that we will be dealing with far higher accretion rates in the Population III case than we are used to from studies of local star formation.

If we want to improve on this simple scaling argument and derive a more accurate figure for the accretion rate, then there are three main ways in which we can go about it. One possible approach is to construct a simplified model for the collapsing protostellar core from which an approximation to the true accretion rate can be derived analytically (or with only minor use of numerical calculations). For example, if we assume that the protostellar core is isothermal and spherically symmetric, then there is a whole family of similarity solutions that could potentially be used to describe the collapse (Hunter, 1977; Whitworth & Summers, 1985), including the familiar Larson-Penston solution (Larson, 1969; Penston, 1969), or the Shu solution (Shu, 1977).

An example of this approach is given in Omukai & Nishi (1998). These authors used a spherically symmetric Lagrangian hydrodynamical code to simulate the formation of a Population III protostar, and found that prior to core formation, the gravitational collapse of the gas could be well described with a Larson-Penston similarity solution, with an entropy parameter $K = p/\rho^\gamma = 4.2 \times 10^{11}$ (in cgs units) and an effective adiabatic index $\gamma_{\text{eff}} = 1.09$. Omukai & Nishi (1998) were unable to continue their numerical study past the point at which the protostar formed, for the reasons addressed above, but assumed that the same similarity solution would continue to apply. By making this assumption, they were therefore able to derive the following accretion rate for the protostar

$$\dot{M} = 8.3 \times 10^{-2} \left(\frac{t}{1 \text{ yr}} \right)^{-0.27} M_\odot \text{ yr}^{-1}. \quad (66)$$

In a similar study, using a more sophisticated treatment of the microphysics of the collapsing gas, Ripamonti et al. (2002) also found that the initial flow was well described as a Larson-Penston similarity solution, but derived a different accretion rate

$$\dot{M} = 6.0 \times 10^{-2} \left(\frac{t}{1 \text{ yr}} \right)^{-0.343} M_\odot \text{ yr}^{-1}. \quad (67)$$

Another example of this approach comes from Tan & McKee (2004). They model the accretion flow onto a Pop. III protostar as a spherical, isentropic polytrope, and derive an accretion rate that is a function of three parameters: the entropy parameter

K , the polytropic index γ_p (which, for an isentropic flow, is equal to the adiabatic index γ), and ϕ_* , a numeric parameter of order unity, which is related to the initial conditions of the flow. Tan & McKee (2004) use the results of Omukai & Nishi (1998) and Ripamonti et al. (2002) to argue that $\gamma_p = 1.1$, and use the 3D simulation results of Abel, Bryan & Norman (2002) to set the other two parameters to $\phi_* = 1.43$ and $K = 1.88 \times 10^{12} K'$ (in cgs units), where

$$K' = \left(\frac{T_{\text{eff}}}{300 \text{ K}} \right) \left(\frac{n_{\text{H}}}{10^4 \text{ cm}^{-3}} \right)^{-0.1}, \quad (68)$$

and where the effective temperature $T_{\text{eff}} = P_{\text{eff}}/(nk)$ accounts for the contribution made to the pressure by small-scale, subsonic turbulence in addition to the standard thermal pressure. Based on this, they then derive the following rate for the accretion of gas onto the protostar and its associated accretion disk

$$\dot{M} = 7.0 \times 10^{-2} K'^{3/2} \left(\frac{t}{1 \text{ yr}} \right)^{-0.30} \text{ M}_{\odot} \text{ yr}^{-1}. \quad (69)$$

This can be directly compared to the other determinations of \dot{M} if we assume that all of the gas reaching the accretion disk is eventually accreted by the star, which is a reasonable assumption for models that do not include the effects of gravitational fragmentation or protostellar feedback.

Instead of using simulation results to select a particular collapse model (e.g. Larson-Penston collapse) and then calculating \dot{M} from the model, the second main approach used to determine \dot{M} attempts to infer it from the state of the gas in the simulation at the point at which the protostar forms, using the information that the simulation provides on the density and velocity distributions of the gas. This approach was pioneered by Abel, Bryan & Norman (2002), who considered two simple models for the time taken for a given fluid element to accrete onto the central protostar. In the first of these models, they assumed that the time taken for the gas within a spherically-averaged shell of radius r to accrete onto the protostar was given by the ratio between the mass enclosed within the shell, $M(r)$, and the rate at which gas was flowing inward at that radius, i.e.

$$t_{\text{acc}} = \frac{M(r)}{4\pi r^2 \rho(r) |v_r(r)|}, \quad (70)$$

where $\rho(r)$ and $v_r(r)$ are the spherically-averaged density and radial velocity in the shell. In the second model for t_{acc} , they used an even simpler approximation, setting t_{acc} to the time that it would take for the gas to reach the protostar if it merely maintained its current radial velocity, i.e.

$$t_{\text{acc}} = \frac{r}{v_r}. \quad (71)$$

Abel, Bryan & Norman (2002) show that other than at the very earliest times, these two approaches yield very similar values for t_{acc} , and hence very similar values

for the accretion rate. This strategy has subsequently been used by many other authors to derive predicted protostellar accretion rates from their simulations (see e.g. Yoshida et al., 2006; O’Shea & Norman, 2007; McGreer & Bryan, 2008; Turk et al., 2011). Of particular note is the study by O’Shea & Norman (2007), who perform multiple simulations of Population III star formation using different random realizations of the cosmological density field. They find that minihalos assembling at higher redshifts form more H_2 than those assembling at lower redshifts, owing to the higher mean density of the virialized gas in the high redshift minihalos. They show that in their simulations, this leads to the gas at densities $n > 10^4 \text{ cm}^{-3}$ having significant differences in its mean temperature in the different halos. In the most H_2 -rich minihalos, the dense gas can be as cold as 200 K, while in the minihalos with the least H_2 , it can be as high as 1000 K. As a result, the predicted accretion rates for the different minihalos span more than an order of magnitude, thanks to the strong scaling of \dot{M} with temperature. Unfortunately, it is necessary to treat these results with a degree of caution, as the O’Shea & Norman (2007) simulations did not include the effect of three-body H_2 formation heating, which is known to have a significant influence on the temperature of the dense gas. It is unclear whether simulations that include this effect would produce dense gas with such a wide range of temperatures and accretion rates, although a study that is currently being carried out by Turk and collaborators should address this issue in the near future (M. Turk, private communication).

The third main approach used to determine the accretion rate involves measuring it directly in a simulation of the later evolution of the gas around the protostar. If we replace the protostar with a sink particle, then we can measure \dot{M} simply by measuring the rate at which the sink particle mass increases. This approach was first used by Bromm & Loeb (2004), in a study of Population III star formation in which a sink particle was created once the gas density exceeded a threshold value $n_{\text{th}} = 10^{12} \text{ cm}^{-3}$ (we will have more to say about this study below). Bromm & Loeb (2004) showed that the rate at which gas was accreted by the sink particle could be approximated as a broken power-law

$$\dot{M} = \begin{cases} 5.6 \times 10^{-2} \left(\frac{t}{\text{lyr}}\right)^{-0.25} \text{ M}_{\odot} \text{ yr}^{-1} & t \leq 10^3 \text{ yr} \\ 6.3 \times 10^{-1} \left(\frac{t}{\text{lyr}}\right)^{-0.6} \text{ M}_{\odot} \text{ yr}^{-1} & t > 10^3 \text{ yr} \end{cases} \quad (72)$$

for times $t < 10^4 \text{ yr}$. Bromm & Loeb halted their simulation at $t \sim 10^4 \text{ yr}$ and hence could not directly measure the evolution of \dot{M} at later times, although they did consider what the final mass of the protostar would be if one simply extrapolated Equation 72 over the three million year lifetime of a massive star.

Accretion rates have also been measured using the sink particle technique in the group of simulations carried out by Clark et al. (2011a,b), Greif et al. (2011a) and Smith et al. (2011) that find evidence for fragmentation of the gas (see Section 3.2 below). The accretion rates onto the individual sinks show a considerable degree of variability in these calculations, but the *total* accretion rate, i.e. the rate of change of

the sum of all of the sink particle masses, evolves more smoothly with time, and is of a similar order of magnitude to the other estimates plotted above.

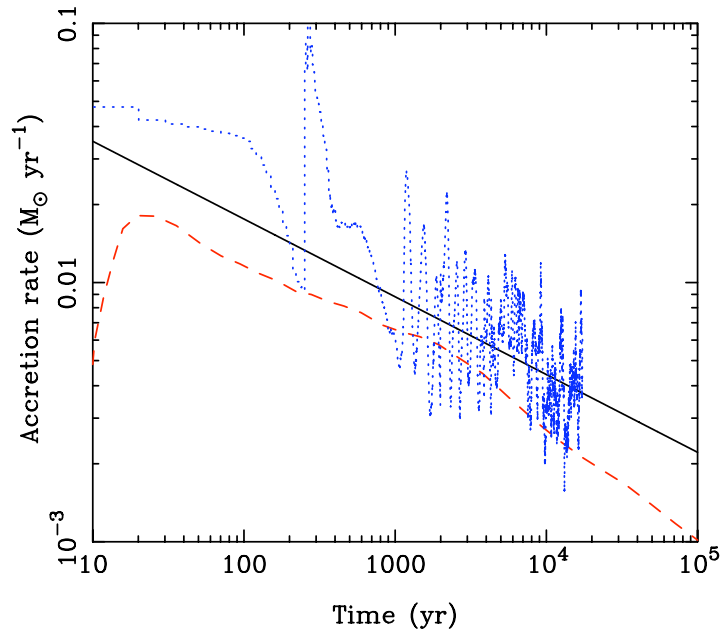


Fig. 3 Three different estimates for the accretion rate onto a Pop. III protostar, taken from Tan & McKee (2004; solid line), Turk et al. (2011; dashed line) and Smith et al. (2011; dotted line), as described in the text. Results from the Smith et al. (2011) simulation are only plotted for the period covered by the simulation, i.e. $t < 2 \times 10^4$ yr.

In Figure 3 we compare several of these different estimates for the accretion rate. We plot three examples, derived using different techniques: a rate based on the Tan & McKee (2004) formalism, computed assuming that $K' = 1$; a rate inferred from the results of one of the adaptive mesh refinement simulations presented in Turk et al. (2011) – specifically, the simulation that was run using the Palla, Salpeter, & Stahler (1983) rate coefficient for three-body H_2 formation; and a rate measured using sink particles, taken from Smith et al. (2011).

At very early times ($t < 100$ yr), the three different techniques yield rather different estimates for \dot{M} , but this is primarily a consequence of the limited resolution of the numerical simulations. At later times, we see that both the Tan & McKee (2004) formalism and the Turk et al. (2011) simulation predict a similar form for the accretion rate, but disagree by about a factor of two on the normalization, which may simply indicate that our adopted value of K' is slightly too large. We also see the

same general trend in the Smith et al. (2011) results, but in this case there is considerable and rapid variation in \dot{M} with time. This is a result of the fragmentation of the gas in this simulation, which produces a set of sink particles that undergo chaotic N-body interactions (see Section 3.2 below). A similar effect is seen in simulations of protostellar accretion in present-day star-forming regions (see e.g. Stamatellos, Whitworth & Hubber, 2011).

Regardless of whether \dot{M} varies smoothly or erratically with time, one fact that is clear from Figure 3 is that the protostellar accretion rate remains very large for a considerable time. This implies that the total mass of gas that is converted to stars can become fairly large after a relatively short time. For example, if we take the Tan & McKee (2004) estimate with $K' = 1$ as a guide, then we find that the total mass in stars increases with time as:

$$M_* = 0.1 \left(\frac{t}{1 \text{ yr}} \right)^{0.70} M_\odot \text{ yr}^{-1}. \quad (73)$$

This means that after 5×10^4 yr (the Kelvin-Helmholtz relaxation time for a $100 M_\odot$ star), we have $M_* \simeq 195 M_\odot$, while after 2×10^6 yr (the typical lifetime for an O star), we have $M_* \simeq 2575 M_\odot$. Therefore, if the gas does not fragment and protostellar feedback is ineffective, one is led to the prediction that the resulting Population III star will be extremely massive. In practice, the gas probably does fragment (see Section 3.2 below), and protostellar feedback cannot be completely ignored, but even so, we would expect to be able to form massive Population III stars relatively easily.

Finally, it should be noted that so far we have considered accretion only in the standard H_2 -dominated case, i.e. in a minihalo with a minimum gas temperature of around 200 K. In minihalos that reach much lower temperatures through HD cooling, the predicted accretion rates are smaller, as one would expect from the simple dimensional analysis given at the start of this section. For example, if one uses the Tan & McKee (2004) formalism to estimate the accretion rate, then Equation 69 still applies, but the value of K' is significantly smaller. Taking $n = 10^6 \text{ cm}^{-3}$ and $T_{\text{eff}} = 150 \text{ K}$ as plausible values to substitute into Equation 68, we find that $K' \simeq 0.3$, and hence the predicted accretion rate is roughly a factor of six smaller than in the H_2 -dominated case. Values estimated from numerical simulations using the Abel, Bryan & Norman (2002) approach agree fairly well with this simple estimate (see e.g. Yoshida, Omukai & Hernquist, 2007; McGreer & Bryan, 2008).

3.1.2 Protostellar structure and evolution

Having established how quickly gas will be accreted by the protostar in the absence of feedback, the obvious next step is to examine how this will be modified by protostellar feedback. Before doing this, however, we must first spend a little time discussing what is known about the internal structure of Population III protostars, and how this evolves with time. This is important if we want to understand how the

radius and luminosity of a given Pop. III protostar evolve, and these quantities are obviously of great importance when determining the influence of that protostar on the surrounding gas.

The internal structure of a Pop. III protostar, and how this evolves as the protostar ages and accretes matter from its surroundings was first studied in detail by Stahler, Palla & Salpeter (1986a,b). They assume that the accretion process can be treated as a series of quasi-steady-state accretion flows onto a hydrostatic core, which is bounded by a strongly radiating accretion shock. Within the core, the standard stellar structure equations are solved. Outside of the core, the treatment depends on the optical depth of the gas. If the gas is optically thin to the radiation from the accretion shock, then the accretion flow is assumed to be in free-fall. Otherwise, a more detailed calculation is made that incorporates the effects of the radiation force on the infalling gas. The accretion shock itself is treated as a simple discontinuity.

In their initial study, Stahler, Palla & Salpeter (1986a) began with a core mass of $0.01 M_{\odot}$ and followed the growth of the protostar until its mass reached $10.5 M_{\odot}$. They assumed a constant accretion rate $\dot{M} = 4.41 \times 10^{-3} M_{\odot} \text{ yr}^{-1}$, and found that for this choice of accretion rate, the evolution of the protostar could be divided into three qualitatively distinct phases.

In the first phase, which lasts until the protostellar mass $M_* = 0.1 M_{\odot}$, the protostar relaxes from its initial entropy profile into one consistent with the selected accretion rate. Stahler, Palla & Salpeter (1986a) dub this a ‘decay of transients’ phase, and the fact that it quickly comes to an end shows that although the initial conditions used in the Stahler, Palla & Salpeter (1986a) study are probably incorrect in detail, the flow soon loses all memory of them, and therefore any inaccuracy at this stage is unlikely to affect the later results.

Once the initial transients have died away, the protostar enters the second phase of its evolution. During this phase, its central temperature remains low ($T_c \sim 10^5 \text{ K}$), resulting in a high interior opacity and hence a low interior luminosity. Consequently, the evolution of the core during this phase is almost adiabatic; although the core continues to gradually contract, this contraction does not lead to any increase in the central entropy. Since the postshock entropy increases over time due to the increasing strength of the accretion shock (which is itself a natural result of the increasing protostellar mass), the core develops an off-centre distribution of entropy and temperature.

The gas surrounding the accretion shock remains optically thick throughout this period. This is a direct result of the high accretion rate, which produces a highly luminous accretion shock. This produces sufficient radiation to partially ionize the preshock gas in the vicinity of the shock, creating a structure known as a radiative precursor. The H^- opacity of the dense, partially ionized gas in this radiative precursor is more than sufficient to make it optically thick. Stahler, Palla & Salpeter show that the core radius during this period evolves as

$$R_* = 48.1 \left(\frac{M_*}{M_{\odot}} \right)^{0.27} \left(\frac{\dot{M}}{\dot{M}_0} \right)^{0.41} R_{\odot}, \quad (74)$$

where $\dot{M}_0 = 4.41 \times 10^{-3} M_\odot \text{ yr}^{-1}$, while the photospheric radius evolves as

$$R_p = 66.8 \left(\frac{M_*}{M_\odot} \right)^{0.27} \left(\frac{\dot{M}}{\dot{M}_0} \right)^{0.41} R_\odot, \quad (75)$$

so $R_p > R_*$ throughout. The strong H^- opacity also keeps the photospheric temperature low ($T_p \sim 6000 \text{ K}$), which prevents the protostar from being able to ionize material outside of its photosphere.

This near-adiabatic accretion phase comes to an end once the cooling time of the core, given approximately by the Kelvin-Helmholtz timescale

$$t_{\text{KH}} = \frac{GM_*^2}{R_* L_*}, \quad (76)$$

becomes comparable to the accretion timescale $t_{\text{acc}} = M_*/\dot{M}$. This occurs for a core mass $M \sim 1 M_\odot$, and results in the core entering a phase of homologous collapse, while energy and entropy are transferred outwards in the form of a ‘luminosity wave’. The radial position of the luminosity peak moves outwards towards the accretion shock, reaching it at about the time that the core mass has reached $8 M_\odot$. This results in a rapid swelling of the outermost layers, which weakens the accretion shock and leads to it becoming optically thin. Stahler, Palla & Salpeter terminate their simulation shortly afterwards, once the core mass has reached $10.5 M_\odot$.

Stahler, Palla & Salpeter (1986b) simulate the later stages of the evolution of a primordial protostar. Their initial protostellar core has a mass of $5 M_\odot$, and they evolve this core forward in time, assuming that no further accretion occurs (i.e. the protostellar mass remains fixed at $5 M_\odot$). They find that deuterium burning within the protostar begins after only 6000 years, but that hydrogen ignition does not occur until $t = 2 \times 10^5 \text{ yr}$, and the protostar does not reach the zero-age main sequence (ZAMS) until $t \sim 10^6 \text{ yr}$.

An improved treatment of the later stages of the evolution of the protostar was made by Omukai & Palla (2001). They used a very similar setup to that in Stahler, Palla & Salpeter (1986a), albeit with improved zero metallicity opacities, and adopted the same constant accretion rate, $\dot{M} = 4.41 \times 10^{-3} M_\odot \text{ yr}^{-1}$. However, unlike Stahler, Palla & Salpeter (1986a), they initialized their simulation at the point at which the core mass was $M = 8 M_\odot$, but did not halt the simulation once the core had grown to $10.5 M_\odot$. Instead, they continued to follow the growth of the protostar until well after hydrogen ignition. They found that deuterium burning within the core began once the core mass was $12 M_\odot$ (corresponding to a time $t = 1000 \text{ yr}$ after the beginning of the simulation, given the assumed accretion rate), and that it was complete by the time the mass had reached $30 M_\odot$ (corresponding to $t = 5000 \text{ yr}$). Hydrogen ignition followed roughly 11000 years later, at $t = 1.6 \times 10^4 \text{ yr}$ after the beginning of the simulation, at which time the mass of the protostar was $80 M_\odot$. At this point, the internal luminosity of the protostar is very close to the Eddington value, which leads to the outer layers of the protostar developing oscillatory behaviour: the high luminosity leads to expansion, the expansion causes the accretion

luminosity to drop, the reduced luminosity can no longer maintain the expansion, leading to contraction of the core, and the contraction raises the accretion luminosity, allowing the whole cycle to begin again. Finally, once the core mass reaches $300 M_{\odot}$, at $t \sim 6.6 \times 10^4$ yr, the contribution of nuclear burning to the protostellar luminosity becomes large enough to drive a final phase of expansion that is strong enough to terminate accretion onto the protostar. Omukai & Palla (2001) halt their simulation at this point.

In a follow-up study using a similar spherically-symmetric setup, Omukai & Palla (2003) performed the same analysis for a range of different values of \dot{M} , looking at models with $\dot{M} = (0.25, 0.5, 1.0, 2.0) \times \dot{M}_{\text{fid}}$ (where \dot{M}_{fid} was the rate adopted by Stahler, Palla & Salpeter 1986a and Omukai & Palla 2001), as well as a model using the time-dependent accretion rate predicted by Abel, Bryan & Norman (2002). The earliest stages of protostellar evolution are qualitatively the same in all of these models: we see again the same sequence of adiabatic growth, propagation of a luminosity wave that triggers expansion of the outer layers, and then rapid contraction. Although some quantitative differences are apparent, significant differences in behaviour do not occur until the end of the contraction phase. At this point, the further evolution of the protostar is governed by the size of the accretion rate. For accretion rates greater than some critical value \dot{M}_{crit} , the luminosity of the protostar becomes large enough to halt the accretion. On the other hand, for $\dot{M} < \dot{M}_{\text{crit}}$, the lower accretion luminosity means that the total luminosity of the protostar remains below L_{Edd} , and accretion continues unabated.

Omukai & Palla (2003) solve for \dot{M}_{crit} by equating the total luminosity of a zero-age main sequence Pop. III protostar (including accretion luminosity) with the Eddington luminosity, and find that

$$\dot{M}_{\text{crit}} \simeq 4 \times 10^{-3} M_{\odot} \text{yr}^{-1}, \quad (77)$$

coincidentally close to \dot{M}_{fid} . In principle, one would expect \dot{M}_{crit} to have a dependence on the current mass of the protostar, but in practice, Omukai & Palla (2003) show that this dependence is weak and may be neglected.

Finally, Omukai & Palla (2003) show that in the time-dependent accretion model, the key factor is the size of the accretion rate at the end of the contraction phase. If this is greater than \dot{M}_{crit} , then one would expect accretion to be halted, while if it is less than \dot{M}_{crit} then accretion can continue. In practice, Omukai & Palla (2003) show that if one adopts the Abel, Bryan & Norman (2002) estimated accretion rate, then $\dot{M} < \dot{M}_{\text{crit}}$, implying that accretion can continue even once the protostar reaches the zero-age main sequence.

The main limitation of the approach outlined above is the neglect of the effects of rotation. In reality, rotation can have profound effects on stellar structure and evolution, particularly for massive stars (Maeder & Meynet, 2000), and it will also have a large influence on how matter reaches the protostar in the first place. The first detailed study of the pre-main sequence evolution of a Pop. III protostar to account for the effects of rotation was carried out by Tan & McKee (2004). In contrast to previous authors, they did not assume spherical symmetry. Instead, they assumed that

a protostellar accretion disk would form, and fixed the size of the disk by assuming angular momentum conservation within the supersonic portion of the accretion flow. They used the polytropic accretion flow model described in the previous section to compute the accretion flow onto the disk. To solve for the disk structure, they made use of the standard theory of steady, thin viscous accretion disks (as outlined in Shakura & Sunyaev 1973), with a spatially constant viscosity parameter α . As sources for α , they considered the magnetorotational instability Balbus & Hawley (1991, 1998) and gravitational instability. With the disk structure in hand, they could then solve for the structure of the protostar itself, using a modified version of an approach developed by Nakano, Hasegawa & Norman (1995) and Nakano et al. (2000). In the zero angular momentum case, Tan & McKee (2004) show that they successfully reproduce the previous results of Stahler, Palla & Salpeter (1986a) and Omukai & Palla (2001, 2003). In more realistic models, Tan & McKee (2004) show that the presence of an accretion disk has little influence on the evolution of the protostar, which still evolves through the same progression of adiabatic growth, terminated by the emergence of a luminosity wave, followed by rapid contraction to the ZAMS. However, Tan & McKee (2004) do find that the photosphere surrounding the protostar behaves very differently in this case than in the spherical case. Because most of the gas accretes onto the protostar via the disk, the gas density is significantly reduced in the polar regions. Consequently, the optical depth of these regions is also significantly reduced, with the result that the flow becomes optically thin early in its evolution. For example, in the model with $f_{\text{Kep}} = 0.5$, the photosphere vanishes once the protostellar mass reaches $1 M_{\odot}$ and does not subsequently reappear. Tan & McKee (2004) argue that this may have a major influence on the effectiveness of radiative feedback from the protostar, a topic that we will return to in the next section.

3.1.3 Feedback effects

Accretion of gas onto the protostar liberates a significant amount of energy, with most of this energy being emitted from regions close to the protostellar surface. This can be shown very simply by considering how the gravitational potential energy of a test mass changes as we move it close to a protostar of mass M_* and radius R_* . At a distance of $2R_*$, the gravitational potential energy of a fluid element with mass dM is

$$W = -\frac{GM_*dM}{2R_*}, \quad (78)$$

while at the protostellar surface it is

$$W = -\frac{GM_*dM}{R_*}. \quad (79)$$

Therefore, the amount of energy that must be dissipated by the fluid element as it moves from $2R_*$ to R_* is as large as the amount that it must have dissipated while

falling in from $R \gg R_*$ to $2R_*$, or in other words, *half* of the total binding energy dissipated by the gas is dissipated while its distance from the protostellar surface is less than R_* . In addition, once the protostar reaches the main sequence, it will start generating additional energy in its own right, via nuclear fusion. The energy that is released in the vicinity of the protostar is therefore quite considerable, and it is reasonable to suppose that this will have some effect on the behaviour of the surrounding gas. It is therefore not surprising that considerable attention has been paid to the issue of protostellar feedback in the context of Pop. III star formation.

In order for the protostar to substantially reduce the rate at which matter flows onto it, it must be able to transfer a significant amount of energy and/or momentum to the infalling gas. The various mechanisms by which this can be accomplished fall under two broad headings: *mechanical feedback*, where the protostar transfers energy and momentum to some form of outflow, which subsequently transfers it to the infalling material, and *radiative feedback*, where radiation from the protostar transfers energy and momentum directly to the infalling gas.

Mechanical feedback

In the local Universe, stellar winds are an almost ubiquitous phenomenon, and play an important role in the evolution of the most massive stars (Chiosi & Maeder, 1986). However, there are good reasons to expect that metal-free stars will be much less effective at driving winds than the roughly solar metallicity stars that we are familiar with in the Milky Way. Strong stellar winds are invariably radiation-driven, and at solar metallicities, the largest contribution to the radiative acceleration of the gas comes from the absorption and scattering of ultraviolet photons in the lines of the many metal atoms and ions present in the outflowing gas (Castor, Abbott, & Klein, 1975). In metal-free gas, on the other hand, the only significant sources of opacity within an outflow will come from the lines of He^+ (atomic hydrogen is typically fully ionized), and from Thomson scattering by free electrons. These provide orders of magnitude less radiative acceleration per unit luminosity than do the metal lines in a solar metallicity gas, and hence one can show that a metal-free Population III star can produce a line-driven wind only if the stellar luminosity is already very close to the Eddington limit (Kudritzki, 2002).

Of course, as a Population III star evolves, it will not remain metal-free. It will start to produce carbon, nitrogen and oxygen internally once the stellar core begins to burn helium, and if the star is rotating, these elements can become well-mixed within the star (Meynet, Ekström & Maeder, 2006). This will provide an additional source of opacity in the stellar atmosphere which may allow the most massive Population III stars to produce a weak CNO-driven wind (Krtićka & Kubát, 2009). However, the mass-loss rate will be small, and the fraction of the stellar mass that can be lost in this way is unlikely to be larger than about 1%.

It is also possible that very massive Population III stars with luminosities close to the Eddington luminosity may produce eruptive, continuum-driven winds, similar to those we see coming from nearby luminous blue variables (LBVs) such as η Car

(Smith & Owocki, 2006). However, as the cause of these LBV eruptions is not yet fully understood even for nearby objects, it is difficult to say with certainty whether they will actually be produced by Pop. III stars. More work on this topic is clearly necessary.

Finally, mechanical feedback can also be generated in the form of hydrodynamical or magnetohydrodynamical jets or outflows. We have already discussed the magnetically-driven disk winds produced in the Machida et al. (2006, 2008) simulations, which are able to eject roughly 10% of the infalling gas from the disk. Although, as we noted previously, these simulations only modelled the very earliest stages in the formation of the protostellar accretion disk, their value for the mass ejection rate is in good agreement with the predictions of a semi-analytical study of Pop. III disks and outflows carried out by Tan & Blackman (2004). If this value is correct, then it implies that the reduction in the protostellar accretion rate brought about by these outflows is small, and hence that they will not significantly limit the final stellar mass. However, one should bear in mind that their interaction with the star-forming halo on larger scales has not yet been modelled in any detail, and hence it is difficult to be certain regarding their final impact.

Radiative feedback

There are several different forms of radiative feedback that could potentially affect the accretion of gas by a Pop. III protostar. First, if the radiation is absorbed or scattered, then it will exert a force on the gas. If this force is comparable to or larger than the gravitational force acting on the gas, then it may suppress accretion onto the protostar, or even prevent it completely. Second, radiation may destroy the H_2 molecules responsible for cooling the gas. In the absence of cooling, the gas will evolve adiabatically, which again may reduce the rate at which it can be accreted. Third, the radiation may heat the gas. If radiative heating raises the gas temperature to a point at which the thermal energy of the gas exceeds the gravitational binding energy of the system, then this again will strongly suppress accretion.

In local star-forming regions, the first of these three forms of radiative feedback is believed to be the most important. Radiation pressure exerted on infalling dust grains by radiation from the protostar results in a substantial momentum transfer to the dust, and from there to the gas, since the dust and gas are strongly coupled. In spherically symmetric models, the radiative force exerted by the radiation on the dust can be strong enough to bring accretion to a complete halt (Wolfire & Cassinelli, 1987). In primordial gas, there is no dust, and so this process cannot operate. However, radiation pressure can also work directly on the gas, and so it is worthwhile investigating whether this process is likely to significantly suppress accretion.

Let us start by assuming that the bolometric luminosity of the protostar is given by the Eddington luminosity

$$L_{\text{Edd}} = \frac{4\pi GM_* c}{\kappa_T}, \quad (80)$$

where M_* is the protostellar mass, and $\kappa_T \equiv \sigma_T/m_p \simeq 0.4 \text{ cm}^2 \text{ g}^{-1}$ is the opacity due to Thomson scattering for a fully ionized gas composed of pure hydrogen, with σ_T the Thomson scattering cross-section of the electron and m_p the mass of the proton. In this case, then we know from the definition of the Eddington luminosity that the radiative force exerted on a fluid element will be equal to the gravitational force exerted on it by the protostar when the opacity of the fluid element is equal to κ_T . More generally, we can write the ratio of the forces acting on the fluid element as

$$\frac{F_{\text{rad}}}{F_{\text{grav}}} = \frac{L_*}{L_{\text{Edd}}} \frac{\kappa}{\kappa_T}, \quad (81)$$

where F_{rad} is the radiative force, F_{grav} is the gravitational force, L_* is the protostellar luminosity, and κ is the mean opacity of the fluid element. Since the protostar is unlikely to be stable if $L_* > L_{\text{Edd}}$, this implies that in order for the radiative force to significantly affect the gas, it must have a mean opacity $\kappa \sim \kappa_T$ or higher. In practice, the luminosity of a Pop. III protostar before it reaches the main sequence will often be significantly less than the Eddington luminosity (see e.g. Smith et al., 2011), in which case an even higher mean opacity is required.

The mean opacity of metal-free gas has been computed by a number of authors, most recently by Mayer & Duschl (2005b). They present tabulated values for both the Rosseland mean opacity

$$\kappa_R^{-1} = \frac{\int_0^\infty (\partial B_\nu / \partial T) \kappa_\nu^{-1} d\nu}{\int_0^\infty (\partial B_\nu / \partial T) d\nu}, \quad (82)$$

and the Planck mean opacity

$$\kappa_P = \frac{\int_0^\infty B_\nu \kappa_\nu d\nu}{\int_0^\infty B_\nu d\nu}, \quad (83)$$

where κ_ν is the frequency-dependent opacity and B_ν is the Planck function. For our purposes, we are most interested in the Planck mean. Strictly speaking, this Planck mean opacity is the same as the mean opacity in Equation 81 only if the protostar has a black-body radiation field and a photospheric temperature that is the same as the gas temperature, and in general this will not be the case. However, if the protostar is still in the pre-main sequence phase of its evolution, it will have a photospheric temperature $T_p \sim 6000 \text{ K}$ (Stahler, Palla & Salpeter, 1986a) and a spectrum that does not differ too greatly from a black-body, while the temperature of the surrounding gas will typically be of the order of 1000-2000 K or higher (Clark et al., 2011b; Greif et al., 2011a; Smith et al., 2011). In these conditions, the error we make by using the Planck mean opacity in Equation 81 should not be excessively large.

There are two regimes in which the tabulated values of κ_P in Mayer & Duschl (2005b) exceed κ_T . The first occurs at very high densities ($n > 10^{22} \text{ cm}^{-3}$), where $\kappa_P > \kappa_T$ for a wide range of temperatures. However, these extreme densities are

only reached *within* the protostar and hence this regime is of no relevance when we are considering feedback from the protostar on the surrounding gas. The second regime in which κ_p grows to the required size is at temperatures above 8000 K, for a wide range of densities. At these temperatures, the dominant source of opacity is the scattering of photons in the Lyman series lines of hydrogen, primarily Lyman- α . The effects of Lyman- α radiation pressure in metal-free gas were considered by Oh & Haiman (2002), in the context of the formation of massive star-forming minihalos with virial temperatures $T > 10^4$ K. They argued that the Lyman- α photons produced by the cooling of the hot gas would not be important (see also Rees & Ostriker, 1977), but that the Lyman- α photons produced by a massive star and its associated HII region would have a pronounced effect on the gas, and could significantly delay or even halt the inflow of the gas. However, they did not carry out a full quantitative investigation of the effects of Lyman- α radiation pressure. More recently, this issue was revisited by McKee & Tan (2008), who studied it in some detail. They found that in a rotating flow, most of the Lyman- α photons would eventually escape along the polar axis of the flow, as it is here that the optical depths are smallest. They showed that if the rotational speed of the gas were at least 10% of the Keplerian velocity, then Lyman- α radiation pressure would be able to reverse the direction of the flow along the polar axis once the protostellar mass reached $20 M_\odot$. The radiation would therefore blow out a polar cavity, allowing more Lyman- α photons to escape. This prevents the radiation pressure from rising further, and McKee & Tan argue that it never becomes large enough to significantly affect the inflow of gas from directions far away from the polar axis (e.g. from the accretion disk). For this reason, they conclude that Lyman- α radiation pressure is unlikely to be able to significantly reduce the protostellar accretion rate.

Let us now turn our attention to the second form of radiative feedback mentioned above: the photodissociation of H_2 and the consequent dramatic reduction in the cooling rate. As we have already discussed, at early times the photospheric temperature of the protostar is too low for it to produce significant quantities of far-ultraviolet radiation, and hence radiation from the protostar does not significantly affect the H_2 . Once the protostar reaches the main sequence, however, it can become a significant source of far-ultraviolet radiation, provided that it has a mass greater than around $15 M_\odot$ (McKee & Tan, 2008). Studies by Omukai & Nishi (1999) and Glover & Brand (2001) considered the effect that this radiation would have on the H_2 surrounding the protostar, and showed that the time required to photodissociate the H_2 would be significantly less than the lifetime of the protostar. The removal of the H_2 from the gas means that it is no longer able to cool effectively at temperatures $T < 10^4$ K, and hence one would expect that as the H_2 in the accreting gas is destroyed, the gas will begin to evolve adiabatically until it reaches this temperature. McKee & Tan (2008) consider whether this switch to adiabatic evolution is sufficient to halt accretion, and conclude that it is not. If no protostar were present, then the switch to adiabatic evolution would be enough to stabilize the gas and prevent further collapse. The presence of the protostar, however, serves to destabilize the gas, allowing accretion to continue even when the evolution of the gas is fully adiabatic. McKee & Tan (2008) use the treatment of protostellar accretion introduced

in Fatuzzo, Adams & Myers (2004) to investigate the issue numerically, and show that an increase in the effective adiabatic index of the gas from $\gamma_{\text{eff}} = 1.1$ (which approximately characterizes the temperature evolution of the gas at $n > 10^4 \text{ cm}^{-3}$; see e.g. Omukai & Nishi 1998) to $\gamma_{\text{eff}} = 5/3$ reduces the accretion rate by only 20%.

The third possible form of radiative feedback involves the heating of the surrounding gas by radiation from the protostar. If the temperature of the gas can be increased to a point at which its thermal energy exceeds its gravitational binding energy, then it will no longer be gravitationally bound to the protostar, and hence will not be accreted. A convenient way to quantify the relative importance of thermal and gravitational energy is to compare the sound-speed of the gas with the escape velocity of the system, v_{esc} : gas with $c_s > v_{\text{esc}}$ will not be gravitationally bound.

For an isolated protostar of mass M_* , we can write v_{esc} at a distance R from the protostar as:

$$v_{\text{esc}} = \sqrt{\frac{2GM_*}{R}}, \quad (84)$$

where G is the gravitational constant. If we rewrite this expression in more convenient units, we find that

$$v_{\text{esc}} \simeq 4.2 \left(\frac{M_*}{1 M_\odot} \right)^{1/2} \left(\frac{R}{100 \text{ AU}} \right)^{-1/2} \text{ km s}^{-1}. \quad (85)$$

For a primordial, fully molecular gas, $c_s = 4.2 \text{ km s}^{-1}$ at a temperature $T \sim 3400 \text{ K}$, and hence gas within 100 AU of a one solar mass protostar must be heated up to a temperature of thousands of Kelvin in order to unbind it. At larger distances, the required temperature would appear at first to be much smaller, but the reader should recall that this expression is for an *isolated* protostar, i.e. one which is not surrounded by gas. It is therefore only valid when the protostellar mass M_* is much larger than the mass of gas within a distance R of the protostar, and once we start considering scales $R \gg 100 \text{ AU}$, this is unlikely to be a good approximation. If we include the influence of this gas by replacing M_* in Equation 84 by $M_{\text{tot}} = M_* + M_{\text{gas}}$, and use the facts that prior to star formation, the mass enclosed within a sphere of radius 100 AU is roughly $5 M_\odot$ and increases at larger distances as $M_{\text{enc}} \propto R^{0.8}$, then at distances $R > 100 \text{ AU}$, we have

$$v_{\text{esc}} \simeq 9.4 \left(\frac{R}{100 \text{ AU}} \right)^{-0.1} \text{ km s}^{-1}. \quad (86)$$

In other words, once we account for the mass of the infalling gas in addition to the mass of the protostar, we find that the escape velocity is of the order of 10 km s^{-1} , with little dependence on the distance from the protostar. An escape velocity of this order of magnitude corresponds to a gas temperature of order 10^4 K . This immediately tells us that heating of the gas by radiation from the protostar during the pre-main sequence phase of its evolution is unlikely to significantly affect the accretion rate due to the low photospheric temperature of the protostar during this phase

– clearly, a protostar with an effective temperature of 6000 K will not be able to heat up distant gas to a temperature of 10000 K. On the other hand, once the protostar reaches the main sequence, its photospheric temperature will sharply increase, and hence it may be able to heat up the surrounding gas to a much higher temperature. In particular, if the protostar is massive enough to emit a significant number of ionizing photons while on the main sequence, then it will easily be able to produce temperatures in excess of 10^4 K within the gas that it ionizes.

The idea that the formation of an HII region may strongly suppress or completely terminate protostellar accretion was discussed long ago in the context of present-day star formation (see e.g. Larson & Starrfield, 1971), but has recently been re-examined by several authors in the context of primordial star formation. On large scales ($R > 0.1$ pc), the behaviour of an HII region produced by a Pop. III star is relatively simple. The radial density profile of the gas on these scales is approximately $\rho \propto R^{-2.2}$, and hence the density falls off too quickly to trap the HII region within the minihalo (see e.g. Whalen, Abel & Norman, 2004; Alvarez, Bromm & Shapiro, 2006; Abel, Wise & Bryan, 2007; Yoshida et al., 2007). The ionization front therefore expands rapidly, as an R-type front, with a velocity that is controlled by the rate at which ionizing photons are being produced by the star. In addition, if we are considering Pop. III star formation within one of the first star-forming minihalos, then it is easy to show that sound speed of the gas within the HII region will be higher than the escape velocity of the minihalo. Consequently, the ionized gas begins to flow out of these small minihalos, significantly reducing the mean gas density. It is therefore clear that once the HII region reaches a size of 0.1 pc or above, it will act to prevent any further infall of gas from these scales onto the protostar. However, this leaves unanswered the question of how long it takes for the HII region to expand to this scale.

In the case of steady, spherically-symmetric infall, Omukai & Inutsuka (2002) showed that in order for the HII region to avoid being trapped on scales close to the protostar, the flux of ionizing photons must exceed a critical value

$$\dot{N}_{\text{crit}} = 6.4 \times 10^{52} \left(\frac{R_{\text{in}}}{10 R_{\odot}} \right)^{-1} \left(\frac{M_{*}}{100 M_{\odot}} \right)^2 \text{ s}^{-1}, \quad (87)$$

where R_{in} is the inner radius of the HII region, which we can take to be equal to the radius of the massive star. Given reasonable values for R_{in} and M_{*} , this expression yields a value for \dot{N}_{crit} that is much larger than the number of photons that will actually be produced by any massive star, leading Omukai & Inutsuka (2002) to conclude that the HII region would remain trapped close to the star. However, this conclusion depends crucially on the assumed spherical symmetry of the flow. In the more realistic case in which our protostar is surrounded by an accretion disk, McKee & Tan (2008) show that the HII region can expand in all directions other than those close to the midplane of the disk once the stellar mass reaches a value of around 50–100 M_{\odot} , where the precise value required depends on how rapidly the gas is rotating. McKee & Tan (2008) also show that the accretion disk can survive for a considerable period after the HII region has broken out, and that the protostar

will stop accreting from the disk only once the rate at which gas is lost from the disk by photoevaporation exceeds the rate at which fresh gas is falling onto the disk. In their models, this occurs for $M_* \sim 140 M_\odot$, leading them to conclude that radiative feedback from the protostar on the surrounding gas cannot prevent the protostellar mass from becoming very large. On the other hand, initial attempts to model this process in 2D or 3D (Hosokawa et al., 2011; Stacy, Greif & Bromm, 2012) find significantly smaller final masses, $M_* \sim 30\text{--}40 M_\odot$, although these detailed models have so far explored only a small part of the potential parameter space.

3.2 *The fragmentation model*

3.2.1 Early studies

The first simulations of primordial gas to make use of sink particles were the SPH simulations of Bromm, Coppi & Larson (1999, 2002). They studied the formation of isolated dark matter minihalos and the cooling and gravitational collapse of gas within them using a somewhat idealized set of initial conditions. At an initial redshift $z = 100$, they created a spherical, uniform density region containing both gas and dark matter, and with an initial velocity field corresponding to the Hubble expansion. The density of this spherical region was taken to be higher than the cosmological background density, and was fixed such that the region would gravitationally collapse and virialize at a specified redshift, chosen to be $z = 30$ in most of the models that they examined. Small-scale structure was introduced into the dark matter distribution by perturbing the particles slightly from their initial positions using the Zel'Dovich (1970) approximation. The amplitudes of these random perturbations were fixed such that the small-scale density structure in the dark matter would begin to evolve in the non-linear regime at the virialization redshift. Both the dark matter and the gas were also assumed to be in solid body rotation, with some specified angular velocity.

Bromm, Coppi & Larson examined several different choices for the halo mass and initial angular velocity of the gas, and showed that starting from these initial conditions, the gas and dark matter would initially collapse in a similar fashion, but that the gas would subsequently form H_2 , dissipate energy, and sink to the center of the minihalo. In most of the cases they studied, the gas would then form a rotationally-supported disk, with a radius of order 10 pc. This disk would then break up into clumps with masses $M_{\text{cl}} \sim 100\text{--}1000 M_\odot$, comparable to the Jeans mass in the disk. As these clumps were gravitationally unstable, they of course underwent gravitational collapse, and Bromm, Coppi & Larson (2002) therefore introduced sink particles to represent clumps that collapsed to densities greater than 10^8 cm^{-3} in order to avoid the timestep constraints discussed earlier, allowing the further evolution of the clumps to be studied.

Unfortunately, the fragmentation observed by Bromm, Coppi & Larson in their simulations is probably not realistic. One major problem lies in their choice of initial

conditions, specifically in their use of solid-body rotation. Although the total angular momentum of the gas and dark matter in their simulations is comparable that measured for minihalos in more realistic cosmological simulations (Jang-Condell & Hernquist, 2001; Davis & Natarajan, 2010), their adoption of solid-body rotation leads to the gas having an incorrect radial profile for this angular momentum. This causes the collapse of the gas to be considerably more ordered than it would be in a real minihalo, leading to the formation of an over-large disk. Disks of this kind do not appear to form in simulations of small star-forming minihalos that start from more realistic cosmological initial conditions (e.g. Abel, Bryan & Norman, 2002; Yoshida et al., 2006). A second major problem lies in the neglect of stellar feedback. Within the disk, the dynamical timescale is of the order of a million years, which is much longer than is needed for a massive Pop. III star to reach the main sequence. Therefore, if a massive star forms within the first clump to be produced within the disk, the radiation from this star may well be able to photodissociate the H_2 in the disk before a second clump can form (Omukai & Nishi, 1999; Glover & Brand, 2001).

The next attempt to use sink particles to study the formation of Pop. III stars was made by Bromm & Loeb (2004). The initial setup of their simulation was similar to that used by Bromm, Coppi & Larson (2002), but to gain improved resolution in the centre of the minihalo, they used a technique called particle splitting (Kitsonas & Whitworth, 2002; Bromm & Loeb, 2003). The evolution of the minihalo was followed until cold, dense gas started to build up in the centre of the halo. The simulation was then paused, and the gas within a radius of 3.1 pc of the centre of the minihalo (corresponding to roughly $3000 M_\odot$ of material) was resampled using SPH particles with much smaller masses, using the resampling technique described in Bromm & Loeb (2003). The mass resolution within this resampled region was thereby improved from $M_{\text{res}} = 200 M_\odot$ to $M_{\text{res}} = 4 M_\odot$. Bromm & Loeb then restarted the simulation, and followed the further gravitational collapse of the gas within this central, higher resolution region until the gas density reached $n \sim 10^{12} \text{ cm}^{-3}$, at which point a sink particle was created. They then followed the accretion of gas onto this sink for roughly 10^4 years, as we have already described above. Bromm & Loeb (2004) found no evidence for fragmentation within the central clump of dense gas, but did note that a second dense clump formed nearby, with a final separation from the star-forming clump of roughly 0.25 pc. However, the free-fall collapse time of this clump was about 3 Myr, and so it was unclear whether it would survive for long enough to form a second star, or whether it would be destroyed by negative feedback from a massive star forming within the first clump.

3.2.2 The importance of turbulence

Although the Bromm & Loeb (2004) study undoubtedly represented a significant step forwards in resolution compared to Bromm, Coppi & Larson (2002), it still had a mass resolution which was more than two orders of magnitude greater than the actual size of a Pop. III protostar at the moment that it forms, and hence it was unable

to investigate the behaviour of the gas on scales smaller than about 100 AU. The first work using sink particles that did manage to probe this regime was Clark, Glover & Klessen (2008). Although the main focus of their study was on the fragmentation brought about by dust cooling in low metallicity systems (see e.g. Omukai et al. 2005, Schneider et al. 2006 or Dopcke et al. 2011 for more on this topic), they also studied the behaviour of the gas in the $Z = 0$ case for the purpose of comparing it with the results on their low metallicity runs. As the initial conditions for their simulations, Clark, Glover & Klessen (2008) considered a uniform density cloud, with a mass of $500 M_{\odot}$, a radius of 0.17 pc and a number density of $5 \times 10^5 \text{ cm}^{-3}$. The gas within this cloud was given a low level of initial turbulence, with a turbulent energy equal to 10% of the gravitational potential energy, and was also assumed to be rotating uniformly, with an initial rotational energy equal to 2% of the gravitational potential energy. Two different simulations were performed, with different numbers of particles: a low resolution simulation that used only two million SPH particles, and hence had a mass resolution of $0.025 M_{\odot}$, and a high resolution simulation that used 25 million particles, corresponding to a mass resolution of $2 \times 10^{-3} M_{\odot}$. Aside from the somewhat artificial initial conditions, the main simplification made in these simulations was the use of a tabulated equation of state to follow the thermal evolution of the gas. The results of the Omukai et al. (2005) one-zone model were used to derive internal energy densities and thermal pressures for the gas at a range of different densities, and this data was then used to construct a look-up table that could be used by the SPH code to compute the internal energy and pressure corresponding to a given gas density.

Clark et al. followed the collapse of the gas in their simulation down to a physical scale of less than an AU (corresponding to a gas density of over 10^{16} cm^{-3}). Regions collapsing to even smaller scales were replaced by sink particles, created using the standard Bate, Bonnell & Price (1995) prescription. Clark et al. showed that at the point at which the first sink particle formed, the radial profiles of quantities such as the gas density or the specific angular momentum were very similar to those found in previous studies of Pop. III star formation that were initialized on cosmological scales (e.g. Abel, Bryan & Norman, 2002; Yoshida et al., 2006). They noted that at this point in the simulation, there is no sign of any fragmentation occurring, and argued that if the simulation were stopped at this point (as would be necessary if the sink particle technique were not being used), one would probably conclude that the gas would not fragment, but would merely be accreted by the protostar. However, they show that this is not what actually happens when the simulation is continued. Instead, the gas fragments, forming 25 separate protostars after only a few hundred years. Clark et al. stopped their simulations after $19 M_{\odot}$ of gas had been incorporated into sink particles, and showed that at this point the protostars have masses ranging from $0.02 M_{\odot}$ to $5 M_{\odot}$, but that the mass distribution is relatively flat, with most of the mass locked up in the few most massive protostars. There is no significant difference between the mass function of sinks in the low and high resolution calculations, suggesting that fragmentation is well-resolved in both cases.

This is an intriguing result, but several reasonable concerns could be raised regarding the numerical technique adopted by Clark, Glover & Klessen (2008). First,

the initial conditions for the gas are an idealized version of what one would find within a real star-forming minihalo, and although there are indications that the gas loses its memory of the initial conditions prior to fragmentation occurring, inevitably a few doubts remain. Second, and more importantly, the use of a tabulated equation of state represents a major simplification of the thermal evolution of the gas, and one which may make fragmentation more likely to occur. For example, this technique does not allow one to model the formation of the hot, shocked regions noted by Turk, Norman & Abel (2010) in which much or all of the H_2 is dissociated, and it is likely to underestimate the temperature of gas falling in at later times, when the typical infall velocity is larger than during the initial assembly of the protostar. The Clark et al. calculation also neglects the effects of radiative feedback from the protostars, and assumes that protostars do not merge, even if they come within sub-AU distances of each other.

In a follow-up study, Clark et al. (2011a) addressed one of these concerns – the use of a tabulated equation of state – by performing simulations that replaced this with a detailed treatment of the chemistry and cooling of primordial gas. In their study, they investigated the role that low Mach number turbulence might play in triggering fragmentation in the gas by performing a set of simulations of the collapse of unstable Bonnor-Ebert spheres. They considered three initial configurations: a $1000 M_\odot$ cloud with an initial temperature of 300 K; a $150 M_\odot$ cloud with an initial temperature of 75 K; and a $1000 M_\odot$ cloud with an initial temperature of 75 K. In each case, the central density of the Bonnor-Ebert sphere was taken to be $n_c = 10^5 \text{ cm}^{-3}$. The first set of initial conditions were intended to correspond to the conditions that one would expect to find within one of the first star-forming minihalos, while the second set were intended to correspond to the conditions within a minihalo dominated by HD cooling. Simulations with the third set of initial conditions were run to allow the effects of lowering the temperature and lowering the total mass to be distinguished. Within the Bonnor-Ebert spheres, a turbulent velocity field was imposed, with a three-dimensional RMS velocity Δv_{turb} .

Clark et al. (2011a) did not claim that this was a completely accurate model of the physical state of the gas within a real star-forming minihalo. Instead, they treated this study as a kind of physics experiment, allowing them to investigate the effect of varying a single important parameter – the turbulent kinetic energy – without varying any of the other parameters in the problem, something that it would not be possible to do if using initial conditions derived from a cosmological simulation. For the first two setups described above, they performed four simulations, with $\Delta v_{\text{turb}} = 0.1, 0.2, 0.4$ and $0.8 c_s$, respectively, where c_s was the initial sound speed. For the third setup (the large, low temperature clouds), they performed only two simulations, with $\Delta v_{\text{turb}} = 0.4$ and $0.8 c_s$, respectively. The clouds were modelled using two million SPH particles in each case, yielding a mass resolution of $0.05 M_\odot$ for the $1000 M_\odot$ clouds and $0.0075 M_\odot$ for the $150 M_\odot$ clouds. Sink particles were created once the gas density exceeded 10^{13} cm^{-3} , and the sink accretion radius was 20 AU.

Clark et al. (2011a) found that fragmentation occurred in almost all of their simulated clouds. In the case of the massive, warm clouds, the only case in which frag-

mentation did not occur was the simulation with $\Delta v_{\text{turb}} = 0.1 c_s$. In this simulation, the gas simply collapsed to form a single, massive protostar. In the simulations with larger turbulent energies, however, the formation of the first protostar was followed within a couple of hundred years by the fragmentation of the infalling gas and the formation of a significantly larger number of protostars. The relationship between the turbulent energy and the degree of fragmentation is not straightforward: the $\Delta v_{\text{turb}} = 0.4 c_s$ run fragmented more than the $\Delta v_{\text{turb}} = 0.2 c_s$, as one might expect, but the $\Delta v_{\text{turb}} = 0.8 c_s$ run fragmented *less* than the $\Delta v_{\text{turb}} = 0.4 c_s$ run (although still more than the $\Delta v_{\text{turb}} = 0.2 c_s$ run). Clark et al. hypothesize that this difference in behaviour is due to the amount of angular momentum retained within the collapsing region, which in this case was larger in the $\Delta v_{\text{turb}} = 0.4 c_s$ run than in the other runs, but note that this may not always be the case, and that a much larger series of realizations of the turbulent velocity field would be needed to make a definitive statement about the relationship between the turbulent energy and the degree of fragmentation (c.f. Goodwin, Whitworth, & Ward-Thompson, 2004, who come to a similar conclusion regarding present-day star formation). The total amount of mass accreted by the sinks is very similar in all four runs, and hence the runs that fragment more tend to form lower mass objects than the runs that fragment less.

In the low-mass, colder clouds, Clark et al. find a much lower degree of fragmentation, despite the fact that the initial number of Jeans masses in these clouds is the same as in the $1000 M_\odot$, $T = 300$ K clouds. In this case, fragmentation occurs only in the $\Delta v_{\text{turb}} = 0.2 c_s$ and $\Delta v_{\text{turb}} = 0.8 c_s$ simulations, and only a small number of fragments are formed in each case. Clark et al. investigate whether this is due to the lower cloud mass by modelling the collapse of $1000 M_\odot$ clouds with the same lower initial temperature, and find that although more fragmentation occurs in this case, the gas still fragments less than in the $1000 M_\odot$, $T = 300$ K case. They suggest that this somewhat counterintuitive behaviour is due to the greater stiffness of the effective equation of state in the colder clouds. In both cases, the gas must heat up from its initial temperature at 10^5 cm^{-3} to a temperature of roughly 1000 K at 10^{10} cm^{-3} , and so when the initial temperature is lower, the gas must heat up more rapidly with increasing density, meaning that it has a larger effective adiabatic index. This makes it more difficult to generate the small-scale non-linear structures that are the seeds for later fragmentation, and also delays the collapse, allowing more of the turbulent energy to dissipate. A similar effect has previously been noted by Yoshida, Omukai & Hernquist (2007) and Tsuribe & Omukai (2008), and calls into question the common wisdom that minihalos in which the cooling becomes HD-dominated will inevitably form lower mass stars.

3.2.3 Models using cosmological initial conditions

In order to establish whether the fragmentation seen in the Clark, Glover & Klessen (2008) model was simply a consequence of the highly idealized initial conditions used in that study, several recent follow-up studies have re-examined the issue using simulations initialized on cosmological scales (i.e. scales significant larger than

the virial radius of the minihalo). One of the first of these studies was carried out by Stacy, Greif & Bromm (2010). They first performed a medium resolution cosmological simulation, which allowed them to determine the formation site of the first minihalo large enough to cool effectively and form stars. They then used a hierarchical zoom-in procedure (Navarro & White, 1994; Tormen, Bouchet & White, 1997; Gao et al., 2005) to improve the resolution within a region centered on this formation site, allowing them to achieve a mass resolution of $1.5 M_{\odot}$ within the centre of the star-forming minihalo.⁵ In contrast to Clark, Glover & Klessen (2008), the thermal and chemical evolution of the gas was followed in detail during the collapse. Once the gravitationally collapsing gas reached a density of 10^{12} cm^{-3} , it was converted into a sink particle, along with all of the gas within an accretion radius $r_{\text{acc}} = 50 \text{ AU}$. Stacy et al. show that following the formation of this first sink, the infalling gas collapses into a flattened disk. At a time $t = 250 \text{ yr}$ after the formation of the first sink particle, this disk has a radius of 200 AU, but it grows with time and has reached a radius of 2000 AU by $t = 5000 \text{ yr}$, the end of the simulation. H_2 cooling allows the gas within the disk to remain at a temperature of roughly 1000 K, and the disk soon becomes gravitationally unstable, forming a second sink particle after roughly 300 yr, and a further three sinks after 4000-5000 years of evolution. At the end of the simulation, the first two sinks to form have become very massive, with masses of $43 M_{\odot}$ and $13 M_{\odot}$ respectively, while the three newer sinks still have masses $\sim 1 M_{\odot}$, close to the resolution limit of the simulation. Stacy, Greif & Bromm (2010) do not include the effects of accretion luminosity in their simulation directly, but do assess its effects during a post-processing stage. They investigate the possible effects of radiation pressure, but show that this remains unimportant within their simulation throughout the period that they simulate, in agreement with our analysis above.

The main drawback of the Stacy, Greif & Bromm (2010) study is their choice of mass resolution. At the point at which it fragments, the protostellar accretion disk in their simulation has a mass of roughly $35 M_{\odot}$, and hence is resolved with only a few thousand SPH particles. This is two orders of magnitude smaller than the number of particles typically used to model gravitationally unstable accretion disks in the context of present-day star formation (see e.g. Rice, Lodato & Armitage, 2005), and it is questionable whether a few thousand particles is enough to properly model the dynamics of the disk. It is therefore possible that the results of Stacy, Greif & Bromm (2010) may have suffered from some degree of artificial fragmentation.

More recently, a study by Clark et al. (2011b) has dramatically improved the mass resolution used to model the build-up of a protostellar accretion disk around the first Population III protostar. Clark et al. use a similar basic strategy to Stacy et al., starting with a medium resolution cosmological simulation to identify the first star-forming minihalo, and then using a hierarchical zoom-in procedure to im-

⁵ The value quoted here for the mass resolution of the Stacy, Greif & Bromm (2010) simulation assumes that 100 or more SPH particles are required to resolve gravitationally bound structures, which is the typical resolution limit adopted in studies of present-day star formation. Stacy, Greif & Bromm (2010) assume that only 48 SPH particles are required, and hence quote a mass resolution that is roughly a factor of two smaller.

prove the resolution within the gas forming this minihalo. They run this zoomed-in simulation until the maximum density of the gravitationally collapsing gas reaches 10^6 cm^{-3} . At this point, they extract a spherical region containing $1000 M_\odot$ of gas from the centre of the minihalo, and resimulate this region at much higher resolution, using several nested levels of particle splitting (Kitsionas & Whitworth, 2002; Bromm & Loeb, 2003). At the final level of splitting, the particle mass is $10^{-5} M_\odot$ and the mass resolution is $10^{-3} M_\odot$, several orders of magnitude better than in the Stacy, Greif & Bromm (2010) simulation.

In addition to the extremely high mass resolution, the other main improvement in the Clark et al. study compared to previous work is its inclusion of the effects of accretion luminosity feedback directly within the simulation. To model this, the authors start by writing the bolometric accretion luminosity produced by a given protostar as

$$L_{\text{acc}} = \frac{G\dot{M}M_*}{R_*}, \quad (88)$$

where \dot{M} is the accretion rate onto that protostar, M_* is the protostellar mass, and R_* is the protostellar radius. As Clark et al. attempt to model only the first few hundred years of the evolution of the gas after the formation of the first protostar, i.e. a timescale much less than the protostellar Kelvin-Helmholtz relaxation timescale, they assume that the protostars remain in the adiabatic accretion phase of their evolution, with masses and radii that are related by (Stahler, Palla & Salpeter, 1986a)

$$R_* = 26R_\odot \left(\frac{M_*}{M_\odot}\right)^{0.27} \left(\frac{\dot{M}}{10^{-3} M_\odot \text{ yr}^{-1}}\right)^{0.41}. \quad (89)$$

The only remaining uncertainty is then \dot{M} , which can be directly measured within the simulation. Clark et al. next assume that the gas is heated by the accretion luminosity at a rate

$$\Gamma_* = \rho \kappa_{\text{p}} \frac{L_{\text{acc}}}{4\pi r^2}, \quad (90)$$

where ρ is the mass density, r is the distance to the protostar, and κ_{p} is the Planck mean opacity of the gas, calculated using the tabulated values given in Mayer & Duschl (2005b). This expression assumes that the gas is optically thin, and hence will tend to overestimate the heating rate.

Clark et al. model protostar formation using sink particles, which are created using the standard Bate, Bonnell & Price (1995) algorithm, with a density threshold $n_{\text{th}} = 10^{17} \text{ cm}^{-3}$. The sink accretion radius was set to 1.5 AU. At the point at which the first sink particle forms, the state of the gas in the Clark et al. simulation (e.g. the density profile and the distribution of specific angular momentum) is very similar to that seen in other high resolution simulations of Pop. III star formation. However, the authors show that at later times, a protostellar accretion disk begins to build up around the central protostar, just as in the Stacy et al. study. The significantly higher resolution of the Clark et al. simulation allows them to model the build up of this disk on scales much closer to the central protostar, and to resolve the disk with a

far larger number of SPH particles. The growth of the accretion disk is followed for around 100 years after the formation of the first protostar, and Clark et al. show that after around 90 years (corresponding to around 1.5 orbital periods for the disk), the accretion disk begins to fragment, forming several low-mass protostars. At the time at which it fragments, the disk contains several solar masses of gas (and hence is resolved with several hundred thousand SPH particles), compared to around $0.4M_{\odot}$ in the central protostar, and the disk radius is a few tens of AU. The state of the disk at the onset of fragmentation is illustrated in Figure 4.

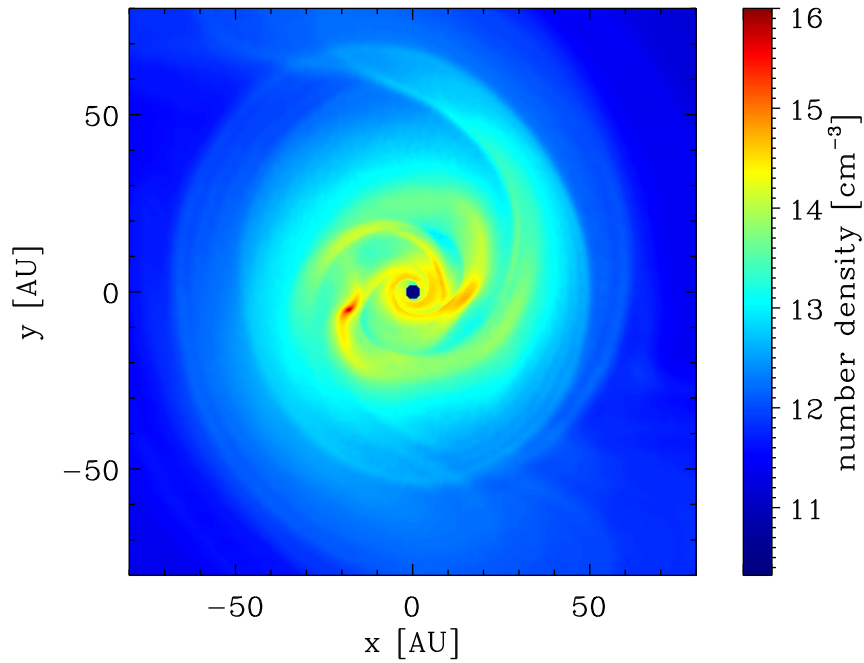


Fig. 4 The volume density of the protostellar accretion disk in the Clark et al. (2011a) simulation immediately prior to fragmentation. The ‘hole’ in the centre of the disk corresponds to the location of the sink particle representing the first protostar to form, and occurs because we have not accounted for the mass in the sink particle when calculating the density. The accretion disk is gravitationally unstable, and has formed several spiral arms, one of which has begun to fragment.

Clark et al. argue that the reason that the protostellar accretion disk fragments is that it is unable to transfer gas onto the protostar fast enough to keep up with the rate at which fresh gas is falling onto the disk. This causes the surface density of the disk to increase, which eventually results in it becoming gravitationally unstable and fragmenting. This argument can be made somewhat more quantitative if one treats the disk using the standard Shakura & Sunyaev (1973) thin disk model, and hence writes the mass flow rate through the disk at a radius r as

$$\dot{M}(r) = 3\pi\alpha c_s(r)\Sigma(r)H(r), \quad (91)$$

where α is the viscosity parameter, and $c_s(r)$, $H(r)$ and $\Sigma(r)$ are the sound speed, disk thickness and surface density, respectively, at a radius r . Clark et al. use the values of c_s , H and Σ provided by their simulation to show that $\dot{M}(r)$ is smaller than the accretion rate onto the disk for a wide range of radii, even if one adopts $\alpha = 1$ (which already presupposes that the disk is gravitationally unstable). The growth of the disk therefore appears to be unavoidable, leading to its fragmentation once portions of it develop a Toomre stability parameter $Q < 1$, where $Q \equiv c_s\kappa/\pi G\Sigma$, with κ here being the epicyclic frequency.

Previous semi-analytical studies of the structure of Pop. III accretion disks came to a somewhat different conclusion regarding their stability, predicting that $Q \gg 1$ throughout the disk (Tan & McKee, 2004; Tan & Blackman, 2004; Mayer & Duschl, 2005a). However, these models neglected the effect of H_2 cooling, motivated by the assumption that the H_2 content of a Pop. III protostellar accretion disk is negligible (J. Tan, private communication). This assumption leaves H^- as the primary source of opacity at temperatures $T \sim 7000$ K and below (Lenzuni, Chernoff & Salpeter, 1991; Mayer & Duschl, 2005b). For gas in chemical equilibrium, the opacity of H^- decreases sharply with decreasing temperature, and consequently these models find the equilibrium temperature of the accretion disk to be high, $T \sim 6000$ K. In comparison, Clark et al. show that when the effects of H_2 are taken into account, the characteristic temperature of the gas in the disk lies in the range of 1500 to 2000 K. The disks in these previous semi-analytical models could therefore transfer mass onto the protostar more rapidly than the disk in the Clark et al. simulation, owing to their higher sound-speed and larger thickness, but at the same time were also more stable against gravitational fragmentation. It is therefore not surprising that these previous studies predicted that the accretion disk should be stable, and highlights the crucial role played by H_2 cooling in enabling disk fragmentation.

In addition to the simulation described above, in which the value of \dot{M} used to calculate the accretion luminosity was measured directly, Clark et al. also performed two additional simulations in which \dot{M} was kept fixed, allowing them to investigate the role played by accretion luminosity heating. They considered cases with $\dot{M} = 10^{-3} M_\odot \text{yr}^{-1}$ (somewhat smaller than the measured value) and $\dot{M} = 10^{-2} M_\odot \text{yr}^{-1}$ (larger than the measured value), and showed that as \dot{M} (and hence L_{acc}) increase, the disk becomes warmer and thicker and takes longer to fragment. However, fragmentation still occurs in every case, demonstrating that accretion luminosity heating is unable to prevent the disk from fragmenting (c.f. Krumholz, 2006, who argues that it plays a crucial role in suppressing fragmentation in local star-forming systems).

One drawback of the Clark et al. (2011b) study is that they examined only a single star-forming minihalo, and although they showed that the properties of this halo (e.g. mass, spin parameter, formation redshift) were similar to those of the minihalos modelled in previous studies of Pop. III star formation, nevertheless the suspicion remains that perhaps this particular minihalo was unusual in some way. This concern was addressed by Greif et al. (2011a). They used the new moving-

mesh code AREPO (Springel, 2010) to study Pop. III star formation in five different minihalos, using a sink particle algorithm to allow them to follow the evolution of the gas past the point at which the first protostar formed. In all five of the systems that they modelled, they found similar behaviour to that in the Clark et al. study: an accretion disk built up around the first protostar, became gravitationally unstable, and began to fragment after only a few years. These results suggest that Clark et al. were right to claim that disk fragmentation, and the resulting formation of Pop. III binary systems, or higher order multiple systems, is an almost inevitable outcome of Population III star formation.

Greif et al. (2011a) also examined the issue of whether the objects represented by the individual sink particles would truly survive as separate protostars, or whether they would simply merge into a single massive protostar as the system evolved further. They considered two different schemes for merging sink particles. In the standard scheme, sink particles coming within a distance of $100 R_{\odot}$ of each other were merged to form a single sink, provided that the total energy of the two-body system was negative. In an alternative model, utilizing what Greif et al. dub as “adhesive” sinks, the energy check was omitted, and sinks were always merged when within a distance of $100 R_{\odot}$ of each other. Greif et al. justify their choice of this critical distance in two ways: first, it is also the accretion radius adopted for their sinks, meaning that the gas flow on smaller scales close to the sinks is not resolved; and second, it is roughly equal to the maximum size of a pre-main sequence protostar predicted by the models discussed in Section 3.1.2.

The majority of the protostars formed in the Greif et al. simulations have at least one close encounter with another protostar, but when the standard merger algorithm is used, many of these encounters result in a purely dynamical interaction, as the total energy of the protostellar pair is too large to allow them to merge. On the other hand, when the adhesive sinks are used, many of these encounters lead to mergers. Greif et al. show that although the total mass incorporated into protostars is roughly the same in both cases, the number of protostars that survive as individual objects is reduced by a factor of up to a few, and the mean protostellar mass is consequently higher. In both cases, the protostars have a relatively flat mass distribution, with most of the protostellar mass being accounted for by a small number of high-mass protostars. The protostars have a broad distribution of radial velocities, ranging from $v_{\text{rad}} \sim 1 \text{ km s}^{-1}$ to $v_{\text{rad}} \sim 100 \text{ km s}^{-1}$, and in many cases the radial velocity is greater than the escape velocity of the central region of the minihalo. It is likely that this leads to a significant fraction of the Pop. III protostars escaping from the minihalo entirely, although Greif et al. do not follow their evolution for long enough to confirm this. It is possible that these protostars will accrete very little additional gas once they escape from the high density region at the centre of the minihalo (see e.g. Johnson & Khochfar, 2011), in which case their final masses would be very similar to the masses that they have at the point at which they are ejected. Greif et al. show that in the standard case, a considerable number of these ejected protostars have masses $M < 1 M_{\odot}$. If these protostars do indeed avoid accreting further gas after their ejection, then they would have lifetimes that are comparable to the current age of the Universe. This suggests that it may be possible for some Population III

stars to survive until the present day. However, when the adhesive sinks are used, the number of ejected protostars with subsolar masses is greatly reduced, demonstrating that this conclusion is highly sensitive to our treatment of protostellar mergers.

The majority of the Greif et al. simulations did not include the effects of the accretion luminosity generated by the collection of protostars. However, they did consider one case in which this was included, using the Clark et al. treatment with a fixed value for the accretion rate used in the determination of the accretion luminosity, $\dot{M} = 0.1 M_{\odot} \text{ yr}^{-1}$. The effect of this was to puff up the disk, causing fragmentation to occur at a slightly larger distance from the initial protostar. However, despite the unrealistically high value adopted for \dot{M} , fragmentation still occurred and the number of protostars that formed was barely affected.

A more detailed study of the effects of accretion luminosity heating was carried out by Smith et al. (2011). They used Gadget to resimulate the central 2 pc of the minihalos simulated by Greif et al. (2011a), starting at a time prior to protostar formation at which the peak density of the gas was around 10^9 cm^{-3} . Smith et al. (2011) evolved these systems past the time at which the first protostar formed, and used sink particles with large accretion radii ($r_{\text{acc}} = 20 \text{ AU}$) to allow them to follow the dynamical evolution of the system for an extended period. For each of the five minihalos, they performed simulations both with and without accretion luminosity heating. When the accretion luminosity heating was included, it was treated in the same fashion as in Clark et al. (2011b). They found that in general, the effect of the accretion luminosity heating was to delay fragmentation and reduce the number of fragments formed. However, they also showed that the effect was relatively small, and had less influence on the number of fragments formed than did the intrinsic variation in halo properties arising from their different assembly histories.

3.2.4 Open questions

As the discussion in the previous section has shown, the past couple of years has seen a large increase in the number of simulations of Pop. III star formation that show evidence for fragmentation, suggesting that the older picture that had Pop. III stars forming in isolation with masses of $100 M_{\odot}$ or more is in need of some revision. However, many aspects of the fragmentation scenario remain unclear. Some of the most important open questions are summarized below.

- Are our treatments of optically thick H_2 cooling and accretion luminosity heating adequate?

The fragmentation of the gas observed in these simulations typically occurs at densities at which H_2 line cooling is optically thick, and hence may depend on the method used to account for the reduction that this causes in the cooling rate. At present, both of the methods in common usage represent relatively crude approximations, and it remains to be seen whether the behaviour of the gas will remain the same if a more accurate treatment is used. Similarly, the method currently used to treat the effects

of accretion luminosity heating also makes a number of major simplifications that may influence the outcome of the simulations.

- What role do magnetic fields play?

If a non-negligible magnetic field can be generated by the turbulent dynamo during the gravitational collapse of the gas, as discussed in Section 2.3, then this may influence the evolution and stability of the disk. The presence of a magnetic field may make the disk unstable via the magnetorotational instability (Tan & Blackman, 2004; Silk & Langer, 2006), although the resulting mass transfer onto the protostar is unlikely to be fast enough to prevent the disk from becoming gravitationally unstable. A more important effect may be magnetic braking of the infalling gas, which could act to significantly reduce the angular momentum of the gas reaching the disk (see e.g. Hennebelle & Ciardi, 2009). Whether either of these effects can significantly suppress fragmentation remains to be determined.

- How often do Population III protostars merge?

Current simulations either ignore mergers entirely (e.g. Clark et al., 2011b; Smith et al., 2011), or treat them using very simple approximations that do not properly account for the effects of tidal forces (e.g. Greif et al., 2011a). However, it is clear from the results of the Greif et al. study that the method used to treat mergers has a significant influence on the number of protostars that survive, their mass distribution and their kinematics. Improving the accuracy with which protostellar mergers are treated within this kind of simulation is therefore an important priority.

- Can we find some way to do without sink particles?

The concerns outlined above regarding the way in which protostellar mergers are treated would be greatly ameliorated if we were able to run the simulations without sink particles, as in this case we would be able to model directly how the gas behaves on scales of the order of $100 R_{\odot}$. To do this, however, it will be necessary to devise some scheme for treating these very small scales that does not fall foul of the Courant time constraint discussed previously. Greif et al. (2012) have recently published the results of an initial effort along these lines, but were only able to simulate the first ten years of the evolution of the disk, owing the extremely high computational cost of the calculation.

- How rapidly does H_2 photodissociation occur?

Fragmentation is dependent on the cooling provided by H_2 and does not occur in models of protostellar accretion disks that omit this effect (Tan & McKee, 2004; Mayer & Duschl, 2005a). It is therefore highly probable that fragmentation will cease once the H_2 has been photodissociated by Lyman-Werner band photons emitted from any massive protostars that form. What is not yet clear is how quickly this will occur. McKee & Tan (2008) show that the number of Lyman-Werner band photons produced by a zero-age main sequence Population III star increases sharply with increasing stellar mass, before levelling off at a value $S_{lw} \sim 10^{49}$ photons s^{-1} for $M_* \sim 30 M_{\odot}$. If we assume that all of these photons are absorbed by H_2 and that

20% of these absorptions lead to dissociation (Draine & Bertoldi, 1996), then the radiation from the star will photodissociate H_2 at a rate $\dot{M}_{\text{dis}} = 0.1 M_{\odot} \text{yr}^{-1}$, leading to complete removal of the H_2 within only a few hundred years. However, it is likely that many of the available photons will not be absorbed by H_2 , either because they never coincide with one of the Lyman-Werner band lines, or because they escape along a direction in which most of the H_2 has already been dissociated, or because they are absorbed by atomic hydrogen (Glover & Brand, 2001), and so the dissociation time for the H_2 could be significantly longer than suggested by this simple estimate, particularly once one accounts for the effects of three-body H_2 formation.

- How rapidly is the gas ionized? Does this completely suppress accretion, or simply suppress fragmentation?

As we have already discussed in Section 3.1.3, the most plausible mechanism for shutting off the supply of cold gas at the centre of the minihalo is the formation of an HII region whose thermal pressure is sufficient to expel most of the gas. However, only a few studies have looked at the interaction between the growth of the HII region and the evolution of the protostellar accretion disk. In particular, the issue has not yet been looked at within the context of the fragmentation model discussed above. It is therefore unclear how rapidly the HII region will grow, and whether it will immediately act to shut off accretion, or whether pockets of dense, cold gas can survive within the HII region for an extended period.

- Do any low-mass Population III stars survive until the present day?

One of the most exciting results of the Greif et al. (2011a) model is that some of the protostars that are ejected from the centre of the star-forming minihalo have masses that are below $0.8 M_{\odot}$, and hence lifetimes that are longer than the current age of the Universe. If these protostars avoided accreting any further gas, then they could have survived until the present-day, raising the possibility of directly detecting truly metal-free stars within the Milky Way. However, as we have already discussed above, the number of protostars with sub-solar masses that are ejected from the star-forming region is very sensitive to the way in which protostellar mergers are treated, and hence is highly uncertain at present. In addition, it is possible that any Pop. III protostars that have survived until the present day have also become too polluted with metals by ongoing accretion from the ISM for us to recognize them as metal-free stars, although the best current estimates (Frebel, Johnson & Bromm, 2009; Johnson & Khochfar, 2011) suggest that the effects of pollution will be very small.

4 Summary

In this review, we have focussed on three main topics: how the first star-forming minihalos come into existence and why they have the properties that they do; how

gas within a representative minihalo cools, collapses and forms a protostar; and how this protostar and the massive clump of gas surrounding it subsequently evolve.

We have seen that on large scales, we now have a relatively good understanding of the physical processes involved in the formation of the first star-forming minihalos. In order for gas to accumulate within a dark matter minihalo, it must be able to overcome the effects of both gas pressure and also the large-scale streaming motion of the gas relative to the dark matter. Since this streaming motion is typically supersonic, the latter effect generally dominates, and the result is that gas is prevented from accumulating in large quantities within minihalos with masses of less than around $10^5 M_\odot$. Within more massive minihalos, the gravitational force exerted by the dark matter is strong enough to overcome the effects of the gas pressure and the coherent streaming, and the gas begins to undergo gravitational collapse, reaching densities that are several hundred times higher than the cosmological background density. As the gas collapses, however, it is heated by compression and shocks. In order for the collapse to continue, the gas must be able to dissipate this energy, which it does through rotational and vibrational line emission from H_2 .

In Section 1.2, we saw that the amount of H_2 formed within a given minihalo is a strong function of the temperature of the gas, with the final molecular fraction scaling roughly as $x_{H_2} \propto T^{3/2}$ with the temperature T . The H_2 cooling rate is also a strong function of temperature. As a result, one finds that there is a critical minihalo virial temperature, $T_{\text{crit}} \sim 1000$ K marking the division between cooler halos that do not dissipate much energy within a Hubble time, and hence which do not form stars, and warmer halos that do manage to cool and form stars. As the virial temperature of a minihalo is a simple function of its mass and redshift, one can derive a critical minihalo mass that must be exceeded in order for the gas to cool effectively. This critical mass scales approximately as $M_{\text{crit}} \sim 1.6 \times 10^6 (1 + z/10)^{-3/2} M_\odot$, given standard values for the cosmological parameters. Combining this constraint with that arising from coherent streaming, one finds that at redshifts $z > 40$, the minimum mass of a star-forming minihalo is set by the need to overcome the effects of the streaming, and is roughly $10^5 M_\odot$, while at $z < 40$, H_2 cooling is the limiting factor, and the minimum mass scale is somewhat larger.

On smaller scales, we have also developed an increasingly good understanding of how the gas evolves as it cools, undergoes runaway gravitational collapse, and forms the first protostar. As outlined in Section 2, the gas first passes through a ‘‘loitering’’ phase, during which cold gas accumulates at the centre of the minihalo. The temperature and density of the gas at this point depend on the nature of the dominant coolant. When H_2 dominates, we have $T \sim 200$ K and $n \sim 10^4 \text{ cm}^{-3}$, while if HD dominates, then $T \sim 100$ K and $n \sim 10^6 \text{ cm}^{-3}$. The loitering phase ends and the collapse of the gas accelerates once the mass of cold gas that has accumulated exceeds the local value of the Bonnor-Ebert mass, which is around $1000 M_\odot$ in the H_2 -dominated case, but only $40 M_\odot$ in the HD-dominated case. The next major event to occur is the onset of three-body H_2 formation at $n \sim 10^8 \text{ cm}^{-3}$ which rapidly converts most of the atomic hydrogen into H_2 . The associated heat input leads to an increase in the gas temperature to $T \sim 1000$ - 2000 K, with the details depending to a significant extent on the rate coefficient chosen for reaction 41, which is poorly

constrained at low temperatures. At $n \sim 10^{10} \text{ cm}^{-3}$, the gas becomes optically thick in the main H_2 cooling lines, but remains optically thin in the continuum. It can therefore continue to cool reasonably effectively at these densities, with the mean temperature only rising relatively slowly with increasing density. At $n \sim 10^{14} \text{ cm}^{-3}$, a new process, collision-induced emission from H_2 , begins to dominate the cooling. However, this does not lead to a significant drop in the gas temperature, as the gas quickly becomes optically thick in the continuum. At densities above $n \sim 10^{16} \text{ cm}^{-3}$, further radiative cooling of the gas is ineffective and the only remaining process capable of slowing the temperature rise is collisional dissociation of the H_2 . While the H_2 fraction in the gas remains significant, the temperature is prevented from rising much above 3000 K, but once most of the H_2 has been destroyed, the temperature in the core rises steeply, and the internal thermal pressure eventually becomes strong enough to halt the collapse. State-of-the-art simulations have followed the gravitational collapse of the gas up to this point, which we can identify as the moment at which the first true Population III protostar forms.

Nevertheless, several uncertainties remain in this picture of Pop. III star formation. As already noted, the uncertainty in the three-body H_2 formation rate limits the accuracy with which we can model the chemical and thermal evolution of the collapsing gas. In addition, current three-dimensional collapse models make use of simplified treatments of the effect of opacity on the H_2 cooling rate, and the uncertainty that this introduces into the models has not yet been properly quantified. Further uncertainty comes from two additional issues which have only recently begun to be addressed: the role played by magnetic fields, and the influence of dark matter annihilation. Although the strength of any seed magnetic field existing prior to the assembly of the first star-forming minihalos is still poorly constrained, it now seems clear that the small-scale turbulent dynamo acting during the collapse of the gas will rapidly amplify even a very weak initial field up to a point at which it could potentially become dynamically significant. However, neither the final strength of the field nor its correlation length are well constrained at present, and without a better understanding of these values it is difficult to say to what extent the magnetic field will influence the details of the collapse. The role played by heating and ionization due to dark matter annihilation is even less well understood. Simple models suggest that it may be extremely important and may result in the formation of “dark stars” supported by the energy released by dark matter annihilation rather than by nuclear fusion, but the only hydrodynamical study performed to date suggests that the influence on the collapse is small, and that dark stars do not actually form.

Finally, there remains the question of how the gas evolves after the formation of the first protostar. For much of the last decade, the leading model for this phase of the evolution of the gas has been what we have termed the “smooth accretion” model. In this model, it is assumed that the gas surrounding the newly formed protostar does not fragment, but instead simply smoothly accretes onto the protostar, primarily via a protostellar accretion disk. Considerable work has been done within the framework of this model to understand the structure of the protostar during the accretion phase, and the effect of protostellar feedback on the surrounding gas. This work has shown that any feedback occurring prior to the protostar joining the main

sequence is unlikely to significantly reduce the accretion rate, and that the most plausible mechanism for terminating the accretion is photoionization of the accretion disk by ionizing radiation from the central star, implying that it must already have grown to some tens of solar masses. This model therefore predicts that Pop. III stars will generally be solitary, with only one or two forming in each minihalo, and massive, with masses $M \gg 10 M_{\odot}$.

Over the past couple of years, however, several new studies have appeared that have cast considerable doubt on the smooth accretion model. These studies have attempted to directly model the evolution of the gas as it begins to be accreted, and have shown that the accretion disk that builds up around the protostar is unstable to gravitational fragmentation even if the stabilizing effects of accretion luminosity feedback from the central protostar are taken into account. Once a few fragments have formed, the dynamical interactions between the individual fragments and between the fragments and the gas can lead to further fragmentation, and to the ejection of low-mass fragments from the system. If we assume that all of the gravitationally bound fragments form protostars, then the result of this model is the assembly of a small, extremely dense cluster of Pop. III protostars with a wide range of masses. As discussed in Section 3.2.4, many aspects of the fragmentation scenario remain unclear and much work remains to be done before we can hope to have a good understanding of the final protostellar mass function. Nevertheless, these results suggest that Population III star formation perhaps has far more in common with present-day star formation than has been previously recognised.

Acknowledgments

The author would like to thank a large number of people with whom he has had interesting and informative discussions about the physics of Population III star formation, including T. Abel, V. Bromm, P. Clark, G. Dopcke, T. Greif, Z. Haiman, T. Hosokawa, R. Klessen, M. Norman, K. Omukai, B. O’Shea, D. Schleicher, B. Smith, R. Smith, A. Stacy, J. Tan, M. Turk, D. Whalen, and N. Yoshida. Special thanks also go to R. Smith and M. Turk for providing some of the data plotted in Figure 3, and to P. Clark for his assistance with the production of Figure 4. Financial support for this work was provided by the Baden-Württemberg-Stiftung via their program International Collaboration II (grant P-LS-SPII/18), from the German Bundesministerium für Bildung und Forschung via the ASTRONET project STAR FORMAT (grant 05A09VHA), and by a Frontier grant of Heidelberg University sponsored by the German Excellence Initiative.

References

- Abel, T., Anninos, P., Zhang, Y., & Norman, M. L.: Modeling primordial gas in numerical cosmology, *New Astron.*, **2**, 181-207 (1997)
- Abel, T., Bryan, G. L., & Norman, M. L.: The Formation and Fragmentation of Primordial Molecular Clouds, *Astrophys. J.*, **540**, 39-44 (2000)
- Abel, T., Bryan, G. L., & Norman, M. L.: The Formation of the First Star in the Universe, *Science*, **295**, 93-98 (2002)
- Abel, T., Wise, J. H., & Bryan, G. L.: The H II Region of a Primordial Star, *Astrophys. J.*, **659**, L87-L90 (2007)
- Alvarez, M. A., Bromm, V., & Shapiro, P. R.: The H II Region of the First Star, *Astrophys. J.*, **639**, 621-632 (2006)
- Balbus, S. A., & Hawley, J. F.: A powerful local shear instability in weakly magnetized disks. I - Linear analysis. II - Nonlinear evolution, *Astrophys. J.*, **376**, 214-233 (1991)
- Balbus, S. A., & Hawley, J. F.: Instability, turbulence, and enhanced transport in accretion disks, *Rev. Mod. Phys.*, **70**, 1-53 (1998)
- Barkana, R., & Loeb, A.: In the beginning: the first sources of light and the reionization of the universe, *Phys. Rep.*, **349**, 125-238 (2001)
- Barkana, R., & Loeb, A.: Probing the epoch of early baryonic infall through 21-cm fluctuations, *Mon. Not. Royal Astron. Soc.*, **363**, L36-L40 (2005)
- Barrow, J. D., Ferreira, P. G., & Silk, J.: Constraints on a Primordial Magnetic Field, *Phys. Rev. Lett.*, **78**, 3610-3613 (1997)
- Bate, M. R., Bonnell, I. A., & Price, N. M.: Modelling accretion in protobinary systems, *Mon. Not. Royal Astron. Soc.* **277**, 362-376 (1995)
- Beck, R., Poezd, A. D., Shukurov, A., & Sokoloff, D. D.: Dynamos in evolving galaxies, *Astron. Astrophys.*, **289**, 94-100 (1994)
- Bergin, E. A., & Tafalla, M.: Cold Dark Clouds: The Initial Conditions for Star Formation, *Ann. Rev. Astron. Astrophys.*, **45**, 339-396 (2007)
- Biermann, L.: Über den Ursprung der Magnetfelder auf Sternen und im interstellaren Raum, *Zeitschrift Naturforschung A*, **5**, 65 (1950)
- Blumenthal, G. R., Faber, S. M., Flores, R., & Primack, J. R.: Contraction of dark matter galactic halos due to baryonic infall, *Astrophys. J.*, **301**, 27-34 (1986)
- Bonnor, W. B.: Boyle's Law and gravitational instability, *Mon. Not. Royal Astron. Soc.*, **116**, 351-359 (1956)
- Bromm, V., Coppi, P. S., & Larson, R. B.: Forming the First Stars in the Universe: The Fragmentation of Primordial Gas, *Astrophys. J.*, **527**, L5-L8 (1999)
- Bromm, V., Coppi, P. S., & Larson, R. B.: The Formation of the First Stars. I. The Primordial Star-forming Cloud, *Astrophys. J.*, **564**, 23-51 (2002)
- Bromm, V., & Loeb, A.: Formation of the First Supermassive Black Holes, *Astrophys. J.*, **596**, 34-46 (2003)
- Bromm, V., & Loeb, A.: Accretion onto a primordial protostar, *New Astron.*, **9**, 353-364 (2004)
- Bryan, G. L., & Norman, M. L.: Statistical Properties of X-Ray Clusters: Analytic and Numerical Comparisons, *Astrophys. J.*, **495**, 80-99 (1998)
- Castor, J. I., Abbott, D. C., & Klein, R. I.: Radiation-driven winds in Of stars, *Astrophys. J.*, **195**, 157 (1975)
- Ciardi, B., & Ferrara, A.: The First Cosmic Structures and Their Effects, *Space Sci. Rev.*, **116**, 625-705 (2005)
- Chiosi, C., & Maeder, A.: The evolution of massive stars with mass loss, *Ann. Rev. Astron. Astrophys.*, **24**, 329-375 (1986)
- Clark, P. C., Glover, S. C. O., & Klessen, R. S.: The First Stellar Cluster, *Astrophys. J.*, **672**, 757-764 (2008)

- Clark, P. C., Glover, S. C. O., Klessen, R. S., & Bromm, V.: Gravitational Fragmentation in Turbulent Primordial Gas and the Initial Mass Function of Population III Stars, *Astrophys. J.*, **727**, 110 (2011a)
- Clark, P. C., Glover, S. C. O., Smith, R. J., Greif, T. H., Klessen, R. S., & Bromm, V.: The Formation and Fragmentation of Disks Around Primordial Protostars, *Science*, **331**, 1040-1042 (2011b)
- Cyburt, R. H., Fields, B. D., & Olive, K. A.: An update on the big bang nucleosynthesis prediction for ${}^7\text{Li}$: the problem worsens, *J. Cosmol. Astropart. Phys.*, **11**, 012 (2008)
- Davis, A. J., & Natarajan, P.: Spin and structural halo properties at high redshift in a Λ cold dark matter universe, *Mon. Not. Royal Astron. Soc.*, **407**, 691-703 (2010)
- Draine, B. T., & Bertoldi, F.: Structure of Stationary Photodissociation Fronts, *Astrophys. J.*, **468**, 269-289 (1996)
- Dopcke, G., Glover, S. C. O., Clark, P. C., & Klessen, R. S.: The Effect of Dust Cooling on Low-metallicity Star-forming Clouds, *Astrophys. J.*, **729**, L3 (2011)
- Ebert, R.: Über die Verdichtung von H I-Gebieten, *Z. Astrophys.*, **37**, 217-232 (1955)
- Fatuzzo, M., Adams, F. C., & Myers, P. C.: Generalized Collapse Solutions with Nonzero Initial Velocities for Star Formation in Molecular Cloud Cores, *Astrophys. J.*, **615**, 813-831 (2004)
- Federrath, C., Sur, S., Schleicher, D. R. G., Banerjee, R., & Klessen, R. S.: A New Jeans Resolution Criterion for (M)HD Simulations of Self-gravitating Gas: Application to Magnetic Field Amplification by Gravity-driven Turbulence, *Astrophys. J.*, **731**, 62 (2011)
- Frebel, A., Johnson, J. L., & Bromm, V.: The minimum stellar metallicity observable in the Galaxy, *Mon. Not. Royal Astron. Soc.*, **392**, L50-L54 (2009)
- Freese, K., Gondolo, P., Sellwood, J. A., & Spolyar, D.: Dark Matter Densities During the Formation of the First Stars and in Dark Stars, *Astrophys. J.*, **693**, 1563-1569 (2009)
- Frommhold, L.: Collision-Induced Absorption in Gases. Cambridge Univ. Press, Cambridge (1993)
- Galli, D., & Palla, F.: The chemistry of the early Universe, *Astron. Astrophys.*, **335** 403-420 (1998)
- Gao, L., White, S. D. M., Jenkins, A., Frenk, C. S., & Springel, V.: Early structure in Λ CDM, *Mon. Not. Royal Astron. Soc.*, **363**, 379-392 (2005)
- Gao, L., Yoshida, N., Abel, T., Frenk, C. S., Jenkins, A., & Springel, V.: The first generation of stars in the Λ cold dark matter cosmology, *Mon. Not. Royal Astron. Soc.*, **378**, 449-468 (2007)
- Glover, S. C. O.: The Formation Of The First Stars In The Universe, *Space Sci. Rev.*, **117**, 445-508 (2005)
- Glover, S. C. O.: Chemistry and Cooling in Metal-Free and Metal-Poor Gas. In: O'Shea, B. W., Heger, A., Abel, T. (eds.) *First Stars III*, pp. 25-29. AIP Press (2008)
- Glover, S. C. O., & Abel, T.: Uncertainties in H_2 and HD chemistry and cooling and their role in early structure formation, *Mon. Not. Royal Astron. Soc.*, **388**, 1627-1651 (2008)
- Glover, S. C. O., & Brand, P. W. J. L.: On the photodissociation of H_2 by the first stars, *Mon. Not. Royal Astron. Soc.*, **321**, 385-397 (2001)
- Glover, S. C. O., & Brand, P. W. J. L.: Radiative feedback from an early X-ray background, *Mon. Not. Royal Astron. Soc.*, **340**, 210-226 (2003)
- Glover, S. C. O., & Savin, D. W.: H_3^+ cooling in primordial gas, *Phil. Trans. Roy. Soc. Lond. A*, **364**, 3107-3112 (2006)
- Glover, S. C. O., & Savin, D. W.: Is H_3^+ cooling ever important in primordial gas?, *Mon. Not. Royal Astron. Soc.*, **393**, 911-948 (2009)
- Glover, S. C. O., Savin, D. W., & Jappsen, A.-K.: Cosmological Implications of the Uncertainty in H^- Destruction Rate Coefficients, *Astrophys. J.*, **640**, 553-568 (2006)
- Gnedin, N. Y.: Effect of Reionization on Structure Formation in the Universe, *Astrophys. J.*, **542**, 535-541 (2000)
- Gnedin, N. Y., & Hui, L.: Probing the Universe with the Ly α forest - I. Hydrodynamics of the low-density intergalactic medium, *Mon. Not. Royal Astron. Soc.*, **296**, 44-55 (1998)
- Gnedin, O. Y., Kravtsov, A. V., Klypin, A. A., & Nagai, D.: Response of Dark Matter Halos to Condensation of Baryons: Cosmological Simulations and Improved Adiabatic Contraction Model, *Astrophys. J.*, **616**, 16-26 (2004)

- Goodwin, S. P., Whitworth, A. P., & Ward-Thompson, D.: Simulating star formation in molecular cloud cores. I. The influence of low levels of turbulence on fragmentation and multiplicity, *Astron. Astrophys.*, **414**, 633-650 (2004)
- Gould, R. J., & Salpeter, E. E.: The Interstellar Abundance of the Hydrogen Molecule. I. Basic Processes, *Astrophys. J.*, **138**, 393-407 (1963)
- Green, A. M., Hofmann, S., & Schwarz, D. J.: The first WIMPy halos, *J. Cosmol. Astropart. Phys.*, **8**, 3 (2005)
- Greif, T. H., Johnson, J. L., Klessen, R. S., & Bromm, V.: The first galaxies: assembly, cooling and the onset of turbulence, *Mon. Not. Royal Astron. Soc.*, **387**, 1021-1036 (2008)
- Greif, T. H., Glover, S. C. O., Bromm, V., & Klessen, R. S.: The First Galaxies: Chemical Enrichment, Mixing, and Star Formation, *Astrophys. J.*, **716**, 510-520 (2010)
- Greif, T., Springel, V., White, S., Glover, S., Clark, P., Smith, R., Klessen, R., & Bromm, V.: Simulations on a Moving Mesh: The Clustered Formation of Population III Protostars, *Astrophys. J.*, **737**, 75 (2011)
- Greif, T., White, S., Klessen, R., & Springel, V.: The Delay of Population III Star Formation by Supersonic Streaming Velocities, *Astrophys. J.*, **736**, 147 (2011)
- Greif, T. H., Bromm, V., Clark, P. C., Glover, S. C. O., Smith, R. J., Klessen, R. S., Yoshida, N., Springel, V.: Formation and evolution of primordial protostellar systems, *Mon. Not. Royal Astron. Soc.*, **424**, 399-415 (2012)
- Haiman, Z., Abel, T., & Madau, P.: Photon Consumption in Minihalos during Cosmological Reionization, *Astrophys. J.*, **551**, 599-607 (2001)
- Haiman, Z., Abel, T., & Rees, M. J.: The Radiative Feedback of the First Cosmological Objects, *Astrophys. J.*, **534**, 11-24 (2000)
- Haugen, N. E., Brandenburg, A., & Dobler, W.: Simulations of nonhelical hydromagnetic turbulence, *Phys. Rev. E*, **70**, 016308 (2004)
- Hennebelle, P., & Ciardi, A.: Disk formation during collapse of magnetized protostellar cores, *Astron. Astrophys.*, **506**, L29-L32 (2009)
- Hosokawa, T., Omukai, K., Yoshida, N., Yorke, H. W.: Protostellar feedback halts the growth of the first stars in the universe, *Science*, **334**, 1250-1253
- Hoyle, F.: On the Fragmentation of Gas Clouds Into Galaxies and Stars, *Astrophys. J.*, **118**, 513-528 (1953)
- Hunter, C.: The collapse of unstable isothermal spheres, *Astrophys. J.*, **218**, 834-845 (1977)
- Hutchins, J. B.: The thermal effects of H₂ molecules in rotating and collapsing spheroidal gas clouds, *Astrophys. J.*, **205**, 103-121 (1976)
- Jang-Condell, H., & Hernquist, L.: First Structure Formation: A Simulation of Small-Scale Structure at High Redshift, *Astrophys. J.*, **548**, 68-78 (2001)
- Jasche, J., Ciardi, B., & Ensslin, T. A.: Cosmic rays and the primordial gas, *Mon. Not. Royal Astron. Soc.*, **380**, 417-429 (2007)
- Johnson, J. L., & Bromm, V.: The cooling of shock-compressed primordial gas, *Mon. Not. Royal Astron. Soc.*, **366**, 247-256 (2006)
- Johnson, J. L., Greif, T. H., & Bromm, V.: Occurrence of metal-free galaxies in the early Universe, *Mon. Not. Royal Astron. Soc.*, **388**, 26-38 (2008)
- Johnson, J. L., & Khochfar, S.: Suppression of accretion on to low-mass Population III stars, *Mon. Not. Royal Astron. Soc.*, **413**, 1184-1191 (2011)
- Kandus, A., Kunze, K. E., & Tsagas, C. G.: Primordial magnetogenesis, *Phys. Rep.*, **505**, 1 (2011)
- Kazantsev, A. P.: Enhancement of a Magnetic Field by a Conducting Fluid, *Sov. Phys. JETP*, **26**, 1031 (1968)
- Kitsionas, S., & Whitworth, A. P.: Smoothed Particle Hydrodynamics with particle splitting, applied to self-gravitating collapse, *Mon. Not. Royal Astron. Soc.*, **330**, 129-136 (2002)
- Komatsu, E., et al.: Seven-year Wilkinson Microwave Anisotropy Probe (WMAP) Observations: Cosmological Interpretation, *Astrophys. J. Suppl. S.*, **192**, 18 (2011)
- Kraichnan, R. H., & Nagarajan, S.: Growth of Turbulent Magnetic Fields, *Phys. Fluids*, **10**, 859-870 (1967)

- Kreckel, H., Bruhns, H., Čížek, M., Glover, S. C. O., Miller, K. A., Urbain, X., & Savin, D. W.: Experimental Results for H₂ Formation from H⁻ and H and Implications for First Star Formation, *Science*, **329**, 69-71 (2010)
- Krtićka, J., & Kubát, J.: CNO-driven winds of hot first stars, *Astron. Astrophys.*, **493**, 585-593 (2009)
- Krumholz, M. R.: Radiation Feedback and Fragmentation in Massive Protostellar Cores, *Astrophys. J.*, **641**, L45-L48 (2006)
- Kudritzki, R. P.: Line-driven Winds, Ionizing Fluxes, and Ultraviolet Spectra of Hot Stars at Extremely Low Metallicity. I. Very Massive O Stars, *Astrophys. J.*, **577**, 389-408 (2002)
- Kulsrud, R. M., & Anderson, S. W.: The spectrum of random magnetic fields in the mean field dynamo theory of the Galactic magnetic field, *Astrophys. J.*, **396**, 606-630 (1992)
- Kulsrud, R. M., Cen, R., Ostriker, J. P., & Ryu, D.: The Protogalactic Origin for Cosmic Magnetic Fields, *Astrophys. J.*, **480**, 481-491 (1997)
- Kulsrud, R. M., & Zweibel, E. G.: On the origin of cosmic magnetic fields, *Rep. Prog. Phys.*, **71**, 046901 (2008)
- Lacey, C., & Cole, S.: Merger rates in hierarchical models of galaxy formation, *Mon. Not. Royal Astron. Soc.*, **262**, 627-649 (1993)
- Larson, R. B.: Numerical calculations of the dynamics of collapsing proto-star, *Mon. Not. Royal Astron. Soc.*, **145**, 271-295 (1969)
- Larson, R. B., & Starrfield, S.: On the formation of massive stars and the upper limit of stellar masses. *Astron. Astrophys.*, **13**, 190-197 (1971)
- Lenzuni, P., Chernoff, D. F., & Salpeter, E. E.: Rosseland and Planck mean opacities of a zero-metallicity gas, *Astrophys. J. Suppl. S.*, **76**, 759-801 (1991)
- Lepp, S., & Shull, J. M.: Molecules in the early universe, *Astrophys. J.*, **280**, 465-469 (1984)
- Low, C., & Lynden-Bell, D.: The minimum Jeans mass or when fragmentation must stop, *Mon. Not. Royal Astron. Soc.*, **176**, 367-390 (1976)
- Machacek, M. E., Bryan, G. L., & Abel, T.: Effects of a soft X-ray background on structure formation at high redshift, *Mon. Not. Royal Astron. Soc.*, **338**, 273-286 (2003)
- Machida, M. N., Omukai, K., Matsumoto, T., & Inutsuka, S.: The first jets in the Universe: protostellar jets from the first stars, *Astrophys. J.*, **647**, L1-L4 (2006)
- Machida, M. N., Matsumoto, T., & Inutsuka, S.: Magnetohydrodynamics of Population III Star Formation, *Astrophys. J.*, **685**, 690-704 (2008)
- Maeder, A., & Meynet, G.: The Evolution of Rotating Stars, *Ann. Rev. Astron. Astrophys.*, **38**, 143-190 (2000)
- Maron, J., Cowley, S., & McWilliams, J.: The Nonlinear Magnetic Cascade, *Astrophys. J.*, **603**, 569-583 (2004)
- Martin, P. G., Keogh, W. J., & Mandy, M. E.: Collision-induced Dissociation of Molecular Hydrogen at Low Densities, *Astrophys. J.*, **499**, 793-798 (1998)
- Mayer, M., & Duschl, W. J.: Stationary Population III accretion discs, *Mon. Not. Royal Astron. Soc.*, **356**, 1 (2005a)
- Mayer, M., & Duschl, W. J.: Rosseland and Planck mean opacities for primordial matter, *Mon. Not. Royal Astron. Soc.*, **358**, 614-631 (2005b)
- McDowell, M. R. C.: On the formation of H₂ in HI regions, *Observatory*, **81**, 240-243 (1961)
- McGreer, I. D., & Bryan, G. L.: The Impact of HD Cooling on the Formation of the First Stars, *Astrophys. J.*, **685**, 8-20 (2008)
- McKee, C. F., & Tan, J. C.: The Formation of the First Stars. II. Radiative Feedback Processes and Implications for the Initial Mass Function, *Astrophys. J.*, **681**, 771-797 (2008)
- Meynet, G., Ekström, S., & Maeder, A.: The early star generations: the dominant effect of rotation on the CNO yields, *Astron. Astrophys.*, **447**, 623-639 (2006)
- Mizusawa, H., Omukai, K., & Nishi, R.: Primordial Molecular Emission in Population III Galaxies, *Pub. Astron. Soc. Japan*, **57**, 951-967 (2005)
- Myers, Z., & Nusser, A.: Neutralino annihilations and the gas temperature in the dark ages, *Mon. Not. Royal Astron. Soc.*, **384**, 727-732 (2008)

- Nagakura, T., & Omukai, K.: Formation of Population III stars in fossil HII regions: significance of HD, *Mon. Not. Royal Astron. Soc.*, **364**, 1378-1386 (2005)
- Nakamura, F., & Umemura, M.: The Stellar Initial Mass Function in Primordial Galaxies, *Astrophys. J.*, **569**, 549-557 (2002)
- Nakano, T., Hasegawa, T., Morino, J.-I., & Yamashita, T.: Evolution of Protostars Accreting Mass at Very High Rates: Is Orion IRc2 a Huge Protostar?, *Astrophys. J.*, **534**, 976-983 (2000)
- Nakano, T., Hasegawa, T., & Norman, C.: The Mass of a Star Formed in a Cloud Core: Theory and Its Application to the Orion A Cloud, *Astrophys. J.*, **450**, 183-195 (1995)
- Navarro, J. F., Frenk, C. S., & White, S. D. M.: A universal density profile from hierarchical clustering, *Astrophys. J.*, **490**, 493-508 (1997)
- Navarro, J. F., & White, S. D. M.: Simulations of dissipative galaxy formation in hierarchically clustering universes-2. Dynamics of the baryonic component in galactic haloes, *Mon. Not. Royal Astron. Soc.*, **267**, 401-412 (1994)
- Naoz, S., & Barkana, R.: Growth of linear perturbations before the era of the first galaxies, *Mon. Not. Royal Astron. Soc.*, **362**, 1047-1053 (2005)
- Naoz, S., & Barkana, R.: The formation and gas content of high-redshift galaxies and minihaloes, *Mon. Not. Royal Astron. Soc.*, **377**, 667-676 (2007)
- Oh, S. P., & Haiman, Z.: Second-generation objects in the Universe: radiative cooling and collapse of halos with virial temperatures above 10^4 Kelvin, *Astrophys. J.*, **569**, 558-572 (2002)
- Oh, S. P., & Haiman, Z.: Fossil H II regions: self-limiting star formation at high redshift, *Mon. Not. Royal Astron. Soc.*, **346**, 456-472 (2003)
- Omukai, K., & Inutsuka, S.: An upper limit on the mass of a primordial star due to the formation of an HII region: the effect of ionizing radiation force, *Mon. Not. Royal Astron. Soc.*, **332**, 59-64 (2002)
- Omukai, K., & Nishi, R.: Formation of Primordial Protostars, *Astrophys. J.*, **508**, 141-150 (1998)
- Omukai, K., & Nishi, R.: Photodissociative Regulation of Star Formation in Metal-free Pregalactic Clouds, *Astrophys. J.*, **518**, 64-68 (1999)
- Omukai, K., Nishi, R., Uehara, H., & Susa, H.: Evolution of Primordial Protostellar Clouds – Quasi-Static Analysis, *Prog. Theor. Phys.*, **99**, 747-761 (1998)
- Omukai, K., & Palla, F.: On the Formation of Massive Primordial Stars, *Astrophys. J.*, **589**, 677-687 (2003)
- Omukai, K., & Palla, F.: Formation of the First Stars by Accretion, *Astrophys. J.*, **561**, L55-L58 (2001)
- Omukai, K., Tsuribe, T., Schneider, R., & Ferrara, A.: Thermal and Fragmentation Properties of Star-forming Clouds in Low-Metallicity Environments, *Astrophys. J.*, **626**, 627-643 (2005)
- O'Shea, B. W., & Norman, M. L.: Population III Star Formation in a Λ CDM Universe. I. The Effect of Formation Redshift and Environment on Protostellar Accretion Rate, *Astrophys. J.*, **654**, 66-92 (2007)
- Palla, F., Salpeter, E. E., & Stahler, S. W.: Primordial star formation - The role of molecular hydrogen, *Astrophys. J.*, **271**, 632-641 (1983)
- Peebles, P. J. E., & Dicke, R. H.: Origin of the Globular Star Clusters, *Astrophys. J.*, **154**, 891-908 (1968)
- Penston, M. V.: Dynamics of self-gravitating gaseous spheres-III. Analytical results in the free-fall of isothermal cases, *Mon. Not. Royal Astron. Soc.*, **144**, 425-448 (1969)
- Pinto, C., Galli, D., & Bacciotti, F.: Three-fluid plasmas in star formation. I. Magneto-hydrodynamic equations, *Astron. Astrophys.*, **484**, 1-15 (2008)
- Pudritz, R. E., & Silk, J.: The origin of magnetic fields and primordial stars in protogalaxies, *Astrophys. J.*, **342**, 650-659 (1989)
- Rees, M. J.: Opacity-limited hierarchical fragmentation and the masses of protostars, *Mon. Not. Royal Astron. Soc.*, **176**, 483-486 (1976)
- Rees, M. J., & Ostriker, J. P.: Cooling, dynamics and fragmentation of massive gas clouds - Clues to the masses and radii of galaxies and clusters, *Mon. Not. Royal Astron. Soc.*, **179**, 541-559 (1977)

- Rice, W. K. M., Lodato, G., & Armitage, P. J.: Investigating fragmentation conditions in self-gravitating accretion discs, *Mon. Not. Royal Astron. Soc.*, **364**, L56-L60 (2005)
- Ripamonti, E., Haardt, F., Ferrara, A., & Colpi, M.: Radiation from the first forming stars, *Mon. Not. Royal Astron. Soc.*, **334**, 401 (2002)
- Ripamonti, E., & Abel, T.: Fragmentation and the formation of primordial protostars: the possible role of collision-induced emission, *Mon. Not. Royal Astron. Soc.*, **348**, 1019-1034 (2004)
- Ripamonti, E., Iocco, F., Ferrara, A., Schneider, R., Bressan, A., & Marigo, P.: First star formation with dark matter annihilation, *Mon. Not. Royal Astron. Soc.*, **406**, 2605-2615 (2010)
- Saslaw, W. C., & Zipoy, D.: Molecular Hydrogen in Pre-galactic Gas Clouds, *Nature*, **216**, 976-978 (1967)
- Savin, D. W., Krstić, P. S., Haiman, Z., & Stancil, P. C.: Rate Coefficient for $H^+ + H_2(X^1\Sigma_g^+, v = 0, J = 0) \rightarrow H(1s) + H_2^+$ Charge Transfer and Some Cosmological Implications, *Astrophys. J.*, **606**, L167-L170 (2004)
- Schleicher, D. R. G., Banerjee, R., & Klessen, R. S.: Reionization: A probe for the stellar population and the physics of the early universe, *Phys. Rev. D*, **78**, 083005 (2008)
- Schleicher, D. R. G., Galli, D., Palla, F., Camenzind, M., Klessen, R. S., Bartelmann, M., & Glover, S. C. O.: Effects of primordial chemistry on the cosmic microwave background, *Astron. Astrophys.*, **490**, 521-535 (2008)
- Schleicher, D. R. G., Banerjee, R., Sur, S., Arshakian, T. G., Klessen, R. S., Beck, R., & Spaans, M.: Small-scale dynamo action during the formation of the first stars and galaxies. I. The ideal MHD limit, *Astron. Astrophys.*, **522**, A115 (2010)
- Schleicher, D. R. G., Galli, D., Glover, S. C. O., Banerjee, R., Palla, F., Schneider, R., & Klessen, R. S.: The Influence of Magnetic Fields on the Thermodynamics of Primordial Star Formation, *Astrophys. J.*, **703**, 1096-1106 (2009)
- Schneider, R., Omukai, K., Inoue, A. K., & Ferrara, A.: Fragmentation of star-forming clouds enriched with the first dust, *Mon. Not. Royal Astron. Soc.*, **369**, 1437-1444 (2006)
- Shakura, N. I., & Sunyaev, R. A.: Black holes in binary systems. Observational appearance, *Astron. Astrophys.*, **24**, 337-355 (1973)
- Shu, F.: Self-similar collapse of isothermal spheres and star formation, *Astrophys. J.*, **214**, 488-497 (1977)
- Silk, J.: Cosmic Black-Body Radiation and Galaxy Formation, *Astrophys. J.*, **151**, 459-471 (1968)
- Silk, J., & Langer, M.: On the first generation of stars, *Mon. Not. Royal Astron. Soc.*, **371**, 444-450 (2006)
- Smith, R. J., Glover, S. C. O., Clark, P. C., Greif, T., & Klessen, R. S.: The Effects of Accretion Luminosity upon Fragmentation in the Early Universe, *Mon. Not. Royal Astron. Soc.*, **414**, 3633-3644 (2011)
- Smith, N., & Owocki, S. P.: On the Role of Continuum-driven Eruptions in the Evolution of Very Massive Stars and Population III Stars, *Astrophys. J.*, **645**, L45-L48 (2006)
- Sobolev, V. V.: *Moving envelopes of stars*. Harvard University Press, Cambridge (1960)
- Spolyar, D., Freese, K., & Gondolo, P.: Dark Matter and the First Stars: A New Phase of Stellar Evolution, *Phys. Rev. Lett.*, **100**, 051101 (2008)
- Springel, V.: E pur si muove: Galilean-invariant cosmological hydrodynamical simulations on a moving mesh, *Mon. Not. Royal Astron. Soc.*, **401**, 791-851 (2010)
- Stacy, A., & Bromm, V.: Impact of cosmic rays on Population III star formation, *Mon. Not. Royal Astron. Soc.*, **382**, 229-238 (2007)
- Stacy, A., Bromm, V., & Loeb, A.: Effect of Streaming Motion of Baryons Relative to Dark Matter on the Formation of the First Stars, *Astrophys. J.*, **730**, L1 (2011)
- Stacy, A., Greif, T. H., & Bromm, V.: The first stars: formation of binaries and small multiple systems, *Mon. Not. Royal Astron. Soc.*, **403**, 45-60 (2010)
- Stacy, A., Greif, T. H., & Bromm, V.: The first stars: mass growth under protostellar feedback, *Mon. Not. Royal Astron. Soc.*, **422**, 290-309 (2012)
- Stahler, S. W., Palla, F., & Salpeter, E. E.: Primordial stellar evolution - The protostar phase, *Astrophys. J.*, **302**, 590-605 (1986a)

- Stahler, S. W., Palla, F., & Salpeter, E. E.: Primordial stellar evolution - The pre-main-sequence phase, *Astrophys. J.*, **308**, 697-705 (1986b)
- Stamatellos, D., Whitworth, A. P., & Hubber, D. A.: The Importance of Episodic Accretion for Low-mass Star Formation, *Astrophys. J.*, **730**, 32 (2011)
- Stancil, P. C., Lepp, S., & Dalgarno, A.: The Lithium Chemistry of the Early Universe, *Astrophys. J.*, **458**, 401-406 (1996)
- Stancil, P. C., Lepp, S., & Dalgarno, A.: The Deuterium Chemistry of the Early Universe, *Astrophys. J.*, **509**, 1-10 (1998)
- Stenrup, M., Larson, Å., & Elander, N.: Mutual neutralization in low-energy $H^+ + H^-$ collisions: A quantum ab initio study, *Phys. Rev. A*, **79**, 012713 (2009)
- Subramanian, K.: Can the turbulent galactic dynamo generate large-scale magnetic fields?, *Mon. Not. Royal Astron. Soc.*, **294**, 718-728 (1998)
- Sur, S., Schleicher, D. R. G., Banerjee, R., Federrath, C., & Klessen, R. S.: The Generation of Strong Magnetic Fields During the Formation of the First Stars, *Astrophys. J.*, **721**, L134-L138 (2010)
- Tan, J. C., & Blackman, E. G.: Protostellar Disk Dynamos and Hydromagnetic Outflows in Primordial Star Formation, *Astrophys. J.*, **603**, 401-413 (2004)
- Tan, J. C., & McKee, C. F.: The Formation of the First Stars. I. Mass Infall Rates, Accretion Disk Structure, and Protostellar Evolution, *Astrophys. J.*, **603**, 383-400 (2004)
- Tan, J. C., & McKee, C. F.: Star Formation at Zero and Very Low Metallicities, In: O'Shea, B. W., Heger, A., Abel, T. (eds.) *First Stars III*, pp. 47-62. AIP Press (2008)
- Tegmark, M., Silk, J., Rees, M. J., Blanchard, A., Abel, T., & Palla, F.: How Small Were the First Cosmological Objects?, *Astrophys. J.*, **474**, 1-12 (1997)
- Tormen, G., Bouchet, F. R., & White, S. D. M.: The structure and dynamical evolution of dark matter haloes, *Mon. Not. Royal Astron. Soc.*, **286**, 865-884 (1997)
- Tseliakhovich, D., Barkana, R., & Hirata, C.: Suppression and Spatial Variation of Early Galaxies and Minihalos, *MNRAS*, **418**, 906
- Tseliakhovich, D., & Hirata, C.: Relative velocity of dark matter and baryonic fluids and the formation of the first structures, *Phys. Rev. D*, **82**, 083520 (2010)
- Tsuribe, T., & Omukai, K.: Physical Mechanism for the Intermediate Characteristic Stellar Mass in Extremely Metal Poor Environments, *Astrophys. J.*, **676**, L45-L48 (2008)
- Turk, M. J., Abel, T., & O'Shea, B.: The Formation of Population III Binaries from Cosmological Initial Conditions, *Science*, **325**, 601-605 (2009)
- Turk, M. J., Norman, M. L., & Abel, T.: High-entropy Polar Regions Around the First Protostars, *Astrophys. J.*, **725**, L140-L144 (2010)
- Turk, M. J., Clark, P. C., Glover, S. C. O., Greif, T. H., Abel, T., Klessen, R. S., & Bromm, V.: Effects of Varying the Three-body Molecular Hydrogen Formation Rate in Primordial Star Formation, *Astrophys. J.*, **726**, 55 (2011)
- Wang, P., & Abel, T.: Dynamical Treatment of Virialization Heating in Galaxy Formation, *Astrophys. J.*, **672**, 752-756 (2008)
- Whalen, D., Abel, T., & Norman, M. L.: Radiation Hydrodynamic Evolution of Primordial H II Regions, *Astrophys. J.*, **610**, 14-22 (2004)
- Whitworth, A., & Summers, D.: Self-similar condensation of spherically symmetric self-gravitating isothermal gas clouds, *Mon. Not. Royal Astron. Soc.*, **214**, 1-25 (1985)
- Wolfire, M. G., & Cassinelli, J. P.: Conditions for the formation of massive stars, *Astrophys. J.*, **319**, 850-867 (1987)
- Xu, H., O'Shea, B. W., Collins, D. C., Norman, M. L., Li, H., & Li, S.: The Biermann Battery in Cosmological MHD Simulations of Population III Star Formation, *Astrophys. J.*, **688**, L57-L60 (2008)
- Young, P.: Numerical models of star clusters with a central black hole. I - Adiabatic models, *Astrophys. J.*, **242**, 1232-1237 (1980)
- Yoshida, N., Abel, T., Hernquist, L., & Sugiyama, N.: Simulations of Early Structure Formation: Primordial Gas Clouds, *Astrophys. J.*, **592**, 645-663 (2003)

- Yoshida, N., Omukai, K., Hernquist, L., & Abel, T.: Formation of Primordial Stars in a Λ CDM Universe, *Astrophys. J.*, **652**, 6-25 (2006)
- Yoshida, N., Oh, S. P., Kitayama, T., & Hernquist, L.: Early Cosmological H II/He III Regions and Their Impact on Second-Generation Star Formation, *Astrophys. J.*, **663**, 687-707 (2007)
- Yoshida, N., Omukai, K., & Hernquist, L.: Formation of Massive Primordial Stars in a Reionized Gas, *Astrophys. J.*, **667**, L117-L120 (2007)
- Yoshida, N., Omukai, K., & Hernquist, L.: Protostar Formation in the Early Universe, *Science*, **321**, 669-671 (2008)
- Zel'Dovich, Ya. B.: Gravitational instability: An approximate theory for large density perturbations, *Astron. Astrophys.*, **5**, 84-89 (1970)